**TÜRKİYE CUMHURİYETİ**
**ADANA ALPARSLAN TÜRKEŞ SCIENCE AND TECHNOLOGY UNIVERSITY**

**GRADUATE SCHOOL**
**FOOD ENGINEERING DEPARTMENT**

# PRODUCTION OF L-METHIONINASE ENZYME, INVESTIGATION OF ITS ANTICARCINOGENIC PROPERTIES AND USAGE AREAS IN THE FOOD INDUSTRY

**SEMİH LATİH İPEK**

**Ph.D.**

**ADANA 2023**

**TÜRKİYE CUMHURİYETİ**
**ADANA ALPARSLAN TÜRKEŞ SCIENCE AND TECHNOLOGY UNIVERSITY**

**GRADUATE SCHOOL**
**FOOD ENGINEERING DEPARTMENT**

# PRODUCTION OF L-METHIONINASE ENZYME, INVESTIGATION OF ITS ANTICARCINOGENIC PROPERTIES AND USAGE AREAS IN THE FOOD INDUSTRY

**SEMİH LATİH İPEK**

**Ph.D.**

**THESIS ADVISOR**
**ASSOC. PROF. DR. DİLEK GÖKTÜRK**

**ADANA, 2023**

# DECLARATION OF CONFORMITY

In this thesis study, which was prepared following the thesis writing rules of the Adana Alparslan Türkeş Science and Technology University Institute of Graduate School, I declare that I provide all the information, documents, evaluations, and results in accordance with scientific ethics and moral codes without resorting to any means or assistance that would be contrary to scientific ethics and traditions. I also declare that I refer to all the articles I used in this study with appropriate references and accept all moral and legal consequences if a situation is found contrary to my statement regarding my work.

31/10/2023

[Signature]

Semih Latif İPEK

# ÖZET


## L-METİYONİNAZ ENZİMİNİN ÜRETİMİ, ANTİ-KANSEROJEN ÖZELLİKLERİNİN VE GIDA ENDÜSTRİSİNDE KULLANIM OLANAKLARININ ARAŞTIRILMASI

Semih Latif İPEK

Doktora, Gıda Mühendisliği Anabilim Dalı

Danışman: Doç. Dr. Dilek GÖKTÜRK

Ekim 2023, 141 sayfa

Bu çalışmada L-metiyoninaz enzimi, yardımcı peynir kültürü olan *Brevibacterium linens* BL2'den kısmen saflaştırılmıştır. Enzimin spesifik aktivitesi 3.055 ünite/mg olarak belirlenmiştir. İlk olarak, L-metiyoninazın Glioblastoma hücrelerine olan sitotoksik etkileri değerlendirilmiştir. U87MG ve T98G glioblastoma hücre hatlarının $IC_{50}$ değerleri, 24 saatlik inkübasyon sonrası nötral kırmızı canlılık analizi ile sırasıyla 5.792 ünite/mL ve 5.215 ünite/mL olarak saptanmıştır. L-metiyoninaz, etoposid ile birlikte kombinasyon halinde kullanıldığında aynı hücre hatlarına karşı sitotoksik etkiyi de artırdığı görülmüştür. Bu, U87MG hücrelerinin canlılığında önemli bir azalmaya yol açmış ve 48 saatlik inkübasyon süresinde kontrol grubuyla karşılaştırıldığında canlılığı %24.35'e azalttığı gözlemlenmiştir. Benzer şekilde, T98G hücrelerinin büyümesi hem L-metiyoninaz hem de etoposid tarafından inhibe edilmiştir. 48 saatlik inkübasyon sonunda hücresel canlılık, kontrol gruba kıyasla %37.74'e düşüş göstermiştir. *Brevibacterium linens* BL2'den saflaştırılan L-metiyoninaz enzimi Fare Embriyonik Fibroblast (MEF) hücreleri ve İnsan Keratinosit Hücre Hattı (HaCaT) üzerinde glioblastoma hücrelerine göre daha düşük sitotoksik etki göstermiştir. L-metiyoninaz ve etoposidin kombinasyon uygulaması, HaCaT hücre canlılığının genel olarak %63.02'ye ve MEF hücre canlılığının %58.99'a düşürmüştür. Giemsa, DAPI ve F-aktin boyama yöntemleri ile hem hücre popülasyonunda hem de morfolojideki değişiklikleri doğrudan tespit edilmiştir. L-metiyoninaz ve etoposidin birlikte uygulanması, glioblastomanın yara iyileştirme yeteneğini azaltmasının yanında, hücresel göçün baskılanmasında dikkate değer bir etkinlik gösterdiği gözlemlenmiştir. Klonojenik deneyler, L-metiyoninaz ve

etoposid uygulanmasının, 21 günlük inkübasyon süresi boyunca glioblastoma hücrelerinin koloni sayısında önemli bir azalmaya neden olduğunu göstermiştir. RT-qPCR sonuçları, L-metiyoninazın, kanser hücrelerinin hayatta kalması için hayati olan Survivin ve C-Myc genlerinin ekspresyonunda azalmaya neden olurken hücre ölümü için gerekli olan Kaspaz-3 geninin ekspresyonunu arttırdığını göstermektedir.

Bu araştırma aynı zamanda L-metiyoninazın çedar peyniri bulamaçlarına uygulanmasının uçucu sülfür bileşikleri üretimi ve peynir mikrobiyomu değişimi üzerindeki etkileri de araştırılmıştır. Çedar bulamacı numuneleri, yeni nesil dizileme ve GC-MS analizi kullanılarak incelenmiştir. Deneyin ilk gününde numunelerde çoğunlukla *Lactococcus* ve *Streptococcus* suşlarının baskın olduğu görülmüştür. Ancak, dokuzuncu günde, tüm örneklerde belirgin bir şekilde *Limosilactobacillus*, *Lactobacillus*, *Enterococcus* ve *Lacticaseibacillus* gibi mikroorganizmaların varlığı ile karakterize edilen mikrobiyal çeşitlilikte kayda değer bir artış gözlenmiştir. İlginç bir şekilde, *Lactococcus* ve Streptococcus, dokuzuncu günde hala baskın türler olarak kalmıştır. Ek olarak, L-metiyoninaz enzimi ve *Brevibacterium linens* BL2'nin ilave edilmesi, Metanetiyol ve Dimetil trisülfür gibi uçucu kükürt bileşiklerinin üretimini teşvik etmiştir. Fermantasyonun erken aşamasında, L-metiyoninaz enzimi çedar bulamaçlarında 1490.2 ± 1.31 (µg/kg kuru madde) metanetiyol ve 65.8 ± 0.04 (µg/kg kuru madde) dimetil trisülfit üretmiştir. Bu sonuçlar, L-metiyoninazın çedar peyniri üretiminde ekonomik değer arttırıcı potansiyele sahip bir gıda endüstrisi enzimi olarak gelecekte kullanılabileceği görüşünü desteklemektedir.

**Anahtar Kelimeler:** L-metiyoninaz, Etoposid, Glioblastoma, Yeni nesil dizileme, Uçucu sülfür bileşikler, Çedar peyniri.

# ABSTRACT


## PRODUCTION OF L-METHIONINASE ENZYME, INVESTIGATION OF ITS ANTICARCINOGENIC PROPERTIES AND USAGE AREAS IN THE FOOD INDUSTRY

Semih Latif İPEK

Ph.D., Department of Food Engineering

Supervisor: Assoc. Prof. Dr. Dilek Göktürk

October 2023, 141 pages

In this study, L-methioninase was partially purified from *Brevibacterium linens* BL2. The specific activity of this enzyme was 3.055 units/mg. The cytotoxic properties of L-methioninase against Glioblastoma cells were evaluated. The $IC_{50}$ values of U87MG and T98G glioblastoma cell lines were found to be 5.792 units/mL and 5.215 units/mL, respectively, using a neutral red viability assay after 24 h of incubation. L-methioninase also increased the cytotoxic effect of etoposide in the same cell lines when combined. This led to a notable decrease in the viability of U87MG cells, with only 24.35% remaining compared with the control group after 48 h of incubation. Similarly, the growth of T98G cells was inhibited by both L-methioninase and etoposide compared to the control group. Following After 48-hour phase of incubation, the cellular viability decreased by 37.74% compared to that of the untreated group. Notably, the cytotoxic effects of the L-methioninase enzyme produced by *Brevibacterium linens* on Mouse Embryonic Fibroblast (MEF) cells and Human Keratinocyte Cell Line (HaCaT) cells, however, were found to be lower than those of etoposide. The combined administration of L-methioninase and etoposide resulted in an overall decrease in HaCaT cell viability to 63.02% and MEF cell viability to 58.99%. The use of staining methods such as Giemsa staining, DAPI staining, and F-actin staining enabled the direct detection of alterations in both cell population and morphology. The co-administration of L-methioninase and etoposide showed notable effectiveness in suppressing cellular migration, as evidenced by the results of a wound healing experiment. In a clonogenic experiment, the administration of L-methioninase and etoposide led to a significant decrease in the number of

colonies observed throughout the 21-day incubation period. According to the RT-qPCR results, L-methioninase caused a decrease in the expression of c-Myc and survivin genes, while simultaneously increasing the expression of Caspase-3.

This study also investigated the effects of applying L-methioninase to cheddar cheese slurries on the production of volatile sulfur compounds and cheese microbiome alteration. The cheddar slurry samples were analyzed using next-generation sequencing and GC-MS analysis. On the first day of the experiment, the samples were mostly dominated by *Lactococcus* and *Streptococcus* strains. On the ninth day, a notable augmentation in microbial diversity was found in all samples, characterized by the presence of *Limosilactobacillus, Lactobacillus, Enterococcus*, and *Lacticaseibacillus* in considerable quantities across all samples. *Lactococcus* and *Streptococcus* were the predominant species. The introduction of L-methioninase and *Brevibacterium linens* BL2 led to the formation of volatile sulfur compounds, namely, Methanethiol and Dimethyl trisulfide. During the first stage of fermentation, the L-methioninase enzyme generated a quantity of 1490.2 ± 1.31 (µg/kg dry matter) of Methanethiol and 65.8±0.04 (µg/kg dry matter) of Dimethyl trisulfide inside the cheddar slurry. The present study provides evidence supporting the possibility of L-methioninase as a promising option for food enzymes in cheddar cheese manufacturing, thus presenting substantial economic benefits.

**Keywords:** L-methioninase, Etoposide, Glioblastoma, Next-generation sequencing, Volatile sulfur compounds, Cheddar cheese.

***To my beloved family***

# ACKNOWLEDGEMENTS

First, I would like to thank my supervisor, Assoc. Prof. Dilek Göktürk, for her limitless support in my academic development and for giving me freedom and self-confidence during my work. I am also thankful to my thesis jury members, Prof. Haşim Kelebek, Prof. Aysun Şener Gedük, Prof. Osman Gülnaz, and Assoc. Prof. Yasemin Saygıdeğer, for their assistance with my thesis.

I appreciate Res. Assist. Dr. Cennet Pelin Boyacı Gündüz for her support and guidance in Applied Microbiology during my studies.

Beyond my thesis studies, I am deeply indebted to Prof. Zafer Erbay, who has always been an inspiration for me to study dairy science, for his valuable help in analyzing cheddar cheese samples. I am also thankful to Dr. Pelin Salum for helping me to evaluate the GC-MS data. I would like to thank Assist especially. Prof. Zeynep İyigündoğdu allowed me to use her microplate reader, which had a huge impact on my quality of work.

I feel so lucky because I have a team member to motivate and help during difficult times. In this respect, I acknowledge Res. Assist. Meryem Damla Özdemir Alkış for helping me every time I am in need.

I am thankful to Prof. Gözde Baydemir Peşint for obtaining a valuable laboratory work environment and supporting my academic life in the best possible way.

I would also like to thank Assoc. Prof. Hatice İmge Oktay Başeğmez, Assoc. Prof. Sibel Özdaş, Assoc. Prof. Rozelin Aydın, Assist. Prof. Mevre Çapkın Yurtsever and Assoc. Prof. Esra Göv for their valuable support during this thesis. During my studies, I urgently needed several chemicals and laboratory apparatus. In this regard, Prof. Osman Kola and Res. Assist. Erva Parıldı always provided urgent goods and chemicals if available. I appreciate their generous support.

My special thanks to my friend Barış Tansalar for his support in facilitating contact with biotechnology companies to acquire the necessary culture for my thesis. We would also like to thank Chr. Hansen and Danisco companies supply cheese cultures.

Finally, I would never be able to be successful without my family. I acknowledge that they are always with me.

This project had been supported by ATÜ Scientific Projects Unit with 21103010 and 21803002 project numbers and the TÜBITAK 2211-C Biotechnological Drugs Technology Priority Research Area Domestic Scholarship Program.

# TABLE OF CONTENTS

**CERTIFICATION OF APPROVAL** **i**
**DECLARATION OF CONFORMITY** **ii**
**ÖZET** **iii**
**ABSTRACT** **v**
***Dedication*** **vii**
**ACKNOWLEDGEMENTS** **viii**
**TABLE OF CONTENTS** **x**
**LIST OF FIGURES** **xiv**
**LIST OF TABLES** **xvii**
**LIST OF ABBREVIATIONS** **xviii**
**1. INTRODUCTION** **1**
**2. LITERATURE REVIEW** **7**
2.1. Gliomas and Glioblastoma **7**
2.2. Importance of Methionine in Cancer Metabolism **9**
2.3. L-Methioninase in Cancer Treatment **11**
2.4. L-Methioninase in the Food Industry **17**
**3. MATERIALS AND METHODS** **21**
3.1. Materials **21**
3.2. Method **22**
3.2.1. Production Procedure of L-methioninase Enyzme **22**
3.2.2. Enzyme Activity and Protein Content Analysis **23**
3.2.3. SDS-PAGE Analysis **24**
3.2.4. Methods for Investigation of Cytotoxic Effect of L-Methioninase **27**
3.2.4.1. Cell Culture Conditions **27**
3.2.4.2. Neutral Red Assay **27**
3.2.4.3. Analysis of the Cytotoxic Effect of L-Methioninase on Cancer Cells **28**

3.2.4.4. Clonogenic Assay **29**

3.2.4.5. Wound healing (Migration) Assay **30**

3.2.4.6. Giemsa Staining **30**

3.2.4.7. DAPI and F-Actin Staining **31**

3.2.4.8. RNA Isolation and cDNA Synthesis **31**

3.2.4.9. Gene Expression Analysis (RT-qPCR) **32**

3.2.5. Methods for Evaluation the Effect of the Use of L-Methioninase From *Brevibacterium linens* BL2 on Microbial Community Shift and Volatile Sulfur Compound Development **32**

3.2.5.1. Cheddar Cheese Slurry Preparation and Sampling **33**

3.2.5.2. Total Viable Bacterial Count **34**

3.2.5.3. Total Lactic Acid Bacterial Count **34**

3.2.5.4. DNA Isolation **34**

3.2.5.5. PCR and Gel Electrophoresis **35**

3.2.5.6. 16S rRNA Gene–Based Library Preparation **36**

3.2.5.7. Bioinformatics Analyses of Sequencing Data **37**

3.2.5.8. Determination of Volatile Compounds with GC-MS **38**

3.2.5.9. Statistical Analysis **39**

**4. RESULTS AND DISCUSSION** **41**

4.1. Enzyme Activity and Protein Profile of Enzyme Solution **41**

4.2. SDS-PAGE Analysis **41**

4.3. $IC_{50}$ Determination of L-Methioninase on Glioblastoma Cell Lines via Neutral red assay **42**

4.4. The Concurrent Effect of L-methioninase and Etoposide on Cell Viability **43**

4.5. Evaluation of the Effect of L-Methioninase with Etoposide on Mouse Embryonic Fibroblast (MEF) and Human Keratinocyte (HaCaT) Cells **44**

4.6. Evaluation of the Effect of L-Methioninase on the Migration Characteristics of Glioblastoma Cells **45**

4.7. Giemsa Staining of Glioblastoma Cells after L-Methioninase and Etoposide Administration **50**

4.8. DAPI and F-Actin Staining Results **52**

4.9. Clonogenic Assay Images and Colony Numbers after L-methioninase and Etoposide Administration **53**

4.10. RT-qPCR Results **56**

4.11. Results for evaluation of the effect of the use of L-Methioninase from *Brevibacterium linens* BL2 on microbial community shift and volatile sulfur compound development in raw milk Cheddar cheese slurries **59**

4.11.1.Evaluation of total viable bacterial count and total lactic acid bacterial count **59**

4.11.2. PCR and Gel Electrophoresis **61**

4.11.3. Next Generation Sequences Analyses **61**

4.11.4. Principal Component Analysis (PCA) assessment of 1st day and 9th day of fermentations between samples **74**

4.11.5. Principal Coordinate Analysis (PcoA) Assessment of Samples with Weighted Unifrac Analysis and Bray-Curtis Analysis (Beta Diversity) **76**

4.11.6. Similarity Analysis Using Dendrogram **77**

4.11.7. Cladogram of Genus for 1 and 9 Days of Fermentation Between Samples **80**

4.11.8. Taxonomy, LDA score and Cladogram of Sample a (control slurry) **81**

4.11.9.Taxonomy, LDA score and Cladogram of Sample b (control slurry and methionine) **85**

4.11.10.Taxonomy, LDA score and Cladogram of Sample c (control slurry + methionine + *Br. linens* BL2) **86**

4.11.11.Taxonomy, LDA score and Cladogram of Sample d (control slurry + methionine + L-methioninase) **103**

4.11.12. GC-MS Analysis Results **109**

**5. CONCLUSION** **121**

**6. RECOMMENDATIONS** **123**

**REFERENCES** **124**

**VITA** **141**

# LIST OF FIGURES

**Figure 3.1.** The thermal cycler program for amplification 36
**Figure 4.1.** Bands observed through SDS-PAGE 41
**Figure 4.2.** $IC_{50}$ graph for U87MG cell line 42
**Figure 4.3.** $IC_{50}$ graph for T98G cell line 42
**Figure 4.4.** The cytotoxicity analysis for U87MG cells 43
**Figure 4.5.** The cytotoxicity analysis for T98G cells 44
**Figure 4.6.** Cytotoxicity analysis for MEF, HaCat, U87MG and T98G cells 45
**Figure 4.7.** Wound closure status of U87MG cells over 24 h 46
**Figure 4.8.** The wound closure status of T98G cells over 24 h 46
**Figure 4.9.** Wound area change in U87MG cells 47
**Figure 4.10.** Average wound width change in U87MG 47
**Figure 4.11.** Cell migration rate for U87MG cells 48
**Figure 4.12.** Wound area change for T98G cells 49
**Figure 4.13.** Average wound width change for T98G cells 49
**Figure 4.14.** Cell migration rate for T98G cells 50
**Figure 4.15.** Giemsa staining images of U87MG cells 51
**Figure 4.16.** Giemsa staining images of T98G cells 51
**Figure 4.17.** Normal photos of U87MG cells 51
**Figure 4.18.** Normal photos of T98G cells 51
**Figure 4.19.** DAPI and F-actin staining images of U87MG cells 52
**Figure 4.20.** DAPI and F-actin staining of T98G cells 53
**Figure 4.21.** Colonies of U87MG cells at the end of 21 days 54
**Figure 4.22.** Colony number of U87MG cells at the end of 21 days 54
**Figure 4.23.** Colonies of T98G cells at the end of 21 days 55
**Figure 4.24.** Colony number of T98G cells 55
**Figure 4.25.** The relative expression of Survivin (**a**), C-myc (**b**), Caspase-3 (**c**) 58
**Figure 4.26.** Total Viable Bacteria Count in Cheddar Cheese Slurries during nine days fermentation. Values on the graph are the mean of triplicate measurements 60

**Figure 4.27.** Lactic Acid Bacteria Count in Cheddar Cheese Slurries during nine days fermentation. Values on the graph are the mean of triplicate measurements 60
**Figure 4.28.** Electrophoresis image. The running amplicons from cheese slurry samples, which appear as intense bands 61
**Figure 4.29.** Percent abundance comparison of bacteria species between samples for Sample a 62
**Figure 4.30.** Variation in the bacterial population distribution over time in sample a 62
**Figure 4.31.** Percent abundance comparison of Bacteria species at different days for sample b 64
**Figure 4.32.** Variation in the bacterial population distribution over time in sample b 65
**Figure 4.33.** Percent abundance comparison of Bacteria species at different days for sample c 66
**Figure 4.34.** Variation in the bacterial population distribution over time in sample c 67
**Figure 4.35.** Percent abundance comparison of Bacteria species at different days for sample d 68
**Figure 4.36.** Variation in the bacterial population distribution over time in sample d 69
**Figure 4.37.** Percent abundance comparison of Bacteria species at day 1 70
**Figure 4.38.** Variation in the bacterial population distribution over time in samples at day 1 71
**Figure 4.39.** Percent abundance comparison of Bacteria species at day 9 72
**Figure 4.40.** Variation in the bacterial population distribution over time in samples at day 9 73
**Figure 4.41.** 2-Dimension PCA analysis of samples by all data at 1st day 74
**Figure 4.42.** 2-Dimension PCA analysis of samples by all data at 9th day 75
**Figure 4.43.** 3-Dimension PCA analysis of samples by all data at 1st day 75
**Figure 4.44.** 3-Dimension PCA analysis of samples by all data at 9th day 76
**Figure 4.45.** Beta diversity of 1 and 9 days of fermentation with Weighted Unifrac and Bray-Curtis Analysis 77
**Figure 4.46.** Similarity distance of samples by OTU at 1 day of fermentation 78
**Figure 4.47.** Similarity distance of samples by OUT at 9 days of fermentation 79
**Figure 4.48.** Genus Cladogram of 1 day of fermentation of samples 80
**Figure 4.49.** Genus Cladogram of 9 day of fermentation of samples 81
**Figure 4.50.** LDA score of genus in sample a (control slurry) 84

**Figure 4.51.** Genus cladogram of genus in sample a (control slurry) 85
**Figure 4.52.** Genus cladogram of genus in sample b (control slurry and methionine) 86
**Figure 4.53a.** Detailed information of sample b (control slurry and methionine) 92
**Figure 4.53b.** Detailed information of sample b (control slurry and methionine) 93
**Figure 4.53c.** Detailed information of sample b (control slurry and methionine) 94
**Figure 4.53d.** Detailed information of sample b (control slurry and methionine) 95
**Figure 4.53e.** Detailed information of sample b (control slurry and methionine) 96
**Figure 4.54.** Genus cladogram of sample c (control slurry + methionine + *Br. linens* BL2) 96
**Figure 4.55a.** LDA score of sample c (control slurry + methionine + *Br. linens* BL2) 101
**Figure 4.55b.** LDA score of sample c (control slurry + methionine + *Br. linens* BL2) 102
**Figure 4.55c.** LDA score of sample c (control slurry + methionine + *Br. linens* BL2) 103
**Figure 4.56a.** LDA score of sample d (control slurry + methionine + L-methioninase) 107
**Figure 4.56b.** LDA score of sample d (control slurry + methionine + L-methioninase) 108
**Figure 4.57.**Genus cladogram of sample d (control slurry + methionine + L-methioninase)109
**Figure 4.58.** Methanethiol and dimethyl Trisulfide amount change in time between samples 117

# LIST OF TABLES

**Table 3.1**. Experimental Design 33

**Table 3.2**. Universal 16S primer sequences used in long read platforms 35

**Table 4.1.** Bacterial population distribution of Sample a at 1 day and 9 day with control sample 82

**Table 4.2.** Detailed information of microbial community of sample b 87

**Table 4.3.** Species in sample c detected by next generation sequencing 97

**Table 4.4.** Species in sample d detected by next generation sequencing 104

**Table 4.5.** Volatile compound profile of cheddar cheese slurry at time zero 110

**Table 4.6.** Volatile compound profile of cheddar cheese slurry at 1 day incubation 111

**Table 4.7.** Volatile compound profile of cheddar cheese slurry at 4 days incubation 113

**Table 4.8.** Volatile compound profile of cheddar cheese slurry at 9 days incubation 115

# LIST OF ABBREVIATIONS

| | |
|---|---|
| SAM | : S-Adenosylmethionine |
| SSF | : Solid State Fermentation |
| SmF | : Submerged Fermentation |
| SDS-PAGE | : Sodium Dodecyl-Sulfate Polyacrylamide Gel Electrophoresis |
| 5MTHF | : 5-Methyltetrahydro-Folic Acid |
| PLP | : Pyridoxal-5′-Phosphate |
| PCA | : Plate Count Agar |
| GC | : Gas Chromatography |
| GC-MS | : Gas Chromatography-Mass Spectrometry |
| ANOVA | : Analysis of Variance |

# 1. INTRODUCTION

Every year, a significant number of individuals experience the unfortunate outcome of cancer-related mortality or endure the arduous process of intensive treatment. Despite the considerable financial burden associated with cancer therapy, there is a pressing need to explore novel pharmaceutical agents owing to challenges such as the emergence of medication resistance. In the field of cancer biology, researchers have noted that some cancer cells, referred to as 'methionine-dependent,' have a pronounced need for an external supply of the essential amino acid methionine to facilitate their growth and reproduction. The deprivation of methionine in methionine-dependent cancer cells may induce a malfunction in their protein synthesis apparatus, decelerating the essential cellular processes necessary for their survival. The absence of methionine interrupts protein synthesis, which impedes the proliferation and function of cancer cells at their maximum potential. Consequently, this induces cellular stress that may potentially result in cell death. These phenomena have sparked scientific inquiry into the therapeutic capacity of methionine restriction as a tactic to selectively impede the proliferation of certain cancer cell subtypes. One method of methionine restriction is the application of a methioninase enzyme. One such promising candidate is L-methioninase, which has the potential to augment the antiproliferative properties of chemotherapeutic drugs, consequently reducing the treatment duration for patients. This is accomplished by inhibiting the proliferation of cancer cells in methionine-dependent cancer subtypes and facilitating apoptosis.

L-methioninase (E.C.4.4.1.11) is an enzyme that catalyzes the α- and γ-elimination of the amino acid L-methionine when pyridoxal phosphate coenzyme is present. This enzymatic process leads to the decomposition of l-methionine into α-ketobutyrate, methanethiol, and ammonia (Tanaka et al., 1977). The inhibitory effects of the methioninase enzyme, initially derived from Clostridium sporogenes, on the proliferation of Walker carcinosarcoma cells in mice were first documented by Kreis and Heisson in 1973. This enzyme has various designations, including methionine-gamma-lyase, methioninase, methionine lyase, and methionine demethylase (Suganya et al., 2017).

In recent years, there has been significant interest in exploring the potential of L-methioninase enzyme for the treatment of various cancers (Tan et al., 1996). Unlike normal cells, cancer cells are unable to synthesize functional methionine, leading to the acquisition of methionine from extracellular sources (Hoffman, 1984). The reliance of cancer cells on methionine has paved the way for a potential treatment approach involving the use of the methionase enzyme. This strategy aims to induce death of cancer cells by enzymatically breaking down methionine, thereby impeding their proliferation, growth, and vital functions (Epner et al., 2003; Lu & Epner, 2000).

Previous research has revealed that while the absence of methionine due to enzymatic breakdown allows normal cells to maintain the cell cycle, even in the presence of homocysteine, it results in cell death in most cancer cells. This distinction arises because regular cells do not require methionine for their function, whereas many cancer cells rely heavily on methionine for their metabolic processes (Mecham et al., 1983). This reliance on methionine is due to the inactivity or insufficiency of the enzyme methionine synthase in cancer cells, which prevents them from producing methionine within their environment containing homocysteine (El-Sayed, 2010).

The remarkable specificity of L-methioninase towards cancer cells, while sparing normal cells, establishes methionine as a unique therapeutic target in cancer therapy protocols. L-methioninase is administered for therapeutic purposes to induce methionine breakdown in the plasma, leading to methionine deprivation, specifically in cancer cells. As suggested by Yoshioka et al. (1998), utilizing L-methioninase in catabolic processes presents a promising avenue for advancing alternative therapeutic strategies in the field of cancer therapy. This approach is driven by the fact that traditional chemotherapeutic agents, while targeting cancer cells, also affect normal cells, resulting in adverse side effects (De Vita et al., 1993).

In recent years, there has been significant emphasis on investigating the sources of the L-methioninase enzyme, driven by a growing recognition of its importance. L-methioninase has been identified in various organisms, including bacteria, fungi, plants, and protozoa. Owing to the limited availability of enzymes in plants and the complexities associated with their extraction, researchers have shifted their focus toward producing methionase enzymes derived

from bacteria and fungi. This has been achieved using various microbial fermentation and extraction techniques (Khalaf and El-Sayed, 2009).

As outlined by Suganya et al. (2017), the establishment of a sustainable enzyme production system can be achieved by optimizing the conditions for maximal enzyme production, considering the specific characteristics of the microorganisms involved. Extraction of microbial L-methioninase typically involves conventional purification techniques. Suganya et al. (2017) provided a comprehensive overview of the manufacturing processes involved in the production of methionine enzymes.

When L-methioninase is generated externally by the microorganism in which it resides, the enzyme present in the fermentation medium is extracted using a preprepared buffer solution. The crude enzyme solution can be separated via precipitation using chemicals, such as ammonium sulfate. Further purification techniques, such as gel filtration and ion-exchange chromatography, may be employed to refine the sample.

Glioblastoma is a type of brain neoplasm characterized by the presence of star-shaped cells, including astrocytes, oligodendrocytes, microglia, ependymal cells, and a subset of cancer stem cells, localized within the tissue. Glioblastoma tumors have the capacity to autonomously generate their own vascular network, endowing them with a heightened propensity for proliferation and infiltration into healthy cerebral tissues. Despite the implementation of enhanced treatment approaches and an upsurge in experimental investigations, glioblastoma continues to be fundamentally refractory, exhibiting an average survival duration of 12–18 months and a meager long-term survival rate of less than 5% beyond five years post-diagnosis (D'Alessio et al., 2019). Therefore, the importance of advancing the discovery of novel pharmaceutical interventions for glioblastoma can cannot be overstated.

Deoxyribonucleic acid (DNA) topoisomerases play a key role in the regulation of DNA structure by inducing transient DNA strand breaks. These molecules are essential components of fundamental biological processes, including DNA replication, transcription, maintenance, and chromatin remodeling. There are two distinct categories of topoisomerases, specifically

referred to as type II and type I topoisomerases. Topoisomerase type II, also known as TopoII, induces breaks in double-stranded DNA. Etoposide is a chemotherapeutic agent commonly used in the treatment of cancer. The mechanism of action involves the specific targeting of TopoII activities, thereby impeding the reconnection of DNA strands and subsequently impacting several facets of cellular metabolism. Montecucco et al. (2015) showed that etoposide has a notable affinity for chromatin and histones, in addition to its well-established effect on TopoII.

Cheddar cheese is widely produced and consumed in English-speaking countries, such as the USA, the UK, and Canada. Its popularity is also increasing in western nations and other regions globally (Gosalvitr et al. 2019). Cheese is a sophisticated biological environment containing a wide range of microbial communities (De Filippis et al., 2016). The significance of these microbial communities is their ability to provide sensory and physicochemical information to cheese (Afshari et al., 2020). Next-generation sequencing (NGS) is a contemporary methodology used to enhance the understanding and characterization of the microbiota present in cheese ecosystems (Erhardt et al., 2023). This process facilitates the examination of microbial populations during cheese manufacturing and ripening stages (Dreier et al., 2022). Methionine metabolism leads to the synthesis of methanethiol, a highly sought-after taste compound in cheddar cheese (Dias, 1999). In the literature, methanethiol has often been linked to the development of the distinct taste found in mature cheddar cheese. It is worth noting that the ripening process of cheddar cheese typically spans several months (Aston, 1981).

The current study involved administration of L-methioninase to T98G and U87 MG glioma cells. The L-methioninase used in this study was derived from the bacterial *Brevibacterium linens* BL2 through partial isolation. To assess the combined effect of the enzyme and etoposide, a range of methodologies, including neutral red cell vitality assessments, wound healing experiments, colony formation tests, reverse transcription quantitative polymerase chain reaction (RT-qPCR) investigations focusing on apoptotic genes such as Caspase-3, survivin, and c-myc, as well as DAPI, F-actin, and Giemsa labeling tests, were employed. Furthermore, in this study focusing on cheese flavor and aroma profiles, the incorporation of L-methioninase into cheddar cheese slurries accelerated the production of sulfur compounds.

Next-generation sequencing was employed to assess the bacterial composition of cheddar cheese slurries.

The investigation proceeded by conducting a comprehensive analysis of the existing literature regarding the association of the L-methioninase enzyme with cancer and its applications within the food sector. The Materials and Methods section explains the steps used to achieve the objectives of this study. The primary outcomes of this investigation are defined in the Results and Discussion sections. Finally, the investigation concludes by presenting the findings and offering recommendations.

# 2. LITERATURE REVIEW

## 2.1. Gliomas and Glioblastoma

Glioma is a neuroectodermal tumor that originates in the Central Nervous System (CNS). Globally, it accounts for approximately 2.5% of all cancer-related deaths. Gliomas are the most prevalent neoplasms among pediatric populations, although they are predominantly observed in individuals aged 55 years. Notably, tumors are the third leading cause of cancer-related mortality among individuals aged 15–34 years. Unfortunately, there has been a consistent upward trend in the incidence of these neoplastic growths over the past three decades.

Gliomas, comprising nearly 80% of all brain cancers, are derived from the ependymal, oligodendroglial, and astrocytic cells. Although all gliomas originate from neuroepithelial tissue, there are significant variations in terms of their age at onset, severity, histological characteristics, and potential for growth and metastasis (Behnan et al., 2019; Ohgaki & Kleihues, 2005; Silantyev et al., 2019; Sontheimer, 2008).

Gliomas are categorized into four major classes (I-IV) by the World Health Organization (WHO) based on their histological features, including factors such as cellularity, mitotic patterns, necrosis, and vascular proliferation. These classifications also consider the astrocytic and oligodendroglial phenotypes.

- Grade I gliomas are characterized by pilocytic astrocytomas, which typically affect individuals in their youth.
- Grade II gliomas encompass oligodendrogliomas and astrocytomas, including mixed oligoastrocytomas.
- Grade III gliomas consist of anaplastic astrocytomas and anaplastic oligodendrogliomas.
- Grade IV gliomas are dentified as glioblastoma.

These four primary categories serve as indicators of tumor aggressiveness and are generally associated with a poorer prognosis than oligodendrogliomas of the same grade. Glioblastoma, which is classified as a grade IV glioma, is the most malignant form of glioma (Behnan et al., 2019; Shapiro & Shapiro, 1998).

Glioblastoma (GBM) originates from abnormal astrocytes and other glial cells, and is the predominant and most aggressive form of glioma observed in adults. It accounts for approximately 60% of all primary brain tumors and affects individuals across a broad age range, with a higher incidence observed among those aged 55–64 years. While the worldwide incidence rate of glioblastoma (GBM) is relatively low (less than six cases per 100,000 individuals), it has an extremely unfavorable prognosis and contributes to approximately 2.5% of cancer-related deaths (Lenin et al., 2021; Qiu, Shi, & Jiang, 2017; Yeo, Brown, Gargett, & Ebert, 2021). Notably, the incidence of GBM is higher in men than in women, with a ratio of 1.6:1. Similarly, Caucasians have a higher susceptibility to GBM than other racial groups, as indicated by Di Filippo De Araújo, and Chorilli (2021) and Hanif, Muzaffar, Perveen, Malhi, and Simjee (2017).

Typical manifestations of GBM include headaches, nausea, vomiting, visual field abnormalities, impaired vision, memory deficits, urine incontinence, cognitive impairments, alterations in personality, and seizures, which occur in approximately 25% of cases. Moreover, as GBM progresses, patients experience rapid loss of consciousness (Di Filippo et al., 2021; Hsu et al., 2021; Qiu et al., 2017).

The symptoms exhibited by individuals with GBM primarily depend on the extent of brain tissue damage and the size and location of the tumor. Necrosis within the affected brain tissue contributes to presenting symptoms, such as cognitive impairments and localized neurological deficits, affecting approximately 40–60% of individuals. Symptoms may vary based on the region of the brain affected by the tumor. For example, individuals with tumors in the temporal lobe may encounter challenges related to visual and auditory function. In contrast, patients with frontal lobe tumors may exhibit cognitive deficits and personality changes, with an occurrence rate ranging from 20% to 40%. The presence of a large tumor can lead to gait imbalance and incontinence. Additionally, as tumor size increases and edema around the tumor expands, intracranial pressure rises, resulting in headaches, a prevalent symptom experienced by approximately 30–50% of patients diagnosed with GBM (Hanif et al., 2017).

## 2.2. Importance of Methionine in Cancer Metabolism

Methionine is an essential amino acid that plays a crucial role in various mammalian metabolic processes. It is involved in key metabolic events such as protein synthesis, DNA methylation, and polyamine synthesis (Cavuoto and Fenech, 2012). Methionine is absorbed through digestion of dietary proteins in the small intestine and serves as a fundamental component of protein synthesis (Chaturvedi et al., 2018). In every cell, methionine undergoes catabolism, participates in protein synthesis, and contributes to the de novo pathway, where it is converted to S-adenosylmethionine (SAM), which is the primary methyl donor (Bolander-Gouaille and Bottiglieri, 2003; Cavuoto and Fenech, 2012; Chaturvedi et al., 2018). SAM is then converted to S-adenosylhomocysteine (SAH) during DNA and other protein methylation processes (Cavuoto and Fenech, 2012; Chaturvedi et al., 2018; Zingg and Jones, 1997). Subsequently, SAH undergoes degradation into homocysteine (Hcy), which is further metabolized through the trans-sulfuration or methylation pathways (Bolander-Gouaille and Bottiglieri, 2003; Chaturvedi et al., 2018).

Under normal physiological conditions, approximately 50% of Hcy is remethylated in most tissues via the enzymatic activity of methionine synthase (5-methyltetrahydrofolate-homocysteine methyltransferase, MTR), utilizing vitamin B12 (methylcobalamin) and 5-methyltetrahydrofolate (5-MTHF) as cofactors (Cavuoto and Fenech, 2012; Chaturvedi et al., 2018). Hcy can also be converted to methionine by the betaine-homocysteine S-methyltransferase enzyme found in the liver (Cavuoto and Fenech, 2012; Chaturvedi et al., 2018; Sunden et al., 1997). In the trans-sulfuration pathway, Hcy is converted to cystathionine, a precursor of cysteine. Cysteine is used to synthesize glutathione, which protects cells from oxidative stress by reducing reactive oxygen species (Adeoye et al., 2018; Anderson, 1998; Cavuoto and Fenech, 2012). Additionally, it is involved in the synthesis of polyamines that are effective for cell proliferation, such as spermine, spermidine, and putrescine, in the SAM salvage pathway (Cavuoto and Fenech, 2012; Soda, 2018; Thomas and Thomas, 2001).

Cancer is the leading cause of mortality globally, accounting for approximately 10 million deaths in 2020 alone (Ferlay et al., 2020). Despite the production of numerous chemotherapeutic agents for cancer treatment, their application remains limited due to factors

such as adverse effects on normal human cells, emergence of drug resistance in cancer tissues, and limited selectivity of drugs for target tissues (Majolo et al., 2019; El-Sayed, 2010; Prakash et al., 2013; De Vita et al., 1993). Methionine addiction, a prevalent metabolic anomaly observed in cancer cells, has emerged as a promising therapeutic target in cancer treatment (Chaturvedi and Bertino, 2019; Hoffman, 2019; Kawaguchi et al., 2019). The Hoffman effect, as it is termed, stems from the cancer cells' reliance on the amino acid methionine for their proliferation and dissemination, along with their engagement in transmethylation reactions (Han et al., 2020; Hoffman, 2015; Higuchi et al., 2020).

Remarkably, it has been ascertained that specific types of cancer are unable to grow and ultimately die in methionine-depleted environments (Stern et al., 1984). Perturbation of methionine metabolism is widely recognized as a hallmark of cancer (Hoffman, 2015; Stern et al., 1984). Limiting methionine availability within the cancer cell milieu induces cell cycle arrest during the late S/G2 phase, thereby increasing the sensitivity of cancer cells to chemotherapeutic agents during this phase (Kawaguchi et al., 2019).

Limited levels of methionine synthase in specific cancer cells have been linked to the development of methionine addiction in these cells (Chaturvedi et al., 2018; Kenyon et al., 2002). Furthermore, rapid proliferation necessitates an increased demand for methionine, resulting in cells resorting to external sources to meet their methionine requirement. Mutations in the methylenetetrahydrofolate reductase enzyme exacerbate methionine dependence by affecting the synthesis of 5-methyltetrahydrofolate, a crucial substrate in methionine biosynthesis (Chaturvedi et al., 2018). In contrast, normal human cells are capable of converting homocysteine to methionine in the absence of exogenous methionine. This conversion is catalyzed by the methionine synthase enzyme, with cobalamin and 5-methyltetrahydrofolic acid (5MTHF) serving as cofactors (Epner et al., 2003). It has been observed that methionine-dependent cancer cells experience growth inhibition, a significant halt in mitosis, and eventual cell death when subjected to methionine deficiency in their environment or when methionine is replaced with homocysteine (Hu and Cheung, 2009).
Methionine addiction, observed in some select cancer cells, has designated the amino acid methionine as a promising therapeutic target (Cavuoto and Fenech, 2012). This approach is primarily executed through the dietary restriction of methionine. The concentration of

methionine in the blood plasma diminishes when people consume methionine-depleted foods. It has been demonstrated that restricting dietary methionine not only exerts an inhibitory effect on cancer, but also positively influences the deceleration of the aging process (Cavuoto and Fenech, 2012; Kitada et al., 2021). However, the presence of methionine in a wide range of foods limits the effectiveness of a complete methionine-free diet. Therefore, L-methioninase has emerged as a pivotal pharmaceutical agent for reducing methionine levels in bodily fluids (Cavuoto and Fenech, 2012). This enzyme catalyses the breakdown of methionine into alpha-ketobutyrate, methanethiol, and ammonia. Initial observations, dating back to 1973, revealed that L-methioninase derived from Clostridium sporogenes halted the growth of Walker carcinosarcoma cells in mice (Kreis and Heisson, 1973).

With the advent of recombinant technology, L-methioninase enzymes from *Pseudomonas putida*, which possess a low Michaelis constant (Km), have been widely used (Hori et al., 1996; Hoffman et al., 2019). Recombinant L-methioninase has shown promising inhibition in preclinical in vivo studies involving Yoshida sarcoma (a rat sarcoma cell line) and H460 human lung cancer mouse tumor models (Tan et al., 1996).

The clinical potential of recombinant methioninase in cancer treatment was assessed in phase 1 trials involving patients with advanced cancer, resulting in a reduction of methionine levels in blood plasma without any severe adverse effects. To mitigate potential allergic reactions and extend its half-life, methioninase was conjugated to polyethylene glycol (Hoffman et al., 2019).

### 2.3. L-Methioninase in Cancer Treatment

Methionine is an essential amino acid that plays a pivotal role in multiple metabolic processes in mammals including protein synthesis, DNA methylation, and polyamine production (Cavuoto & Fenech, 2012). Methionine absorption occurs during protein digestion in the small intestine and subsequently contributes to various protein synthesis pathways (Chaturvedi et al., 2018). Methionine undergoes catabolism in all cells and participates in both protein synthesis and the de novo route, where it is transformed into S-adenosylmethionine (SAM), a crucial methyl donor (Bolander-Gouaille and Bottiglieri, 2003; Cavuoto and Fenech, 2012; Chaturvedi et al., 2018).

In the field of biotechnology, bacterial enzymes have gained significant attention owing to their effectiveness in enhancing various industrial biochemical processes. L-methioninase is an illustrative example of a bacterial enzyme with potential applications. El-Sayed (2009) employed solid-state fermentation, using agricultural industrial waste as a substrate, to produce L-methioninase from Aspergillus flavipes. The introduction of different externally supplied vitamins into the fermentation medium had limited effects on L-methionine production. Khalaf and El-Sayed (2009) investigated 21 fungal isolates from eight different genera to target L-methionine through submerged fermentation; Aspergillus flavipes displayed the highest methioninolytic activity. Optimal L-methioninase production occurred when l-methionine and glucose were employed.

To enhance the therapeutic potential of L-methioninase, researchers have explored its application in cancer treatment to enhance the therapeutic potential of l-methioninase. Selim et al. (2015a) assessed L-methioninase as a therapeutic agent against different tumor cell lines, noting its stability across a wide range of pH levels and temperatures. In vitro studies have demonstrated significant anti-cancer efficacy against multiple cell lines. Selim et al. (2015b) investigated the extracellular production of L-methioninase by 60 Streptomyces species using a fast-plate assay, highlighting successful production.

Abu-Tahon and Isaac (2016) evaluated the production of alkaline L-methioninase by 24 fungal species through solid-state fermentation, using various agro-industrial wastes as substrates. Aspergillus ustus, in particular, exhibited significantly higher L-methioninase production via solid-state fermentation than via submerged fermentation under optimal conditions. Al-Zahrani and Bukhari (2019) collected bacterial isolates from marine samples in Saudi Arabia to assess their capacity to produce L-methioninase.

According to the findings of Salim, Santhiagu, and Joji (2019), Trichoderma harzianum, an L-methioninase-producing fungus, was identified as a highly effective organism. This fungus was isolated from soil samples during the study. The enzyme was purified and displayed an apparent molecular mass of 48 kDa when analyzed by Sodium Dodecyl Sulfate-Polyacrylamide Gel Electrophoresis (SDS-PAGE). In a separate study conducted by Mohkam

et al. (2020), the synthesis of L-methioninase derived from Alcaligenes spp was successfully demonstrated. Baghdadi and Danial (2022) evaluated the capacity of a bacterial isolate to generate L-methioninase through solid-state fermentation techniques utilizing a variety of organic byproduct residues as substrates.

The utilization of L-methioninase (EC 4.4.1.11) has been investigated as a prospective therapeutic strategy for various malignancies, including glioblastoma and kidney, breast, lung, and colon cancer (Baghdadi and Danial, 2022). L-methioninase exhibits significant promise in the field of cancer therapy and is currently undergoing clinical trials as a biotechnologically derived pharmaceutical agent, as reported by Hoffman et al. (2019).

Cancer is a significant global health challenge, accounting for approximately 10 million deaths by 2020 (Ferlay et al., 2020). Despite the availability of a wide range of chemotherapeutic drugs for cancer treatment, their effectiveness is often limited by their adverse effects on healthy cells, development of drug resistance in cancerous tissues, and inability to specifically target cancer cells specifically (Majolo et al., 2019; El-Sayed, 2010; Prakash et al., 2013; De Vita et al., 1993).

One promising avenue in cancer therapy is the concept of methionine dependency, which is a common metabolic abnormality in cancer cells (Chaturvedi and Bertino, 2019; Hoffman, 2019; Kawaguchi et al., 2019). The Hoffman effect, characterized by the increased consumption of the amino acid methionine by cancer cells, plays a crucial role in cancer cell growth and proliferation owing to its involvement in transmethylation reactions. This phenomenon has been extensively studied in various studies, including those conducted by Han et al. (2020), Hoffman (2015), and Higuchi et al. (2020).

Stern et al. (1984) demonstrated that many cancer types are unable to proliferate or undergo apoptosis when deprived of methionine, which affects the survival and growth of cancer cells. This altered methionine metabolism has been recognized as a common feature of cancer, making it a potential target for therapeutic investigations (Hoffman, 2015; Stern et al., 1984). Kawaguchi et al. (2019) further elucidated that inhibiting methionine in the cancer cell environment halts the cell cycle of cancer cells in the late S/G2 phase. This disruption renders

cancer cells more vulnerable to the effects of chemotherapeutic drugs. Previous studies have established a compelling link between diminished levels of methionine synthase in certain cancer cells and their heightened dependence on methionine as a critical nutrient. This reduced methionine synthase activity effectively hampers the methionine cycle in these cells. Consequently, these cancer cells have gradually intensified their reliance on exogenous methionine sources to sustain themselves. Notably, cancer cells scavenge methionine from the bloodstream, making it a vital resource for their survival. Depleting methionine levels effectively starves these cancer cells of this essential nutrient, eventually leading to their death. In contrast, normal human cells can endure and function adequately, even in conditions where blood serum methionine levels are insufficient to meet their metabolic demands (Chaturvedi et al., 2018; Kenyon et al., 2002).

Moreover, rapid proliferation of tumor cells increases the demand for methionine. Due to insufficient endogenous methionine synthesis, an organism must meet its methionine requirements from the external environment. Chaturvedi et al. (2018) reported that mutations in the methylene tetrahydrofolate reductase enzyme result in an increased dependency on methionine because of its role in the production of 5-methyl tetrahydrofolate, a critical precursor in methionine synthesis. Epner et al. (2003) reported that human cells could convert homocysteine to methionine in the absence of exogenous methionine. Methionine synthase facilitates this conversion and requires the presence of cobalamin and 5-methyltetrahydro-folic acid. (5MTHF). Previous research has demonstrated that methionine-dependent cancer cells undergo growth arrest, a substantial decrease in mitotic activity, and ultimately cell death when exposed to methionine deprivation or replacement of methionine with homocysteine (Hu & Cheung, 2009).

Therapeutic targeting of methionine amino acids has been driven by the observed reliance on methionine in certain cancer cells (Cavuoto & Fenech, 2012). This approach is primarily implemented through dietary restrictions on the methionine intake. Consumption of methionine-deficient diets results in decreased methionine levels in the blood plasma. Previous studies have demonstrated that limiting dietary methionine has a beneficial effect on delaying aging and suppressing cancer (Cavuoto & Fenech, 2012; Kitada et al., 2021). Including methionine in various dietary sources helps to mitigate the consequences associated

with a methionine-deficient diet. Consequently, L-methioninase has been recognized as a significant pharmacological agent for reducing methionine levels in bodily fluids (Cavuoto & Fenech, 2012).

Hori et al. (1996) successfully cloned and expressed an L-methioninase gene derived from Pseudomonas putida. The implications of their results suggest that the suppression of cell development may be influenced not only by the depletion of l-methionine and its precursors, as previously ascribed, but also by the depletion of l-cysteine. Furthermore, the findings of in vitro cell growth inhibition indicated that leukemia cell lines exhibit high sensitivity to L-methioninase. Therefore, it can be inferred that L-methioninase holds potential as a viable therapeutic option for the treatment of leukemia.

Kokkinakis et al. (1997) investigated the effects of dietary and pharmacological treatments on plasma methionine concentration. The authors outlined strategies for regulating both plasma and tumor methionine levels, while preserving the concentrations of cysteine, glutathione, and homocysteine, which are biochemically linked to methionine and play a pivotal role in cancer progression. Their results revealed a significant association between the availability of plasma methionine and the proliferation of human malignancies in mice serving as hosts.

Peron et al. (2003) demonstrated that MCF-7 breast cancer cells are methionine-dependent. Additionally, the fusion protein showed specific affinity for urokinase receptors located on the surface of these cancer cells. This study indicated that the fusion protein of ATF-methioninase, specifically the amino-terminal fragment consisting of amino acids 1-49, can inhibit the proliferation and migration of human breast cancer cells.

Palwai et al. (2007) conducted a comparative analysis of the effects of the ATF-methioninase fusion protein on two different cell lines, SK-LU-1 lung cancer and PC-3 prostate cancer. This analysis involved comparing the outcomes with those of a fusion protein containing a mutated form of methioninase as well as the effects of L-methioninase alone. According to Palwai et al. (2009), the fusion protein exhibited a significantly stronger inhibitory effect than both L-methioninase alone and the mutant fusion protein. Furthermore, the fusion protein had

a greater inhibitory effect on ovarian cancer cell lines than on normal, non-cancerous cells of similar kind.

Van Rite et al. (2011) demonstrated that the administration of an enzyme prodrug therapy, specifically using the L-methioninase-annexin V fusion protein and selenomethionine as the prodrug, resulted in the potential eradication of both endothelial and cancer cells. This treatment was administered for more than three days.

El-Sayed et al. (2012) demonstrated that l-methioninase has enhanced therapeutic characteristics, including an extended half-life, a reduced pyridoxal-5′-phosphate (PLP)-dissociation ratio, a sustained absence of plasma methionine for approximately 17 h, and less antigenicity.

The research conducted by Van Rite et al. (2013) focused on the development of a novel compound, L-methioninase-annexin V FP, with the specific purpose of targeting and binding to tumor vasculature. The findings of this study indicate that the administration of enzyme prodrug therapy targeting the tumor vasculature resulted in a significant reduction in the growth of MDA-MB-231 breast tumors throughout the course of an 11-day treatment period.

According to Guillen et al. (2014), the use of enzyme prodrug complexes, including L-methioninase-annexin V and purine nucleoside phosphorylase-annexin V, has been proposed as a potential therapeutic option because of their strong affinity for prostate cancer cells and effective induction of apoptosis.

Hassabo et al. (2019) successfully synthesized a metal-organic framework (MOF), UiO-66-COOH, which is based on zirconium. The yeast species Wickerhamomyces was used to isolate and purify L-methioninase. A composite material was synthesized by combining L-methioninase with UiO-66–(COOH). In the in vivo experiments, the composite was administered to mice with tumors, and the findings demonstrated a significant deceleration in tumor development among the treated animals.

According to Salim et al. (2020), the efficacy of l-methioninase derived from Trichoderma harzianum was shown in combination with cancer cell lines, as seen in both in vitro and in vivo experimental settings. Human hepatocarcinoma (Hep-G2) and human breast carcinoma (MCF7) cell lines were subjected to various doses of the enzyme, revealing the antiproliferative effect of L-methioninase in both cell lines.

The anti-proliferative effect of l-methioninase was observed in both MCF7 and Hep-G2 cell lines. In a study conducted by Kavya and Nadumane (2023a), significant levels of l-methioninase activity were observed in Methylobacterium sp. JUBTK33, a recently discovered bacterium.

Furthermore, a study conducted by Kavya and Nadumane (2023b) aimed to investigate the impact of a unique combination of tamoxifen and the semi-purified methioninase enzyme on both in vitro breast cancer cell culture and in vivo breast cancer mice models.

### 2.4. L-Methioninase in the Food Industry

Enzymes, which may be extracted from cellular sources and used to accelerate several commercially relevant processes, are biological catalysts, sometimes referred to as biocatalysts, that enhance the rate of biochemical reactions inside live organisms (Robinson, 2015). Enzymes exhibit diverse actions throughout several domains of daily existence, including essential roles in digestion, food manufacturing, and multiple industrial uses. The use of commercial enzymes in food processing has seen a substantial transformation in recent years, transitioning from a negligible function to an essential component (Kannaujia et al., 2015).

The word "biotechnology" encompasses various technologies that use live microorganisms or their constituents to tackle various social challenges. Enzymes play a vital role in most of these technologies owing to their exceptional selectivity and high activity under ambient conditions (Katsimpouras & Stephanopoulos, 2021). L-methioninase, also known as methionine γ-lyase, has significant biotechnological implications because of its hydrolytic capability to facilitate the α-γ-elimination reaction of L-methionine, an essential amino acid.

This enzymatic process results in the production of α-keto-butyrate, methanethiol, and ammonia (Abozeid, 2023).

*Brevibacterium linens* is important because of the contribution of sulfur compounds in some cheeses (Rattray and Fox, 1999). These bacteria, known for their ability to produce methanethiol, are believed to play a role in enhancing the fragrance and taste characteristics of these types of cheeses (Rattray and Fox, 1999). Tokita and Hosono (1968) studied and characterized the production of sulfur compounds in experimental culture media. They observed that the addition of methionine to the culture medium significantly increased the production of hydrogen sulfide. In their study, the substances in the sample were hydrogen sulfide, mercaptans, and disulfides. Hydrogen sulfide exhibited the highest concentration among these compounds. Additionally, the presence of methanethiol has also been observed (Tokita and Hosono, 1968; Rattray and Fox, 1999). According to Sharpe et al. (1977), seven species of *Brevibacterium linens* produce methanethiol, which is likely to be one of the major bacteria that contribute to the flavor and aroma of surface-smear-ripened cheese containing *Brevibactarium linens* (Sharpe et al., 1977). Limburger, Roquefort, and Stilton cheeses are among the surface-ripened cheese types that contain a large number of *Brevibacterium lines* (Sharpe et al., 1977; Rattray and Fox, 1999).

*Brevibacterium linens* is not used in the traditional production of cheddar cheese (Dias and Weimer, 1998). Few studies have investigated the use of this bacterium and L-methioninase in cheddar cheese production. To improve its flavor, Weimer et al. (1977) successfully used *Brevibacterium linens* BL2 in low-fat cheddar cheeses. In that study, *Brevibacterium linens* BL2 strain successfully increased methanethiol production in a cheese-like environment. The advantage of using *Brevibacterium linens* BL2 is the direct conversion of methionine to methanethiol, alpha-ketobutyrate, and ammonia by an intracellular L-methioninase enzyme. This enzyme has great potential for use in cheese production. However, to the best of our knowledge, there is no industrial application of L-methioninase in the cheese industry. Thus, this study sheds light on the industrial use of L-methioninase from *Brevibacterium linens* BL2.

Many different types of bacterial L-methioninase have been purified and characterized. L-methioninase from various organisms, including *Pseudomonas putida, Aeromonas sp., Pseudomonas ovalis, Citrobacter freun-dii, Citrobacter intermedius, Lactococcus lactis, Brevibacterium linens* BL2, and *Brevibacteium linens,* has different purification processes and characteristics, as documented in the publication by Mohamed et al. (2022).

In recent decades, several researchers have investigated regulated enzymatic production of methanethiol using L-methioninase derived from diverse microorganisms. Lindsay and Rippe (1986) used L-methioninase derived from Pseudomonas Putida for cheddar cheese production. The investigation conducted by Ferchichi, Hemme, Nardi, and Pamboukdjian (1985) focused on the synthesis of methanethiol from methionine utilizing L-methioninase derived from *Brevibacterium linens*. The study conducted by Dias and Weimer (1998) focused on purifying L-methionine γ-lyase (EC 4.4.1.11) from *Brevibacterium linens* BL2, a coryneform bacterium. This bacterium has been effectively used as a supplement to improve the taste of cheddar cheese. Researchers have successfully purified the enzyme in a homogeneous state. Amarita et al. (2004) described a specific gene found in *Brevibacterium linens* responsible for the conversion of L-methionine to methanethiol.

Methionine, *Brevibacterium Linens*, and L-methioninase addition can affect the microbiota of cheese samples. Choi et al. (2020) assessed the microbial community shift in cheddar cheese from raw milk to aging using next-generation sequencing. The use of whole-genome sequencing has gained momentum owing to the recent advancements in next-generation sequencing technologies. This technique has great potential for expediting the process of identifying and selecting strains by aligning genes with certain traits (Kelleher et al., 2015). Thus, this technology provides precise information about microorganisms in cheese or other products at a specific time. Therefore, producers can decide what type of starter or adjuvant culture is used or when developing a desirable product. Producers can also obtain information on when undesirable bacteria form under specific conditions (Kelleher et al., 2015). In this study, next-generation sequencing was used to determine the extent of using the L-methioninase enzyme to produce sulfur compounds without growing undesired bacteria from raw milk using the next-generation sequencing method.

# 3. MATERIALS AND METHODS

## 3.1. Materials

The *Brevibacterium linens* BL2 strain was generously donated by Chr. Hansen Company (Hoersholm, Denmark). Protein ladder was purchased from BioLegend (San Diego, California, USA). The phalloidin-iFluorTM 488 conjugate was purchased from the Cayman Chemical Company (Ann Arbor, Michigan, USA). Fetal bovine serum (FBS), DNase I, and Dulbecco's modified Eagle's medium (DMEM) were purchased from Thermo Fisher Scientific (Waltham, Massachusetts, USA). All other chemicals and compounds were purchased from Merck (Darmstadt, Germany). Milli-Q® Type I water (Merck, Darmstadt, Germany) was used in all experiments. Starter cultures were generously provided by Danisco (Copenhagen, Denmark).

The cell lines employed in this study were as follows: T98G cell line [T98-G] (ATCC® CRL-1690™), U87MG (ATCC® Manassas, VA, USA, HTB-14™), Human Keratinocytes, also known as HaCaT (CLS 300493, DKFZ, Heidelberg, Germany), and mouse embryonic fibroblasts (ATCC® SCRC-1040™).

The apparatuses utilized in this study are as follows:

1. Nüve EC 160 humidified CO2 incubator (Nüve, Ankara, Turkey).
2. IKA 4000 incubation shaker (IKA, Berlin, Germany).
3. Universal 320 R Benchtop centrifuge (Hettich, Germany).
4. Ultrasonic Probe (Bandelin Sonoplus 2450, Bandelin electronic, Berlin, Germany).
5. Magnetic Stirrer (IKA, Germany).
6. Incubator (Memmert, Schwabach, Germany).
7. Cary 60 UV-Vis spectrophotometer (Agilent, Santa Clara, CA).
8. Microplate reader (Spectrostar Nano; BMG Labtech, Ortenberg, Germany).
9. Leica dissecting microscope EZ50 model (Leica Biosystems, Wetzlar, Germany).
10. Inverted microscope (Leica Biosystems, Wetzlar, Germany).
11. LED inverted microscope (Leica DM IL; Wetzlar, Germany; Leica Biosystems).
12. Bio-Rad Mini Protean Tetra Gel SDS-PAGE System (Hercules, CA, USA).
13. Image analysis software developed by Bio-Rad (USA) called Chemidoc Touch.
14. Rotor-Gene Q qPCR instrument manufactured by Qiagen, Hilden, Germany.

### 3.2. Method

#### 3.2.1. Production Procedure of L-methioninase Enyzme

L-methioninase was partially purified using a modified version of the technique described by Dias and Weimer (1998). Initially, liyofilized *Brevibacterium linens* BL2 was cultivated in the tryptic soy broth for 24 h. A 1 mL volume of bacterial solution was then added to individual Erlenmeyer flasks, each containing 500 mL of Tryptic Soy Broth. These cultures were incubated for 36 h on an incubation shaker operating at a speed of 250 rpm and a temperature of 25 °C. After a 36-hour incubation period, a 10 mL solution of the L-methioninase enzyme was generated from a 500 mL bacterial culture.

The cells cultivated in the flasks were harvested using a tabletop centrifuge (manufactured by Hettich, Germany) with a centrifugal force of 6000 g for 15 min at 4 °C. The precipitated bacteria underwent two rounds of washing using a potassium phosphate buffer (KP) with a concentration of 50 mM. This buffer also contained 0.02 mM of prydoxal-5-phosphate (PLP), 2% ethanol, 1 mM of phenylmethylsulfonylfluoride (PMSF), and 1 mM of EDTA. The bacterial cell precipitate was reconstituted in KP buffer using a vortex mixer.

To facilitate the breakdown of the cell wall of *Brevibacterium linens* BL2, lysozyme was introduced at a concentration of 1 mg/mL. Lysozyme functions by catalyzing the breakdown of glucosidic bonds within the peptidoglycan structure of bacterial cell walls, rendering cells inactive. The Incubation with lysozyme occurred at 37°C for 1 h. Following this, a concentration of 0.25 µg/mL DNAse I was introduced and agitated at ambient temperature for 1 hour to prevent DNA contamination.

To further disrupt the bacterial cells, ultrasonic treatment was conducted for 4 min at 70% power and repeated five times. This treatment was performed using an ultrasonic probe at a temperature of 4 °C, with an ice bath used to maintain the desired temperature. Following appropriate centrifugation conditions (10,000× g, 1 h, 4 °C), the supernatant was carefully separated and the resulting decant was used as the crude enzyme for further ammonium sulfate precipitation in the subsequent step.

This treatment was performed at a temperature of 4°C in an ice bath used to maintain the desired temperature. After appropriate centrifugation conditions (10,000× g, 1 h, 4°C), the supernatant was carefully separated, and the resulting decant was used as the crude enzyme for further ammonium sulfate precipitation.

Crude enzyme was gradually added to ammonium with constant stirring until it reached a saturation level of 55%. An ice bath was used to control temperature. After centrifugation of the precipitated proteins at 10,000× g for 20 min at 4 °C, the resulting saturated protein solution was resuspended in KP buffer. The enzyme solution was desalted using Amicon® Ultra-15 centrifugal filters with a molecular weight cut-off of 30 kDa. The Centrifugation was carried out at 4000 × g and 4 °C in a centrifuge.

### 3.2.2. Enzyme Activity and Protein Content Analysis

Enzyme activity was quantified by monitoring the temporal changes in the concentration of unbound thiol groups. The 5,5'-dithiobis (2-nitrobenzoic acid) (DTNB) approach described by reference (Laakso & Nurmikko, 1976), was used in this study. DTNB, also known as Elman's reagent, has a strong affinity for methanethiol, which is released after the enzymatic action of L-methioninase on methionine. This interaction led to the manifestation of a vivid yellow hue. A spectrophotometer can detect changes in the intensity of the yellow color. The enzyme solution was combined with 20 mM L-methionine in phosphate-buffered saline (PBS) at a pH of 7.2. Additionally, 0.1 mM pyridoxal-5-phosphate (PLP) and 0.25 mM of 5,5'-dithiobis (2-nitrobenzoic acid) (DTNB) were added to the mixture. The total volume of the solution was 1 ml. The solution was incubated for one hour at 37 °C. Following the incubation period, absorbance at 420 nm was quantified using a spectrophotometer. A control group was established by conducting experiments using L-methioninase in the absence of its substrate, L-methionine, and by utilizing the substrate in the absence of L-methioninase. Thiol groups associated with methanethiol were quantified using a sodium thiomethoxide standard curve. A calibration curve was generated by the reaction between sodium thiomethoxide and DTNB. Enzyme activity was operationally defined as the quantity of enzyme capable of liberating 1 µmol of free thiol per minute, as per the best experimental conditions, which was also referred to as L-methioninase activity. The assessment of the specific activity of methioninase relies on the measurement of protein content, which is obtained using Bradford protein estimation

methodology (Bradford, 1976; Ulagesan & Kim, 2018). In this experiment, a total volume of 50 µL of methioninase solution was added to 2.5 mL of Bradford protein solution, which was produced using Coomassie blue. Subsequently, the mixture was incubated for 5 min in a light-free environment. The absorbance of blank samples was measured using a spectrophotometer at 595 nm. The standard curve was generated using fixed quantities of BSA or bovine serum albumin in accordance with comparable methodologies. The protein content of the enzyme solution was determined using a standard curve.

### 3.2.3. SDS-PAGE Analysis

Additional evaluation of the specific band formation of the produced enzyme was conducted through implementation of an appropriate SDS-PAGE protocol. The protocol involved using a monomer concentration of 12% (w/v) and incorporating a protein ladder spanning the 10-200 kDa range. This range was chosen because the molecules of interest possess molecular weights that fall within this range. Specifically, L-methioninase weighs 43 kDa.

In order to create a running gel with a monomer (acrylamide) concentration of 12%, the following components were combined:7.2 mL of a 30% acrylamide/bis-acrylamide solution, 3.38 mL of a 2 M Tris-HCl solution at pH 8.8, 180 µL of a 10% SDS solution, and 7 mL of Ultrapure water solution. These components were mixed and homogenized gently using pipetting techniques to minimize any potential foaming that may be induced by the presence of SDS. Subsequently, 180 µL 10% ammonium persulfate (APS) and 20 µL N,N,N',N'-tetramethylethylenediamine (TEMED) were added to the solution. The resulting mixture was gently agitated twice by inversion. Given that APS functions as an initiator and TEMED serves as a catalyst, it is advisable to include these compounds in the polymeric solution in the last step, just before pouring the gel. The final solution was carefully poured into the space between two glass plates until it reached a line that was either 1 cm from the end of the comb or 2 cm from the highest point of the glass plates. In order to achieve a homogenous gel consistency and eliminate the presence of air bubbles, the addition of butanol was promptly performed subsequent to the pouring of the gel. Moreover, the presence of oxygen hindered the polymerization process, whereas the use of butanol effectively isolated the gel from the surrounding air. Subsequently, the gel was allowed to undergo polymerization at ambient temperature for a minimum of 15 min. Following the completion of the procedure, butanol

was eliminated by carefully inverting the gel apparatus and then using Kimwipes to thoroughly eliminate any residual butanol present inside the interstitial region between the two glass plates.

The following procedure was used to synthesize a stacking gel with a monomer (acrylamide) concentration of 4%. A mixture was prepared by combining 0.7 mL of a 30% acrylamide/bis-acrylamide solution, 1.5 mL of a 0.5 M Tris-HCl solution with a pH of 6.8, 60 µL of a 10% SDS solution, and 4 mL of UW. Subsequently, 50 µL of 10% ammonium persulfate (APS) and 10 µL of N,N,N',N'-tetramethylethylenediamine (TEMED) were added to the solution. The resulting mixture was gently agitated twice by inversion. A polymeric solution was carefully introduced into the space between the two glass plates to ensure that the solution reached the uppermost point of the plates. To generate wells, a stacking gel was formed by inserting an SDS-PAGE comb between glass plates. Subsequently, the polymeric system was allowed to undergo polymerization at ambient temperature for a minimum of 20 min.

The procedure for preparing samples, putting them into the wells, and executing the experiment was as follows: The gel running box was used to introduce the gel using glass plates. Electrophoresis buffer was gently poured into the box, first covering the wells to ensure that the gel was entirely submerged. The buffer was poured outside the plates until it reached a designated point. Subsequently, the comb was carefully removed. A total volume of 7.5 µL of loading buffer was combined with an equal volume of the protein sample. To obtain denatured proteins, each sample was boiled for 10 min. The samples were subjected to an electrical potential of 60 volts for approximately 1-2 hours using a power source. This process continued until the visible dyes, which had been introduced into the gel alongside the samples, migrated and accumulated in the lowermost portion of the gel.

The occurrence of "smiling bands" on the gel may be attributed to the use of a greater voltage during gel electrophoresis than the recommended value. This phenomenon arises from the differential migration rates of the central portion of a sample compared with its two ends, resulting in a distorted band shape resembling a smile. Determining the appropriate voltage for the electrophoretic process of a certain gel is of significant importance.

Procedural stages for fixing, staining, and de-staining: The gel was separated from the glass plates and the stacking gel was carefully removed. The residual running gel was washed using a combination of methanol and acetic acid in a shaker for a minimum duration of 30 min. Subsequently, the gel was rinsed with distilled water for a period of time to effectively immobilize the protein samples inside the gel matrix. Subsequently, the gel was immersed in a solution of diluted Coomassie Brilliant Blue dye and agitated for a minimum duration of four hours. This facilitated permeation of the dye into the porous composition of the polyacrylamide gel, enabling it to interact with and adhere to the immobilized protein samples. Subsequently, a remedial solution was used to remove the stain. The de-staining method was conducted to eliminate surplus dye from both the interior and outside of the gel, excluding the dye bound to proteins. This procedure allowed the proteins to be visualized as distinct and unobstructed bands.

Two distinct gels were produced: one with a concentration of 12% for running and the other with a concentration of 4% for stacking. After preparing and immediately placing the running and stacking gels on the SDS-PAGE platform, Tris-glycine buffer was poured into the SDS-PAGE reservoir. The enzyme-containing solutions (10 mL each) were mixed with a loading buffer consisting of bromophenol blue (0.0004%), sodium dodecyl sulfate (4%), glycerol (20%), Tris-HCl (0.125 M) buffer (pH 6.8, and 2-mercaptaethanol (10%). Subsequently, the loading solution was heated to 95ºC for ten minutes.

This heating step occurred at elevated temperatures. Following this, the loading solution and protein ladder were added to the wells of the upper SDS-PAGE gel, also known as the stacking gel. To ensure that all bands migrated to the bottom of the running gel, the SDS-PAGE system was operated at 60 V for a minimum of two hours. This step is crucial for ensuring proper functioning of the system.

After the running process was completed, the SDS-PAGE gels were carefully removed and treated with a solution consisting of 40% methanol and 10% acetic acid for 30 min. The gels were subsequently placed in a container containing the Coomassie Blue staining solution, followed by gentle agitation for four hours. Following destaining, the protein bands were visualized using an imaging system.

### 3.2.4. Methods for Investigation of Cytotoxic Effect of L-Methioninase

#### *3.2.4.1. Cell Culture Conditions*

This study included two distinct types of glioblastoma cancer cell lines. One cell line used in this study was the T98G cell line [T98-G] (ATCC® CRL-1690™). The cells were cultured in Dulbecco's modified Eagle's medium (DMEM/F12) containing 10% fetal bovine serum (FBS). The second cell line used for glioblastoma research was the U87MG (ATCC® Manassas, VA, USA; HTB-14™) cell line. U87 MG cells were cultured in DMEM supplemented with 10% FBS. In this study, we used two non-cancerous cell lines to conduct a comparative analysis of the cytotoxic effects of etoposide and L-methioninase on normal cells. The initial cell line used in this study was the Cell Line derived from human keratinocytes, also called HaCaT (CLS 300493, DKFZ, Heidelberg, Germany), which was cultivated in DMEM containing 10% FBS. Mouse embryonic fibroblasts (ATCC® SCRC-1040™) were cultured in DMEM supplemented with 5% FBS and 55 µM 2-mercaptoethanol. The cell lines were cultured in a humidified incubator at a constant temperature of 37 °C, while maintaining a $CO_2$ level of 5%.

#### *3.2.4.2. Neutral Red Assay*

To assess the cytotoxic effects of etoposide and L-methioninase on cell viability, a neutral red vitality test was performed. This test quantifies cell viability by measuring their ability to uptake and bind the supravital dye neutral red to the lysosomes (Repetto, Del Peso, & Zurit, 2008). The fundamental principle of the neutral red viability experiment is based on the idea that living cells can absorb the dye. Cell viability can be determined by measuring the change in color intensity at 540 nm resulting from dye absorption (Borenfreund & Puerner, 1985; Al-Khedhairy & Wahab, 2022).

Approximately 5000 cells were counted using a Neubauer hemocytometer and seeded into each well of a 96-well plate. Following this, a 24-hour incubation period was initiated to allow the cells to adhere to the well plate surface. L-methioninase was prepared in a buffered solution. As a result, the control group was provided with the buffer alone, excluding the enzyme, to minimize any potential impact of the buffer on the observed cytotoxicity of L-methioninase and etoposide. Subsequently, a neutral red test was conducted after the

incubation period. The viability of the control cells was considered 100%, and the viability of cells treated with the enzyme and etoposide was compared to that of the control cells.

The Neutral Red test is a simple and direct method. The method is dependent on the absorption of neutral red dye by live cells, and the amount of dye accumulated inside the cells is directly proportional to the number of viable cells. The use of the Neutral Red test is advantageous in assessing cell viability in the presence of L-methioninase because of its reduced propensity to interfere with enzymatic activity, thus enabling a more precise evaluation.

The neutral red test was conducted concurrently in all the wells of a 96-well plate. Cells corresponding to the groups under investigation were cultured in DMEM + 10% FBS. A pre-prepared neutral red solution (0.033%) in PBS was applied in sufficient quantities to cover the cell surface. The cells were subsequently incubated with a neutral red solution for 2 h. After a 2-hour incubation period, the neutral red solution was aspirated and replaced with a neutral red dissolving solution consisting of 1% Acetic Acid, 49% deionized H2O, and 50% ethanol. The solution was agitated on a shaker until a uniform mixed precipitate of stained live cells was obtained. Absorbance was measured at 540 nm using a microplate reader.

#### *3.2.4.3. Analysis of the Cytotoxic Effect of L-Methioninase on Cancer Cells*

The $IC_{50}$ value was determined to ascertain the concentration of L-methioninase necessary to induce a 50% decrease in cell viability or cell death. Initially, 5000 U87MG and T98G cells were evenly distributed into individual wells of a 96-well cell plate. The cells were then cultured in a controlled environment: a humid incubator set at 37°C with a carbon dioxide concentration of 5%.

To determine the $IC_{50}$ value of L-methioninase, an enzyme known for its activity in glioblastoma cells, various concentrations of the enzyme (0, 0.88, 1.77, 2.66, 3.55, and 4.44 units/mL) were utilized. $IC_{50}$ values were determined after 24 h of incubation. Cell viability was assessed using the neutral red test, allowing the determination of percentage viability at various concentrations. The $IC_{50}$ value, representing the concentration at which a 50% decrease in cell viability occurred, was calculated based on experimental findings.

The L-methioninase enzyme was stored in an appropriate buffer solution. Consequently, the control group received buffer without the enzyme to mitigate the influence of the buffer on the cytotoxicity of L-methioninase and etoposide.

Several treatment regimens, including etoposide alone, L-methioninase + etoposide, and L-methioninase alone, were used to assess the combined effects of L-methioninase and etoposide on U87MG and T98G cells over 24 and 48 h. The neutral red test was used to determine the effect of the combined $IC_{50}$ values of the L-methioninase enzyme solution and etoposide chemotherapy on cell survival.

According to a previous study conducted by Ozdemir and Gokturk (2018), the $IC_{50}$ value for etoposide in U87MG cells was 40 µM. In a separate study by Sevim et al. (2011) using the T98G cell line, the $IC_{50}$ value of etoposide was determined to be 29 µM, and the cytotoxic effects of etoposide and L-methioninase were evaluated and compared using Mouse Embryonic Fibroblasts (MEF) and Human Keratinocyte (HaCaT) cells as control cell lines. Both MEF and HaCaT cells were cultured for 48 h and subjected to the same experimental design and tests to assess the potential damage caused by etoposide. Forty microliters of etoposide and 5.792 units/mL of L-methioninase, which had the highest $IC_{50}$ values, were utilized in these experiments.

#### *3.2.4.4. Clonogenic Assay*

Clonogenic assays (Gao et al., 2014) were used to assess the colony-forming abilities of U87MG and T98G cells. Cells from these glioblastoma cell lines were cultured in six-well plates and exposed to four experimental conditions: no treatment (control), L-methioninase treatment, etoposide treatment, or a combination of both. The $IC_{50}$ values for etoposide were 40 and 29 µM in U87MG and T98G cells, respectively. L-methioninase was used at $IC_{50}$ concentrations of 5.792 units/mL and 5.215 units/mL for T98G cells. After 24 h of incubation, 500 live cells were counted and seeded into six-well plates. The plates were then incubated for 21 days at 37°C in a 5% $CO_2$ humidified environment to accelerate colony growth. Following incubation, cells were fixed with 4% paraformaldehyde and stained with 2% crystal violet solution. Colonies were counted under a microscope.

### *3.2.4.5. Wound healing (Migration) Assay*

To evaluate the effect of L-methioninase and etoposide on the migration of U87MG and T98G cells, we followed the protocol developed by Suarez-Arnedo et al. (2020). Initially, 2,105 cells were seeded in six-well plates. The following day, the plates were rinsed with phosphate-buffered saline (PBS), and a linear incision was created using a 1 mm pipette tip, resulting in a cell monolayer. Treatments, including L-methioninase and etoposide, a combination of both, and the control culture medium were applied. U87MG and T98G cells were exposed to 40 and 29 µM etoposide, respectively, corresponding to their respective $IC_{50}$ values. L-methioninase was administered at previously determined $IC_{50}$ concentrations for U87MG and T98G (5.792 and 5.215 units/mL, respectively). The plates were then incubated for 24 h. Images of the cells were captured at 0th, 8th, and 24th hours post-treatment using an inverted microscope. ImageJ software (version 1.53t) was used for the quantitative analysis of cell migration and wound closure.

### *3.2.4.6. Giemsa Staining*

Giemsa staining is a histological method used to identify specific cellular components, including chromatin and nuclear membranes. The fluid was then filtered using a 0.22 micron syringe filter. Six-well plates were used to conduct experiments on glioblastoma cell lines U87MG and T98G under four different conditions: control (no treatment), methioninase treatment, etoposide treatment, and a combination of the two. U87MG and T98G cells were exposed to 40 and 29 µM etoposide, respectively, corresponding to their respective $IC_{50}$ values. L-methioninase was administered at a concentration of 5.792 units/mL to U87MG cells and 5.215 units/mL to T98G cells, both of which corresponded to the $IC_{50}$ values for each cell line. After incubating the cells for 24 h, the growth medium was removed and the cells were washed twice with phosphate-buffered saline (PBS). Each well of the plate was filled with 1 mL methanol solution consisting of 60% methanol in phosphate-buffered saline (PBS). The plate was then placed in a room-temperature incubator for 10 min. After the solution was removed, it was subjected to a series of purification steps, including passing it through pure methanol. Giemsa staining solution (concentration:0.01 gr/mL) was added to each well at a volume of 1 mL, and the plates were incubated for 20 min at room temperature. The Giemsa staining solution was removed after incubation and the cells were washed three

times in a row with distilled water. LED-inverted microscopy was used to examine cell morphology.

#### *3.2.4.7. DAPI and F-Actin Staining*

Giemsa staining is a histological technique used to identify cellular components such as chromatin and nuclear membranes. In our experiments, we performed Giemsa staining on two glioblastoma cell lines, U87MG and T98G, under four conditions: control (no treatment), methioninase treatment, etoposide treatment, and a combination of both. U87MG cells were treated with 40 µM Etoposide, while T98G cells received 29 µM etoposide, which are their respective $IC_{50}$ values after 24 h of incubation. L-methioninase was administered at concentrations of 5.792 units/mL to U87MG cells and 5.215 units/mL to T98G cells, based on their $IC_{50}$ values.

After 24 h of incubation, we removed the growth medium, washed the cells with PBS, and exposed them to a methanol solution (60% methanol in PBS) for 10 min at room temperature. Subsequently, the cells were stained with Giemsa staining solution (0.01 gr/mL) for 20 minutes. After staining, the cells were washed thrice with distilled water. Cell morphology was examined using an LED-inverted microscope.

#### *3.2.4.8. RNA Isolation and cDNA Synthesis*

Glioblastoma U87MG and T98G cell lines were cultured on 75 cm2 cell culture plates and divided into four experimental groups: control (no treatment), methioninase treatment, etoposide treatment, and a combination of methioninase and etoposide. The experimental groups included methioninase, etoposide, and a combination of methioninase and etoposide. Dosages for the combination treatment were determined using the 24-hour $IC_{50}$ values of etoposide (40 µM for U87MG and 29 µM for T98G) and L-methioninase (5.792 units/mL for U87MG and 5.215 units/mL for T98G). RNA was extracted during a 24-hour incubation period at 37 °C with 5% $CO_2$.

RNA isolation was performed using the InvitrogenTM PureLinkTM RNA isolation kit (Thermo Fisher Scientific, USA) following the manufacturer's instructions. RNA samples

were used to synthesize cDNA using the Revertaid First Strand cDNA Synthesis Kit (Thermo Fisher Scientific). Thermal cycling was performed using an Agilent Sure Cycler 8800 model consisting of 10 min at 25 ℃, 120 min at 37 ℃, and 5 min at 85 ℃. The quality and quantity of the cDNA were assessed using a NanoDrop 2000 spectrophotometer (Thermo Fisher Scientific, USA).

#### *3.2.4.9. Gene Expression Analysis (RT-qPCR)*

Gene expression analysis of caspase 3, survivin, and C-myc was performed using reverse transcription quantitative polymerase chain reaction (RT-qPCR) with a Rotor-Gene Q qPCR instrument (Qiagen, Germany). The reaction conditions included an initial activation step at 95°C for 12 min, denaturation at 95°C for 15 s, annealing at 55°C for 20 s, and elongation at 72°C for 20 s. The ΔCt data were obtained and normalized to the expression of the β-actin reference gene.

The primer sequences used in this investigation were as follows:

- Survivin forward primer: 5'-TCCACTGCCCCACTGAGAAC-3'
- Survivin reverse primer: 5'-TGGCTCCCAGCCTTCCA-3'
- C-myc forward primer: 5'-TACCCTCTCAACGACAGCAG-3'
- C-myc reverse primer: 5'-TCTTGACATTCTCCTCGGTG-3'
- Caspase 3 forward primer: 5′-TGACTGGAAAGCCGAAACTC-3′
- Caspase 3 reverse primer: 5′-AGCCTCCACCGGTATCTTCT-3’
- β-actin forward primer:5′-GTGGACATCCGCAAAGAC-3′
- β-actin reverse primer:5′-AAAGGGTGTAACGCAACTA-3′

### 3.2.5. Methods for Evaluation the Effect of the Use of L-Methioninase From *Brevibacterium linens* BL2 on Microbial Community Shift and Volatile Sulfur Compound Development

The bacterial strain and growth conditions, partial purification of the L-methioninase enzyme, enzyme activity assay, and protein content analysis are described in the previous section.

### *3.2.5.1. Cheddar Cheese Slurry Preparation and Sampling*

The aseptic cheese curd slurry system protocol has been outlined by Roberts et al.. al. (1995), with minor adjustments. Fresh raw milk was procured from a local market near the production site and stored at 4°C until cheese production. Prior to cheddar cheese production, the raw milk was pasteurized at 63°C for 30 min. After pasteurization, milk was allowed to cool to room temperature. Subsequently, SLAB mesophilic commercial starter cultures CHOOZIT™ RA 21 (a mixture of Lactococcus lactis subsp. Lactis and Lactococcus lactis subsp. Cremoris and Streptococcus thermophilus), and MM 100 starter culture (a mixture of Lactococcus lactis subsp. Lactis, Lactococcus lactis subsp. Cremoris, Lactococcus lactis subsp. Lactis biovar diacetylactis; Danisco, Copenhagen, Denmark), were inoculated at concentrations of $1.6 \times 10^6$ and $1.8 \times 10^6$ cells/mL into pasteurized milk. *Brevibacterium linens* BL2 was added separately following the same steps. Approximately 1 h later, 0.01% rennet (v/w) (Trakya, Chr. Hansen, Hoersholm, Denmark) was used to coagulate milk for 30 min. The curd was cut and allowed to heal for 15 min before being slowly heated in a water bath at 39°C, increasing at a rate of 13°C every 5 min. to facilitate the exchange of lactose and lactate, the curd was maintained at 39°C. Subsequently, the curd was moved to a laminar flow hood and allowed to drain. When the pH reached 5.4, the cheese curd was transferred into sterile stomacher bags and samples were collected for moisture analysis using a moisture analyzer (Ohaus, Parsippany, USA). The water content was adjusted to 73% and the salt content was adjusted to 3% by adding a sterile NaCl solution. Methionine (0.1%) was then added to the bags. Samples were homogenized in a stomacher for 2 min. Homogenized slurries were transferred to 100 mL volume sterile sample containers.

**Table 3.1**. Experimental Design.

| **Trial** | **Supplement** |
|---|---|
| a | None |
| b | L-methionine |
| c | L-methionine + *Brevibacterium linens* BL2 |
| d | L-methionine + L-methioninase |

Four different sampling conditions were designed: Control, Control + L-methionine, L-methionine + *Brevibacterium linens* BL2, and L-methionine + L-methioninase. L-

methioninase enzyme at a concentration of 2.5 unit/mL was added immediately before the experiment commenced. Samples were taken at 0, 1st, and 9th days for sequencing analyses and stored at -20°C until DNA isolation. The experimental design is presented in Table 3.1.

#### *3.2.5.2. Total Viable Bacterial Count*

The total viable bacterial count was determined using the Plate Count Agar (PCA) method employing the pour plate technique. Specifically, 1 mL of the slurry was added to a Petri dish and PCA was poured over the sample with gentle mixing. After 24 h of incubation at 30°C, colony numbers were counted following the procedure outlined by Sanders (2012).

#### *3.2.5.3. Total Lactic Acid Bacterial Count*

To determine the total lactic acid bacteria count, 1 mL of the slurry was placed in a petri dish and De Man-Rogosa-Sharpe agar (MRS) agar was poured over the sample with gentle mixing. After 24 h of incubation at 30°C, colony numbers were counted following the procedure described by Sanders (2012).

#### *3.2.5.4. DNA Isolation*

To prepare cheese samples, approximately 150 µL of each sample was collected and transferred to individual Eppendorf tubes. These samples were homogenized at maximum speed for a maximum of 5 min. Following homogenization, the supernatant was separated by centrifugation at 6,000 × g for 8 min, as described by Pancza et al. (2021).

To isolate the remaining bacteria in the pellet, the Quick-DNA Fecal/Soil Microbe Miniprep Kit (Zymo Research, D6010) was used according to the manufacturer's guidelines. Initially, 600 µL of BashingBeadTM Buffer was added to the pellet and pipetted until homogeneity was achieved. This mixture was then transferred to a BashingBeadTM Lysis Tube. The BashingBeadTM Lysis Tube was vortexed at maximum speed for 40 min and subsequently incubated at 90°C for 10 min. After incubation, the BashingBeadTM Lysis Tube was centrifuged at 13,000 × g for 2 min and 400 µL of the supernatant was transferred to a Zymo-SpinTM III-F Filter in a Collection Tube. This was followed by centrifugation at 8,000 × g for 2 min, and the filter was removed. To the eluted liquid, 1,200 µL of Genomic Lysis Buffer was added and pipetted.

Next, 800 µL of the resulting mixture was added to a Zymo-SpinTM IICR Column in a Collection Tube and centrifuged at 10,000 × g for 2 min. The liquid that passed through the filter was discarded and this step was repeated until the mixture was fully filtered. The Zymo-SpinTM IICR Column was then placed in a new Collection Tube, and 200 µL of DNA Pre-Wash Buffer was added. Centrifugation was performed at 10,000 g for 2 min. Subsequently, 500 µL of gDNA Wash Buffer was added to the Zymo-SpinTM IICR Column in the Collection Tube and centrifuged at 10,000 × g for 2 min.

For the final step, 600 µL of Prep Solution was added to the Zymo-SpinTM III-HRC Filter in the Collection Tube and centrifuged at 8,000 × g for 4 min. After centrifugation, the Zymo-SpinTM III-HRC Filter was transferred to a fresh Eppendorf tube. Additionally, the Zymo-SpinTM IICR Column was transferred to a separate Eppendorf tube, and 50 µL of DNA Elution Buffer preheated to 56°C was directly applied to the filter. Centrifugation was performed for 2 min at 10,000 × g.

After centrifugation, the DNA eluted from the Zymo-SpinTM IICR Column was transferred to the Zymo-SpinTM III-HRC Filter in a new pre-prepared Eppendorf tube (Step 13). Centrifugation was performed for 4 minutes at 16,000 x g. Finally, the eluted DNA concentration was recorded using a Qubit Spectrofluorometer.

#### *3.2.5.5. PCR and Gel Electrophoresis*

PCR and gel electrophoresis were performed to quantify the target genes isolated from the cheese samples. The primer pair used to create the amplicon libraries targeted a region of approximately 1400 bp, covering the V1-V9 region of the 16S rRNA gene. The primer sequences are listed in Table 3.2, as described by Davidov et al. (2020).

**Table 3.2**. Universal 16S primer sequences used in long read platforms.

| | Position | Primer Sequence |
|---|---|---|
| 16S – Forward Primer | 27F | AGAGTTTGATCMTGGCTCAG |
| 16S – Reverse Primer | 1492R | CGGTTACCTTGTTACGACTT |

The isolated genomic DNA (20 ng) was measured and transferred to clean PCR tubes. The final volume of each tube was adjusted to 8 µL using ddH2O. Next, 2 µL of the 10 µM primer pair pool and 10 µL of the HF515 2x HiFi Taq Master Mix (MobiomX) enzyme were added to each tube. The tube contents were mixed by tapping, and after a brief spin, any liquid adhering to the tube walls was collected from the bottom. Subsequently, the tubes were placed in a thermal cycler, and 16S amplification was performed using the program outlined in Figure 3.1.

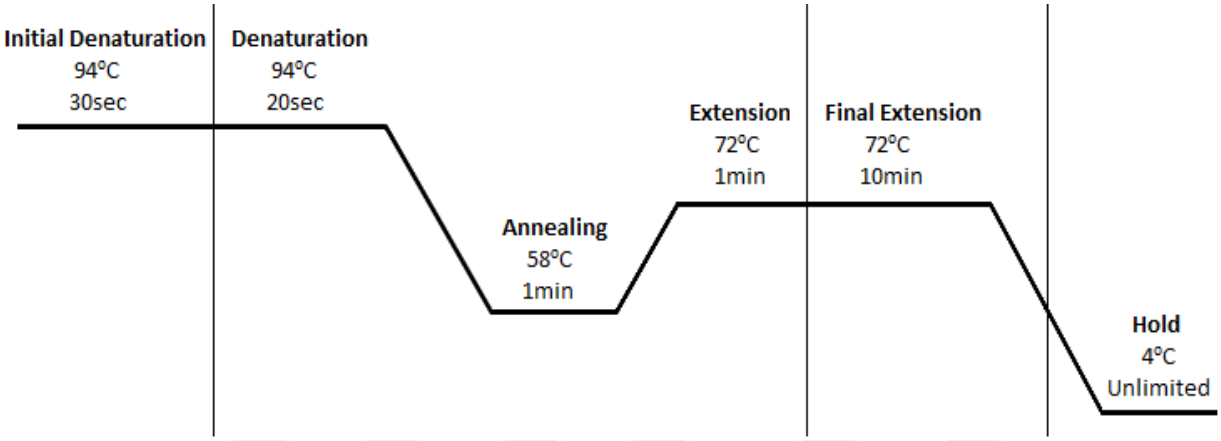


**Figure 3.1.** The thermal cycler program for amplification.

Amplicon sizes (1.5 kb) were verified by electrophoresing the amplicons on a 1% agarose gel at 100 V for 30 min.

### *3.2.5.6. 16S rRNA Gene–Based Library Preparation*

The amplicons were prepared and sequenced using third-generation long-read Oxford Nanopore Technologies (ONT) ligation-based library prep kits. Library preparation and sequencing were conducted on the Mk1C sequencing device (Oxford Nanopore Technologies, UK) using the SQK-NBD114.24 kit (Oxford Nanopore Technologies, UK) and FLO-MIN114 (Oxford Nanopore Technologies, UK) spot-on flow cells.

For the tip and DNA repair steps, 2 µL of the amplicon was mixed with 9 µL of water to reach a final volume of 11 µL. Subsequently, DNA CS (DNA control strand), NEBNext FFPE (formalin-fixed, paraffin-embedded) Repair Mix (M6630, New England BioLabs, UK), and NEBNext Ultra II End Repair/dA-Tailing Module (E7546, New England BioLabs, UK)

were added to the reaction. The Repair/dA-Tailing Module for Next-Generation Sequencing (NGS) facilitates a single-step reaction that combines end-repair, 5' phosphorylation, and dA-tailing processes. This process converts fragmented DNA into DNA fragments that are both 5´-phosphorylated and 3´-dAtailed, enabling direct ligation of NGS sequencing adapters. This mixture was incubated at 20°C for 5 min, and then at 65°C for 5 min. The repaired DNA was purified using magnetic beads (MBD02, MobiomX, Turkey), and barcode sequences were ligated to the fragments by incubating at room temperature for 20 min with NEB Blunt/TA Ligase Master Mix (M0367, New England BioLabs, UK). After the incubation period, the reaction was halted by adding 2 µl of EDTA, and all samples with attached barcodes were pooled into a single tube and purified again using magnetic beads.

Following purification, Native adapters (NA) were bound to the DNA barcoded with Rapid T4 DNA Ligase (MobiomX, Turkey) and purified. DNA was eluted with 15 µL elution buffer (EB), and the library concentration was measured using a Qubit instrument. The flow cell was prepared according to the protocol, and the library of barcoded 16S amplicons, sequencing buffer, and library beads was loaded into the R10.4.1 spot-on flow cell. Sequencing was continued until a minimum of 10,000 reads were obtained for each sample.

#### *3.2.5.7. Bioinformatics Analyses of Sequencing Data*

The bioinformatics analyses of the sequencing data were performed as follows:

1. **Data Conversion:** The sequencing results obtained in fast5 format were converted to fastq format using the Guppy software.

2. **Read Filtering:** Because the 16S rRNA region had an average length of 1500 bp, reads within the 1250–1750 bp range were selected, and reads outside this range were filtered out using Trimmomatic.

3. **Sequence Analysis:** The cleaned reads were subjected to sequence analysis. At this stage, the BLAST algorithm was used to match each sequence.

4. **OTU Creation:** Operational Taxonomic Units (OTUs) were generated based on taxonomic information obtained from sequences with more than 60% reference coverage and 80% pairwise similarity in the matching results.

5. **Diversity Analysis:** Various diversity analyses were conducted, including alpha diversity analysis, PCA (Principal Component Analysis), PCoA (Principal Coordinates Analysis), beta diversity analysis, biomarker analysis, and phenotype analysis. These analyses utilized different indices and tools available on the Qiime2 platform.

6. **Phylogenetic Analysis:** Phylogenetic analyses were performed using the created OTU (. biom) file.

7. **Taxonomic Classification:** Taxonomic classifications were organized, and dynamic Krona charts were prepared using the Mothur platform.

8. **Data Visualization:** Graphics and tables for the analyses were created using Python programming language libraries.

These analyses helped characterize and understand the microbial composition and diversity within the samples, providing valuable insights into the microbiome present in cheese samples.

#### *3.2.5.8. Determination of Volatile Compounds with GC-MS*

The determination of volatile compounds with GC-MS was performed as follows:

1. **Sample Collection:** Cheese slurry samples were collected in 20 mL GC vials, with 5 g of sample in each vial. Samples were collected at four time points: zero day, 1st day, 4th day, and 9th day. These vials were then stored at -20°C until analysis.

2. **Instrumentation:** The analysis was conducted using a Gas Chromatography-Mass Spectrometry (GC-MS) system with an automated injection module. The specific

components of the GC-MS system used were 7890 B GC, 5977A Mass Spectrometer (MSD), and GC Injector 80 (Agilent Technologies, Santa Clara, CA, USA).

3. **Headspace Solid-Phase Microextraction (SPME):** Volatile compounds were isolated from the samples using Headspace SPME. This was achieved using divinylbenzene/carboxen/polydimethylsiloxane (DVB/CAR/PDMS, 50/30 μm) Supelco fibers (57299-U, Supelco). Equipment parameters were set according to the method described by Salum et al. (2017).

4. **Equilibration:** Prior to extraction, all the samples were equilibrated at the extraction temperature for 30 min.

5. **Extraction Parameters:** The agitation on/off times were set at 5/2 s, vial fiber exposure was 22 mm, and vial needle penetration was 11 mm. The extraction temperature used was 54.8°C, the extraction time was 86 min, and the agitation speed was 250 min−1.

6. **Internal Standard:** To calculate the concentration of volatile components, 4-nonanol (9 μg μL-1) was used as the internal standard. The results are presented as μg kg-1 dry matter.

7. **Compound Identification:** Volatile compound identification was conducted using MS libraries, specifically NIST14 and Wiley 7. A mass spectral deconvolution and identification system (AMDIS) from the National Institute of Standards and Technology (NIST) was used for spectral deconvolution.

8. **Retention Index Measurement:** A calibration standard consisting of alkanes (C8-C40, SupelCo, Bellefonte, PA, USA) was used to measure the retention indices.

#### *3.2.5.9. Statistical Analysis*

All experiments were conducted in triplicates. For cell culture assays, statistical analysis was performed using ANOVA and t-tests, with a p-value of 0.001 considered to be statistically significant. Statistical analysis of the cell culture assays was conducted using Microsoft Excel.

For the cheddar cheese slurry experiments, ANOVA and Duncan's post-hoc test were used for statistical evaluation. Statistical analyses were performed using Microsoft Excel and the SPSS software (SPSS ver. 13.0 for Windows, SPSS Inc., Chicago, IL, USA). The significance level was set at $p < 0.05$.

# 4. RESULTS AND DISCUSSION

## 4.1. Enzyme Activity and Protein Profile of Enzyme Solution

Enzyme activity was evaluated using the DTNB method, while total protein content was determined following the Bradford protein estimation protocol. Partially purified methionine exhibited a specific activity of 3.055 U/mg. The specific activity value was calculated by dividing the enzyme units by the total milligrams of protein present in the enzyme solution. The measurement revealed that 10 mL of the enzyme solution contained 21.8 mg of total protein.

## 4.2. SDS-PAGE Analysis

The quantity of L-methioninase within the precipitated protein was determined using SDS-PAGE. In this method, the enzymes are denatured and separated on an SDS-PAGE gel based on their molecular weights. Intensely stained protein bands were observed in the 37–52 kDa range (Figure 4.1).

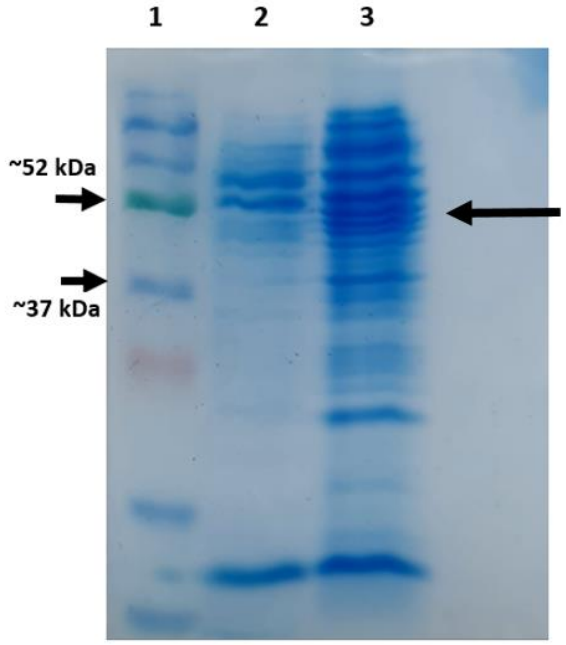


**Figure 4.1.** Bands observed through SDS-PAGE. From left to right: protein ladder (Cat. No: 773302, Broad Range), crude enzyme (acquired through bacterial ultrasonication), and L-methioninase precipitated with 55% ammonium sulfate. The arrow between the 37 and 52 kDa bands indicated the probable position of the L-methioninase band.

### 4.3. $IC_{50}$ Determination of L-Methioninase on Glioblastoma Cell Lines via Neutral red assay

The cytotoxic effects of L-methioninase extracted from *Brevibacterium linens BL2* were assessed using a neutral red assay. For the U87MG and T98G cell lines, the $IC_{50}$ values of L-methioninase were determined to be 5.792 units/mL and 5.215 units/mL after 24 h, respectively ($p < 0.001$) (Figures 4.2 and 4.3). In glioblastoma U87MG and T98G cells, L-methioninase increased the rate of cell death in a concentration-dependent manner. These findings suggest that L-methioninase is more effective in destroying glioblastoma U87MG and T98G cells at higher concentrations.

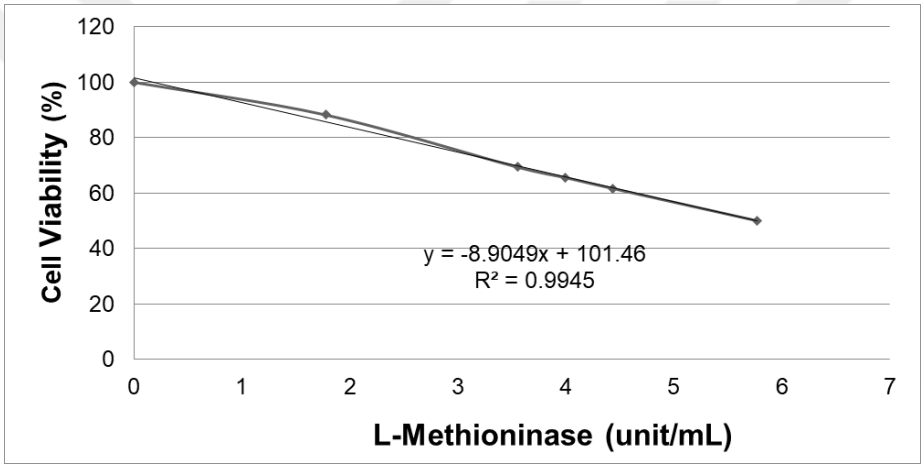


**Figure 4.2.** $IC_{50}$ graph for U87MG cell line.

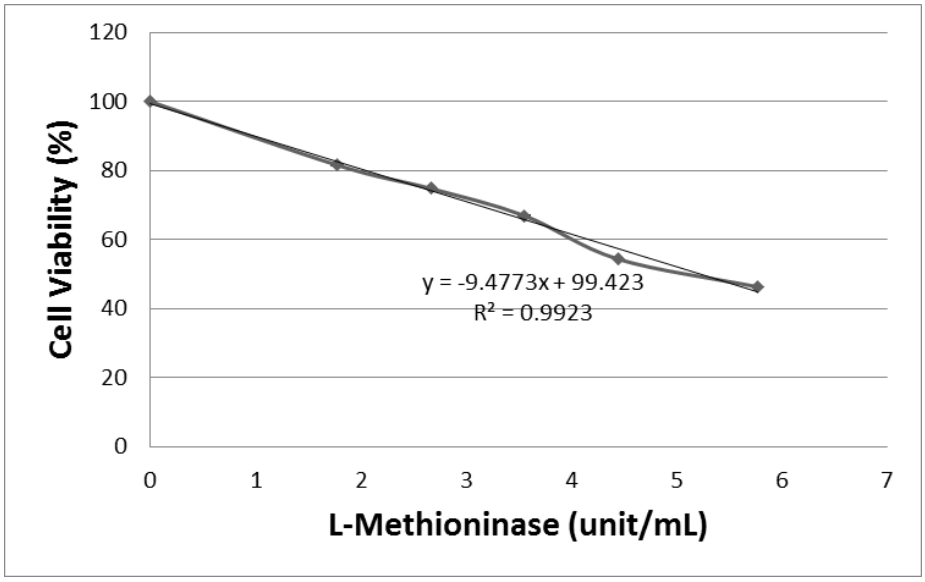


**Figure 4.3.** $IC_{50}$ graph for T98G cell line.

Few studies have applied L-methioninase from different microbial sources to glioma cells. In a study conducted by Hori et al. (1996), recombinant methioninase from *Pseudomonas putida* exhibited an $IC_{50}$ value of 1.5 units/mL in the T98G cell line after 96 h of incubation. $IC_{50}$ values of MGL from *Ps. Putida* for U-87 MG and LN-229 cells were determined to be 0.19 and 0.10 U/ml after 72 h of incubation, respectively (Gay et al., 2017). Intracellular L-methioninase isolated from *Klebsiella oxytoca* BLM-1 demonstrated cytotoxic effects on the U87MG cell line, with an $IC_{50}$ value of 0.009 U/mL after 24 h of incubation (Sharma et al., 2022). The consistent cytotoxicity observed with L-methioninase in two different Glioblastoma cell lines suggests its potential as a candidate adjuvant drug therapy in Glioblastoma treatment.

### 4.4. The Concurrent Effect of L-methioninase and Etoposide on Cell Viability

A neutral red assay was used to assess the combined effects of L-methioninase and etoposide on glioblastoma U87-MG cells.

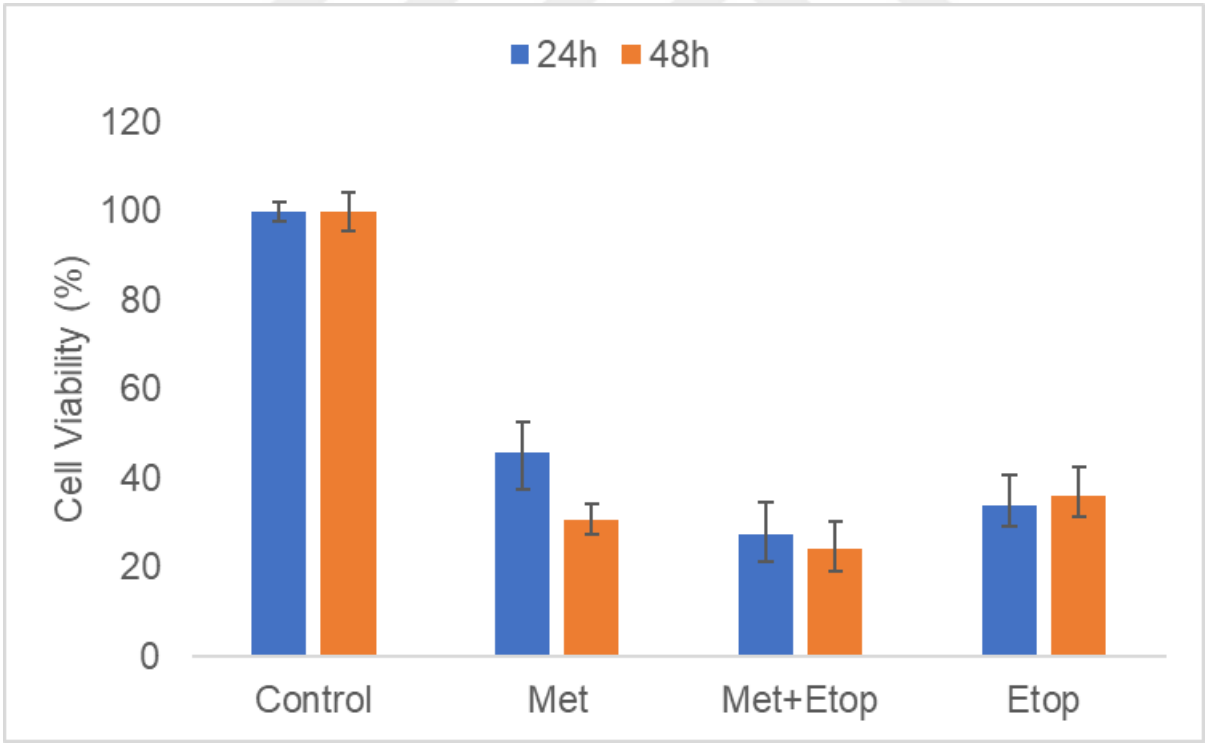


**Figure 4.4.** The cytotoxicity analysis for U87MG cells.

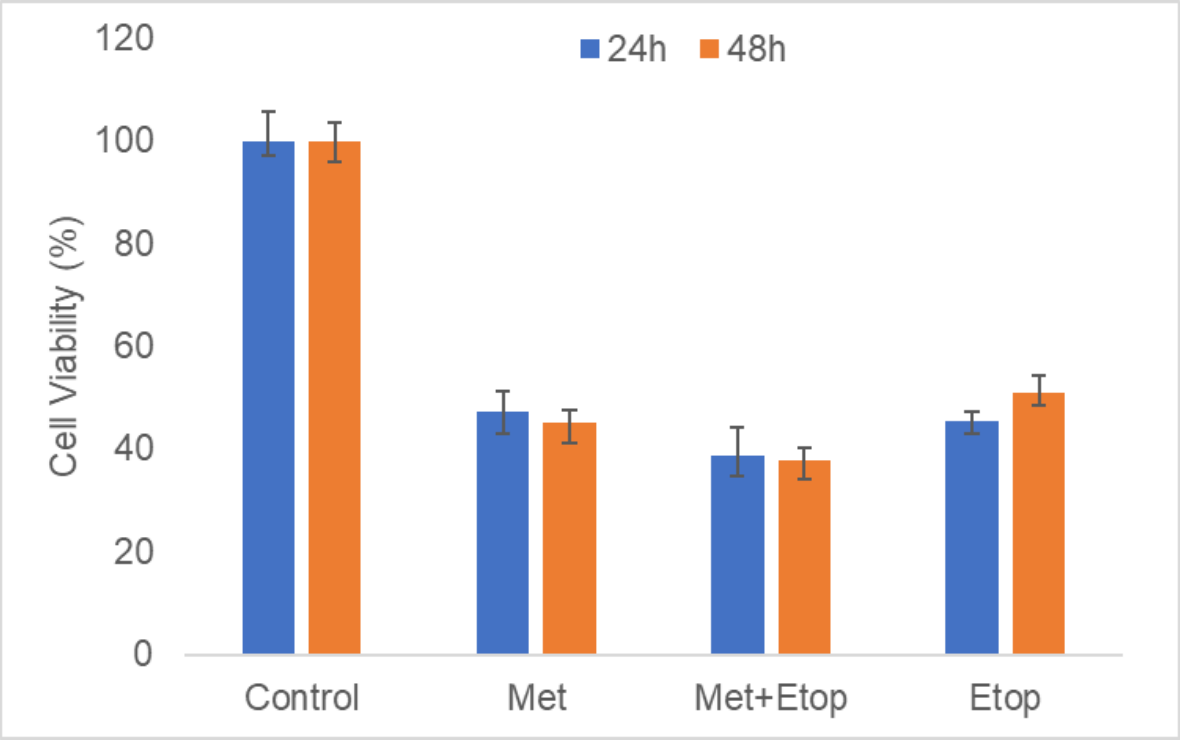


**Figure 4.5.** The cytotoxicity analysis for T98G cells.

These findings indicated that the addition of L-methioninase enhanced the cytotoxicity of etoposide. Both groups cultured with L-methioninase alone and those treated with a combination of L-methioninase and etoposide exhibited increased glioblastoma cell death on the second day. Under both 24-hour and 48-hour culture conditions, the combination of L-methioninase and etoposide resulted in a higher level of cell death in glioblastoma U87MG and T98G cells than either treatment alone. These results demonstrated that L-methioninase can augment the cytotoxic effects of etoposide, leading to increased cell death in glioblastoma U87MG and T98G cell lines ($p < 0.001$) (Figures 4.4 and 4.5).

This pioneering study on the utilization of L-methioninase against Glioblastoma cells has shown that the combined application of L-methioninase and etoposide yielded promising results, offering potential alternative therapeutic approaches for Glioblastoma.

### 4.5. Evaluation of the Effect of L-Methioninase with Etoposide on Mouse Embryonic Fibroblast (MEF) and Human Keratinocyte (HaCaT) Cells

L-methioninase and etoposide were evaluated for their cytotoxicity against glioblastoma U87MG and T98G cells, as well as against normal cells, specifically MEF and HaCaT cells, using a neutral red assay. When MEF cells were cultured for 24 h, L-methioninase exhibited lower cytotoxicity than etoposide. These results indicate that L-methioninase is relatively less toxic to normal cells, even though it mitigates the cytotoxic effects of etoposide on normal mammalian cells and contributes less to its cytotoxic activity (Figure 4.6). To the best of our knowledge, there is no available information in the literature regarding the effect of L-methioninase on MEF and HaCaT cells in combination with etoposide. This is the first study to investigate the effects of L-methioninase on healthy normal cell lines.

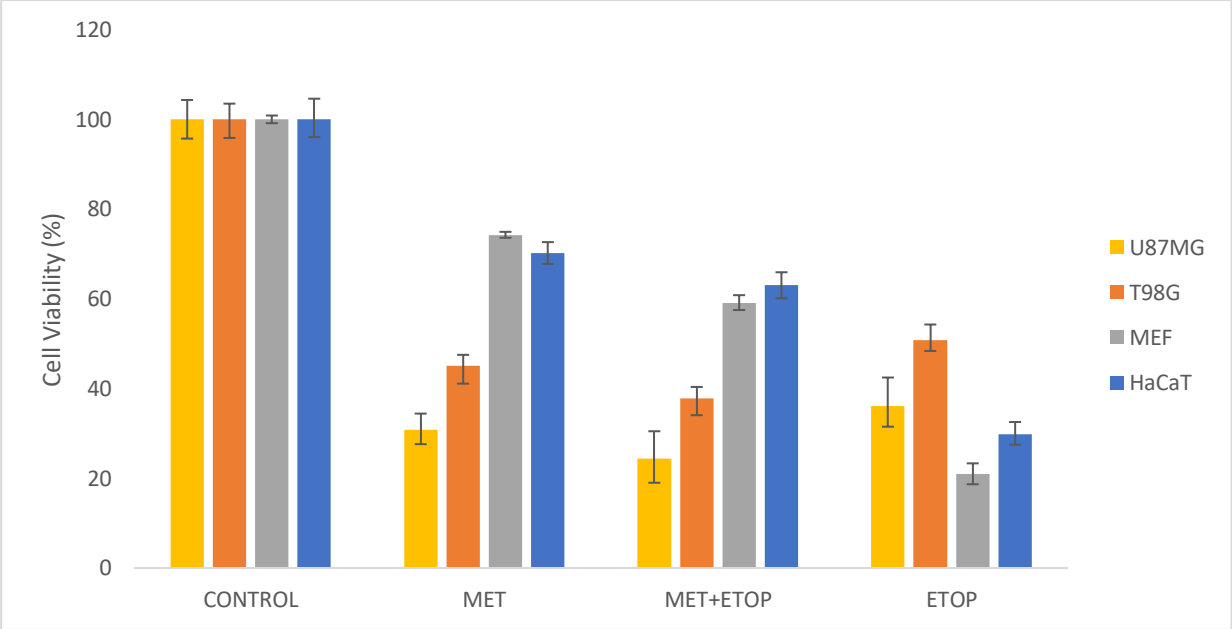


**Figure 4.6.** Cytotoxicity analysis for MEF, HaCat, U87MG and T98G cells.

### 4.6. Evaluation of the Effect of L-Methioninase on the Migration Characteristics of Glioblastoma Cells

A wound healing test was conducted to assess glioblastoma cell migration in response to L-methioninase. 24 hours of $IC_{50}$ values of etoposide (40 µM for U87MG, 29 µM for T98G) and L-methioninase (5.792 units/mL for U87MG, 5.215 units/mL for T98G) were added to the wells, followed by 24 h of incubation. L-methioninase successfully inhibited the migration of U87MG and T98G cells. For both cell lines, the control groups closed the wound within 24 h, whereas L-methioninase and etoposide prevented cell migration, keeping the wound open (Figures 4.7 and 4.8).

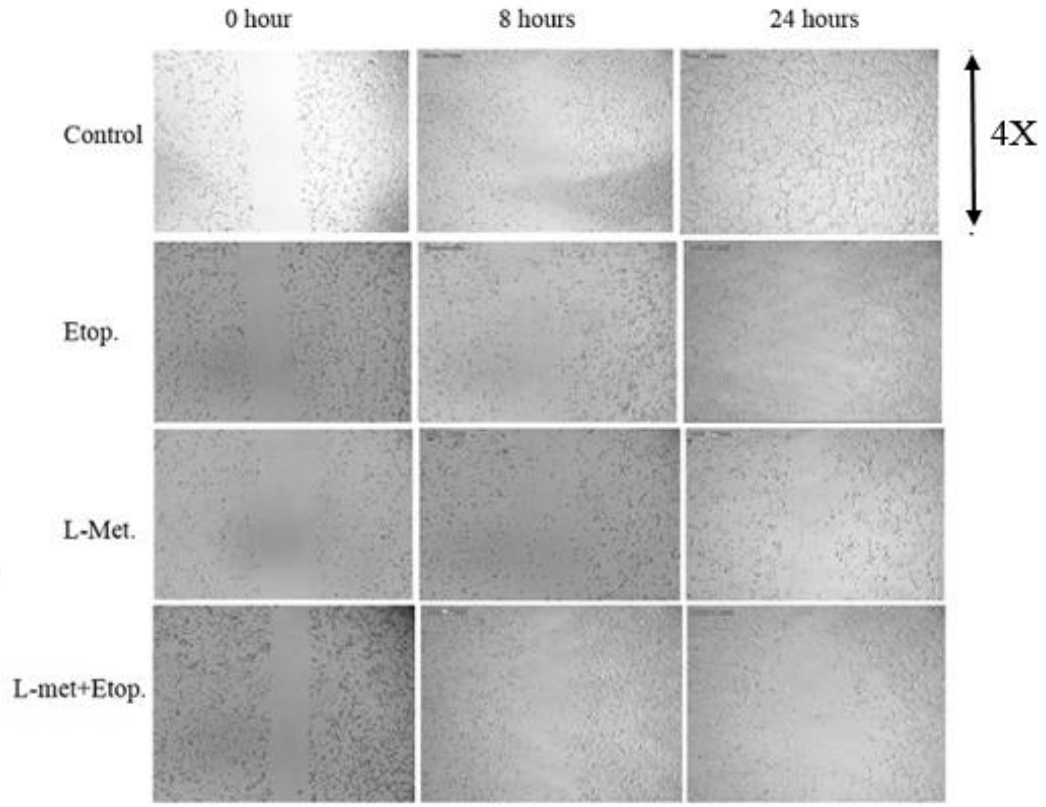


**Figure 4.7.** Wound closure status of U87MG cells over 24 h.

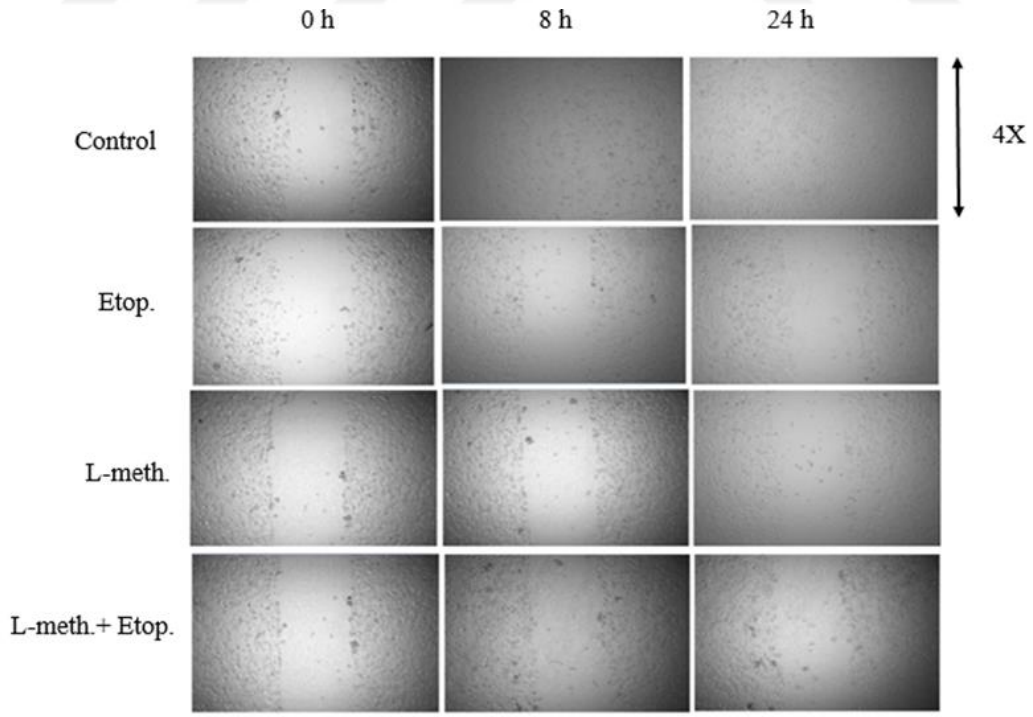


**Figure 4.8.** The wound closure status of T98G cells over 24 h.

These findings suggest that L-methioninase can reduce cell migration, which is a crucial aspect of cancer treatment to prevent metastasis. The graphs of wound width change and area demonstrate that L-methioninase, etoposide, and their combination prevented wound closure in U87MG cells over 24 h (Figures 4.9 and 4.10). After 24 h of incubation, a slight increase in wound width was observed in the wells treated with etoposide and L-methioninase, both of which are potent cytotoxic agents. This increase in wound width was indicative of cell death.

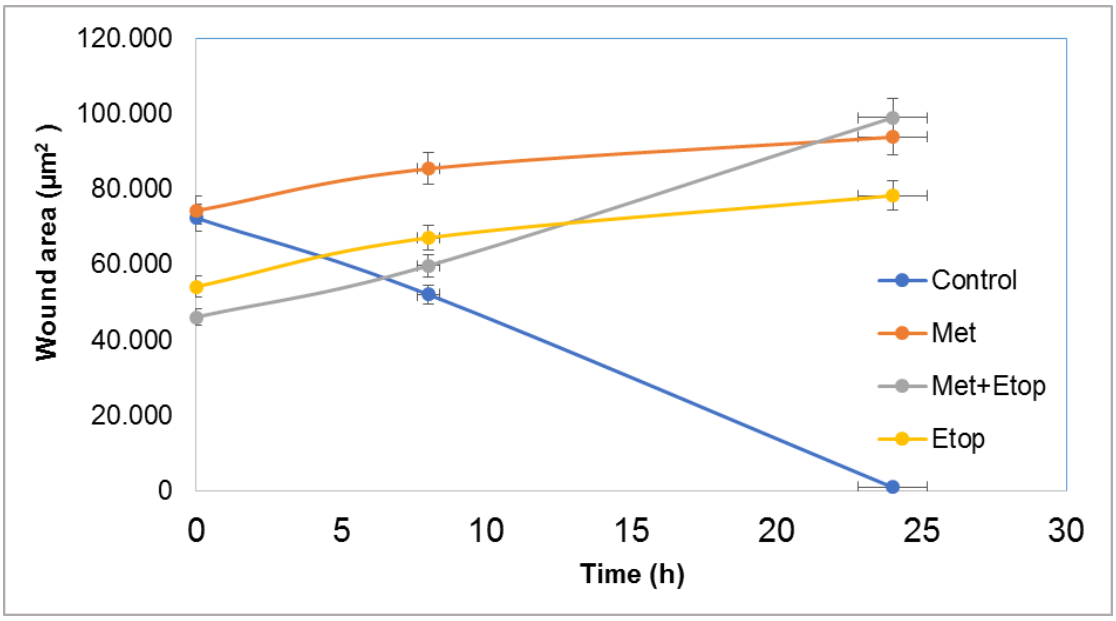


**Figure 4.9.** Wound area change in U87MG cells.

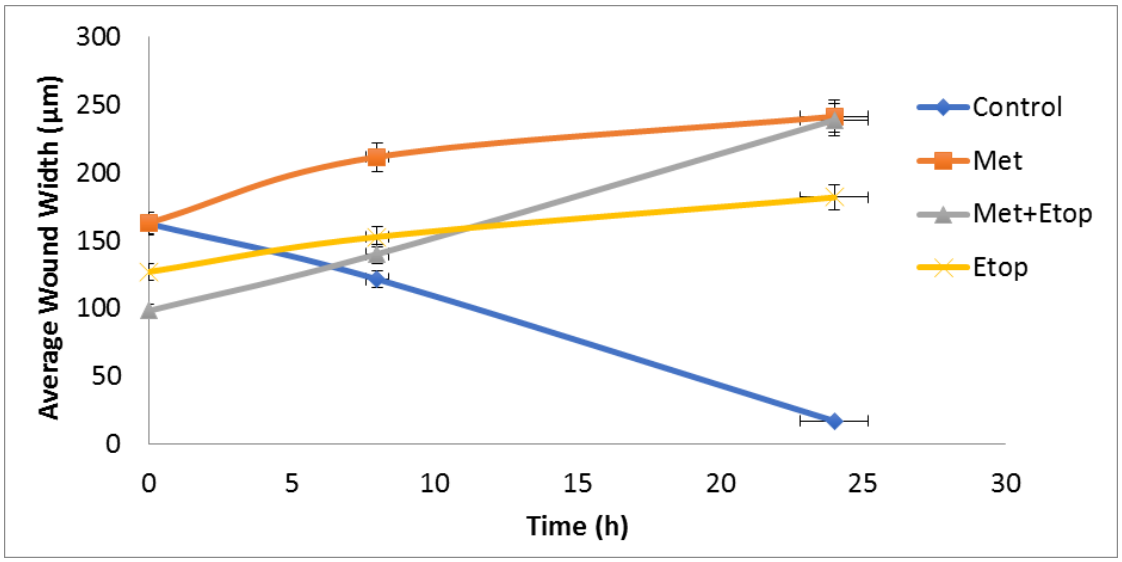


**Figure 4.10.** Average wound width change in U87MG.

The control group exhibited cell migration, leading to wound closure in U87MG cells. In contrast, the experimental groups treated with etoposide and L-methioninase exhibited adverse effects with regard to cell migration and wound closure percentages (Figure 4.11). This observation suggests that treatment with L-methioninase, either alone or in combination with etoposide, may induce cell death, consequently reducing the number of migrating cells.

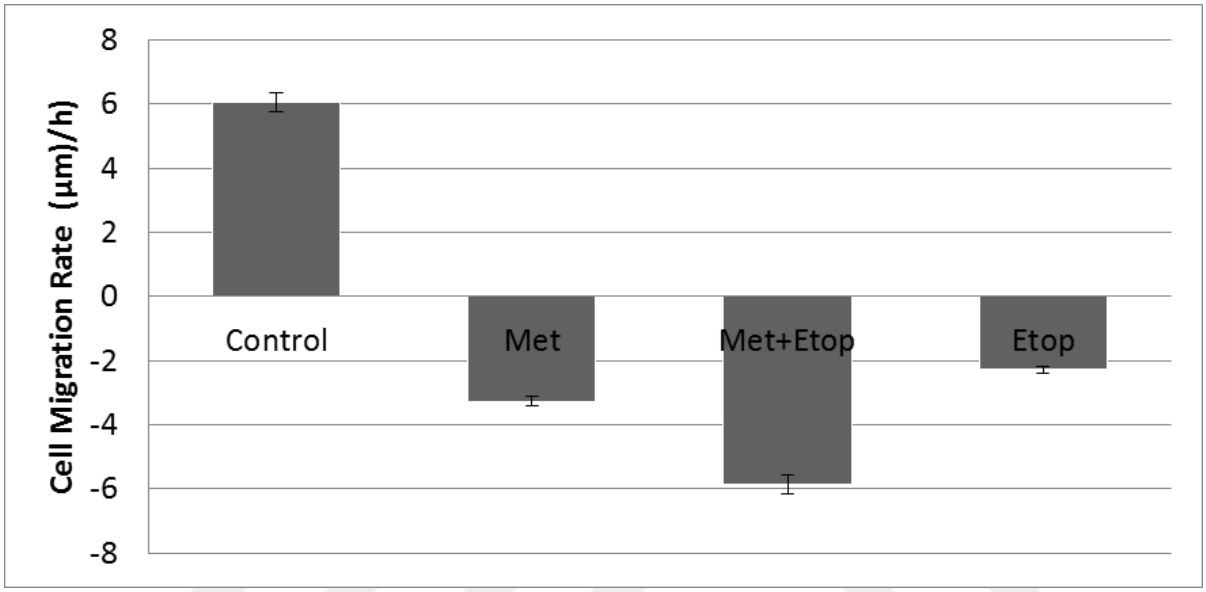


**Figure 4.11.** Cell migration rate for U87MG cells.

Wound healing experiments were repeated in T98G cells, and the findings indicated that etoposide and L-methioninase exhibited properties similar to those observed in U87MG cells. Figures 4.12 and 4.13 depict the changes in wound area and width, respectively. Within 24 h, the wound was completely closed by control cells. However, Figure 4.14 shows that L-methioninase and etoposide prevented wound closure in T98G cells.

In vitro data on cell migration characteristics are crucial for understanding the potential inhibitory effects of L-methioninase in conjunction with etoposide on the mobility of Glioblastoma cells. This information serves as a valuable foundation for guiding future in vivo studies aimed at predicting the impact of metastasis and tumourisation within the human body.

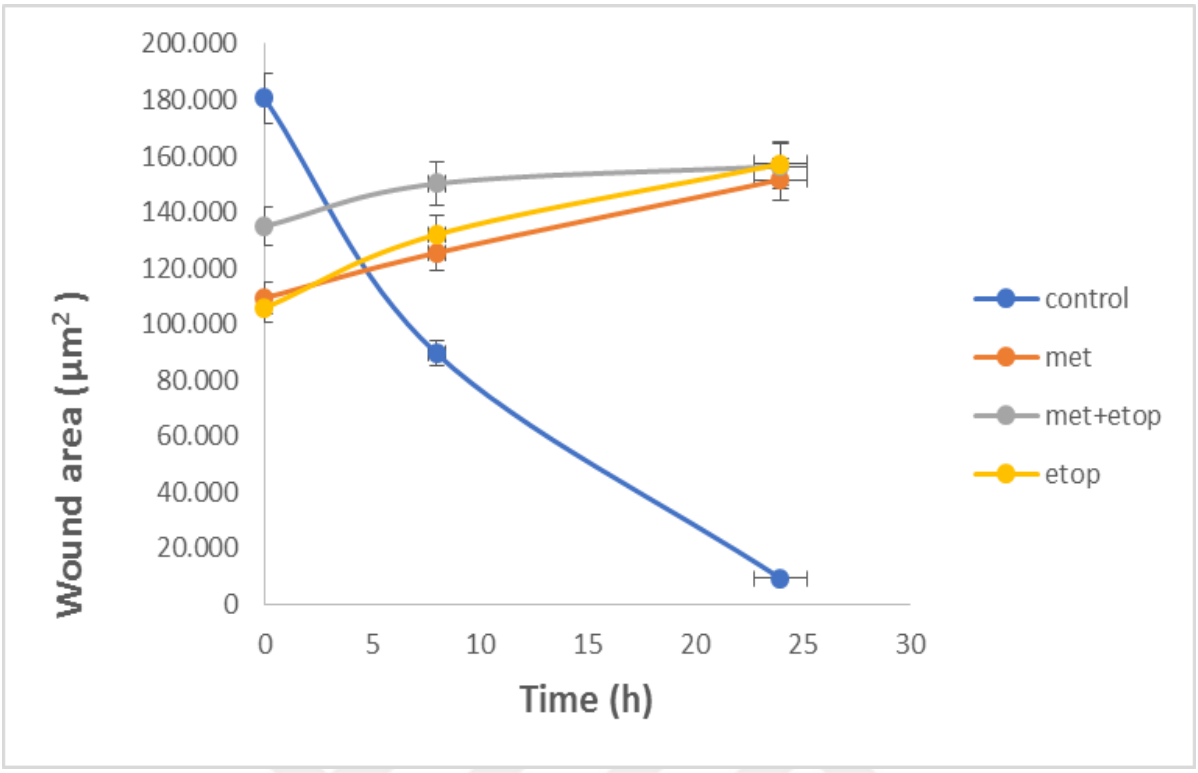


**Figure 4.12.** Wound area change for T98G cells.

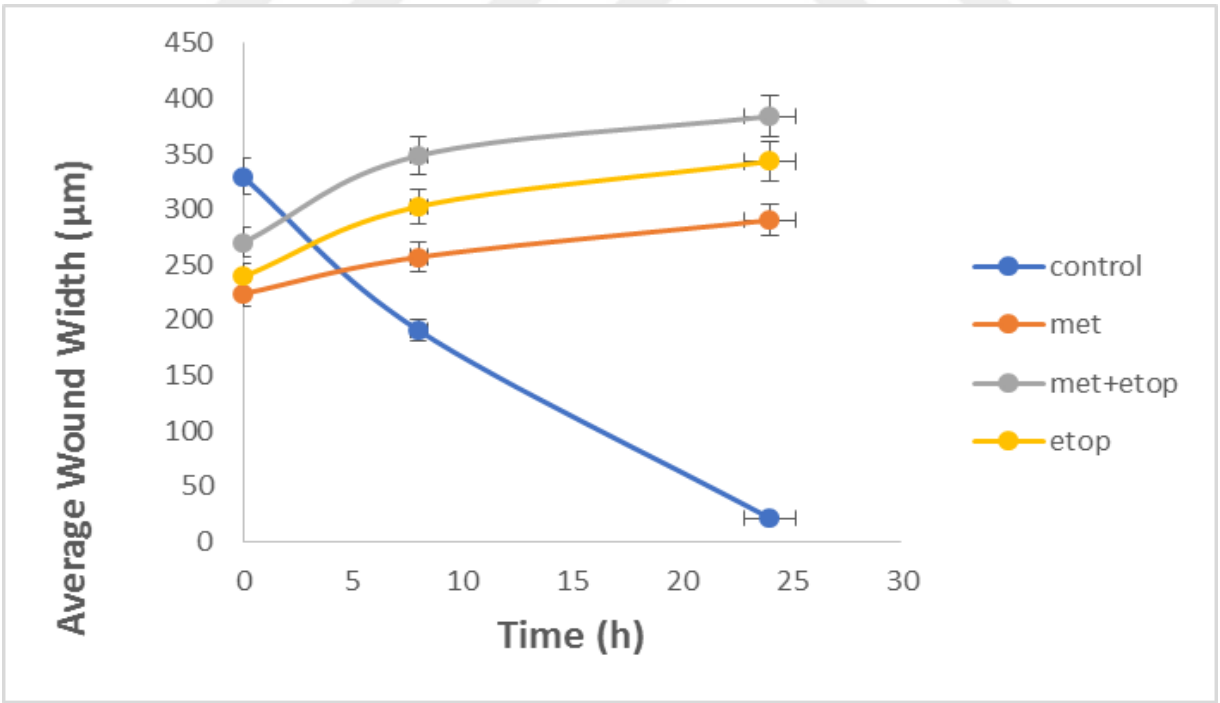


**Figure 4.13.** Average wound width change for T98G cells.

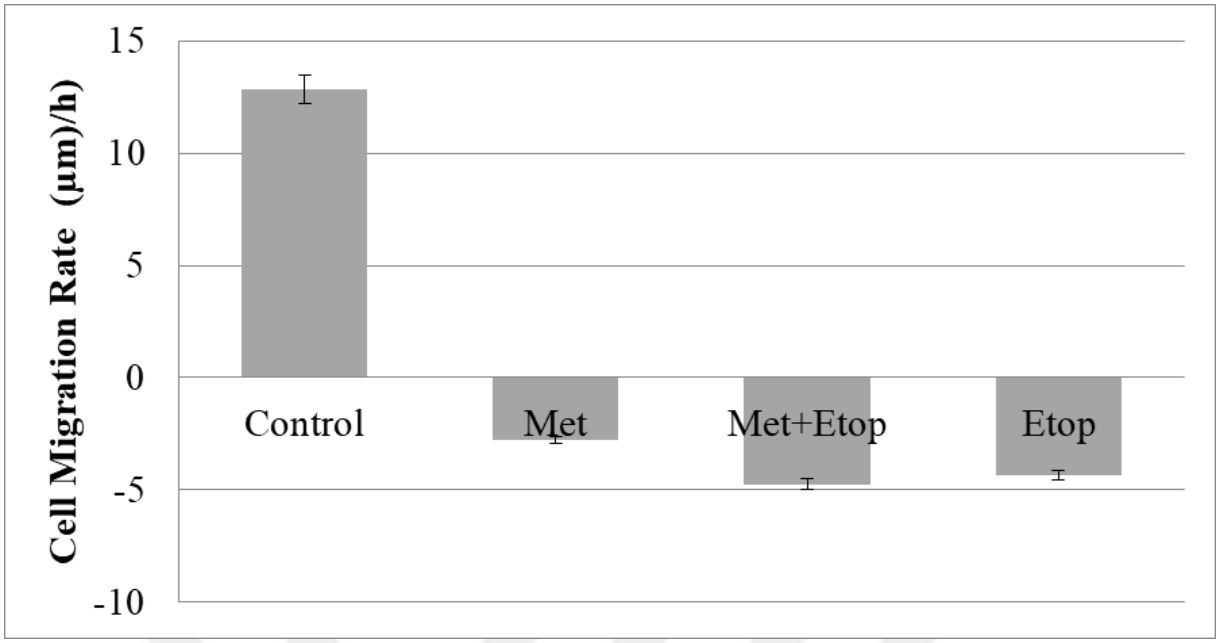


**Figure 4.14.** Cell migration rate for T98G cells.

### 4.7. Giemsa Staining of Glioblastoma Cells after L-Methioninase and Etoposide Administration

Giemsa staining was used to examine the morphology and cytotoxic activity of U87MG and T98G cells following treatment with L-methioninase and etoposide, which induced notable alterations in cell morphology and cytotoxicity. The cells were examined for uniformity and similarity in their properties before Giemsa staining (Figure 4.17 and Figure 4.18). As observed in both Giemsa-stained and unstained cells, the morphology of the cells changed upon administration of L-methioninase (LM) and etoposide. The cells soon lost their star structure and became individual, and cellular adhesion weakened. This change indicates that L-methioninase and etoposide treatment affect the cytoskeletal structure and cellular adhesion of glioblastoma U87MG and T98G cells. Some cells also assumed a rounded form. Cellular stress and triggering of programmed cell death are frequently linked to this shift in cell shape. The rounding up of cells may be an indication that L-methioninase and etoposide have cytotoxic effects on treated cells. The number of cells was also significantly reduced. This suggests that the number of viable cells was significantly decreased as a result of the cytotoxic effects of etoposide and L-methioninase. After Giemsa labeling, both U87MG and T98G cells exhibited altered morphology (Figures 4.15 and Figure 4.16). The cells appeared

weaker and more wounded, resembling the cells in the apoptotic phase. Additionally, the cell intensity decreased owing to the cytotoxic effects of the administered reagents.

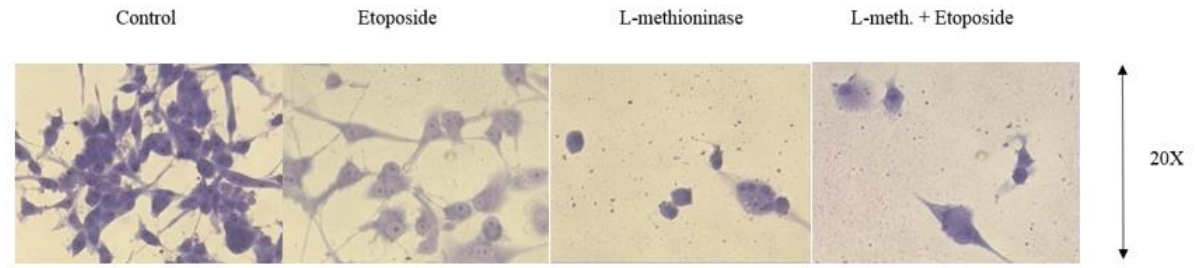


**Figure 4.15.** Giemsa staining images of U87MG cells.

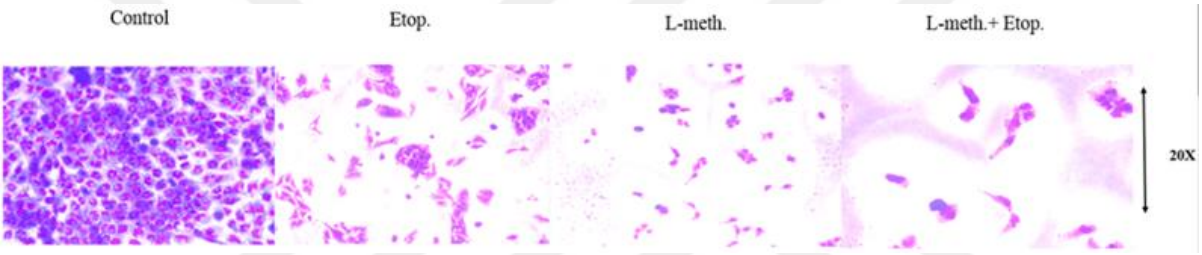


**Figure 4.16.** Giemsa staining images of T98G cells.

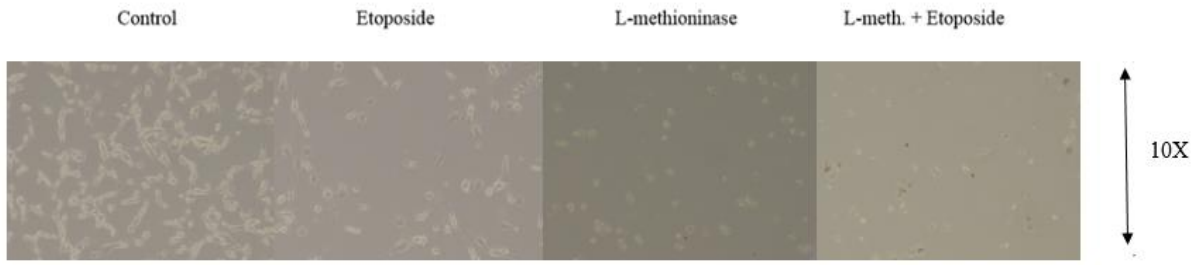


**Figure 4.17.** Normal photos of U87MG cells.

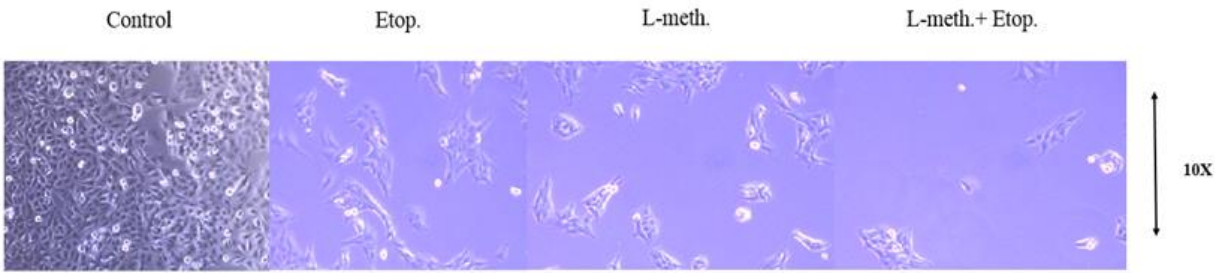


**Figure 4.18.** Normal photos of T98G cells.

Analyzing the alterations in the morphology of Glioblastoma cells following the application of L-methioninase both individually and in combination with etoposide, has yielded a more comprehensive understanding of this topic within the current literature. This research has enhanced our understanding of the apoptotic effects of L-methioninase.

### 4.8. DAPI and F-Actin Staining Results

DAPI and F-actin staining were used to analyze the cellular nuclei and the arrangement of the actin cytoskeleton, respectively, after 24 h of treatment with L-methioninase and etoposide.

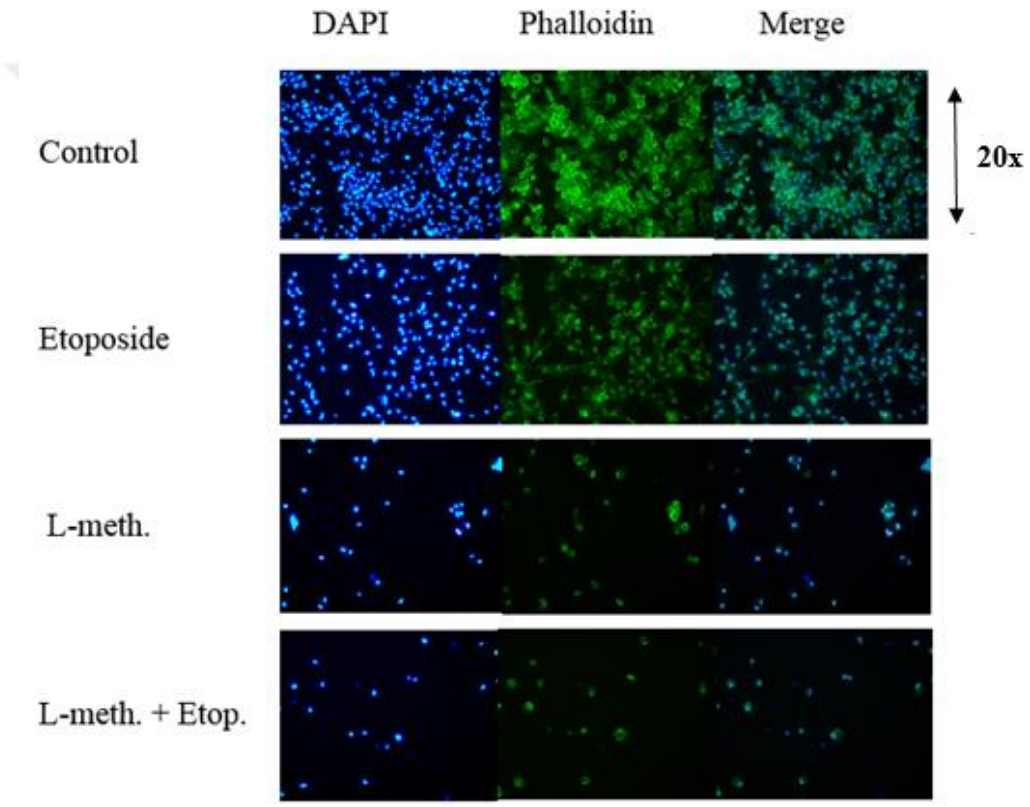


**Figure 4.19.** DAPI and F-actin staining images of U87MG cells.

A decrease in the number of nuclei was observed following L-methioninase treatment. This suggests reduced cell viability or induction of cell death processes such as apoptosis. A rounded form of F-actin filaments, a common feature of apoptosis, was also observed. Furthermore, treatment with L-methioninase and etoposide led to a transition from a star-shaped morphology to a rounded shape, signifying modifications in the cellular structure and potential disruptions in cellular processes. These treatments caused changes in the integrity of

fluorescent nuclei and filaments (Figures 4.19 and 4.20), indicating potential alterations in gene expression, protein levels, or cellular responses in response to the treatments.

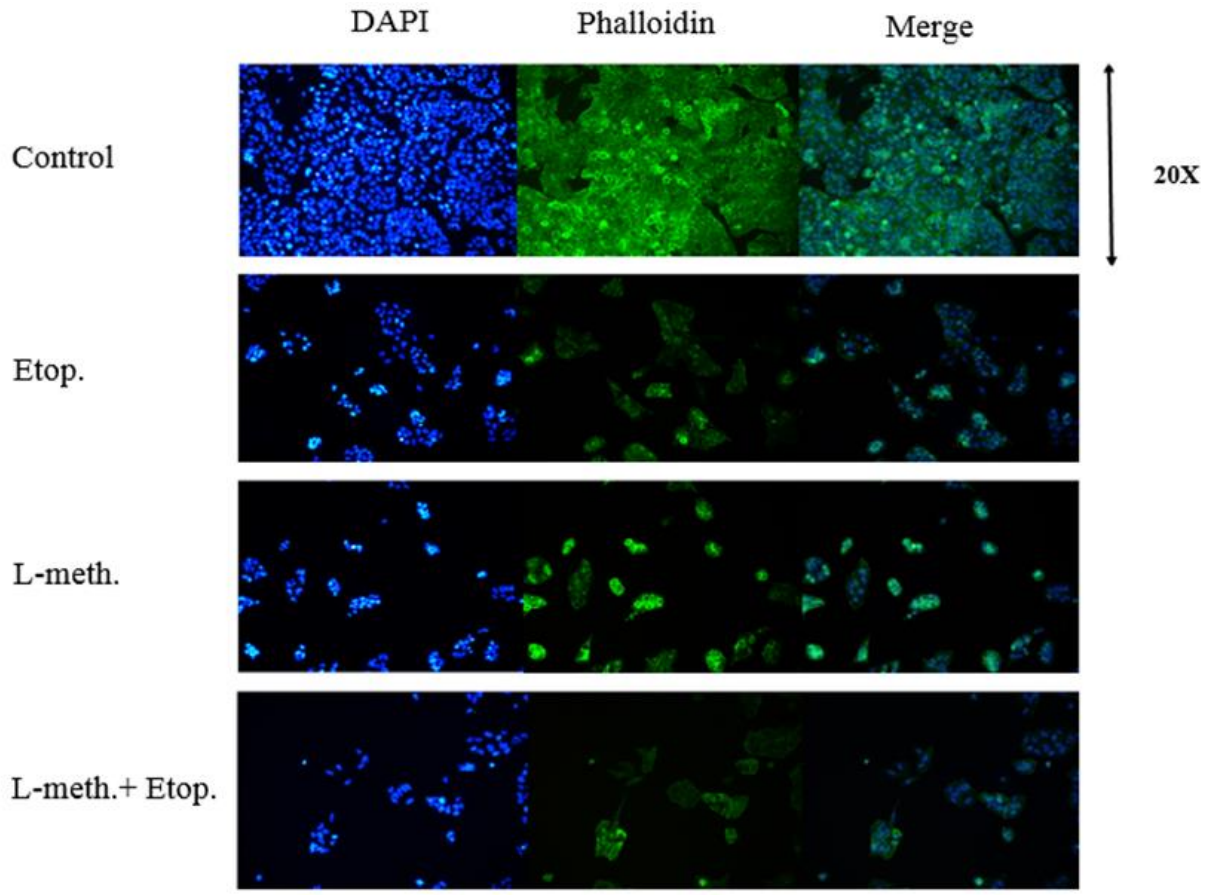


**Figure 4.20.** DAPI and F-actin staining of T98G cells.

Fluorescent images depicting the apoptotic effects of the combination of L-methioninase and etoposide in Glioblastoma cells, especially concerning the nuclei and F-actin filaments, have not been reported in the literature. The observation of apoptotic alterations in both the nucleus and F-actin filaments of Glioblastoma cells significantly increased the depth of this study.

### 4.9. Clonogenic Assay Images and Colony Numbers after L-methioninase and Etoposide Administration

To evaluate the proliferative and clonogenic potential of U87MG and T98G cells treated with etoposide, L-methioninase, or their combination, a colony formation assay was conducted. These results indicated that L-methioninase treatment led to a substantial reduction in colony formation in both U87MG and T98G cells. The number of colonies formed by U87MG and

T98G cells significantly decreased after three weeks of incubation (Figures 4.21 and 4.23). The combined administration of L-methioninase and etoposide reduced the number of colonies to eight in U87MG cells, whereas the control cells formed 41 colonies, as shown in Figure 4.22.

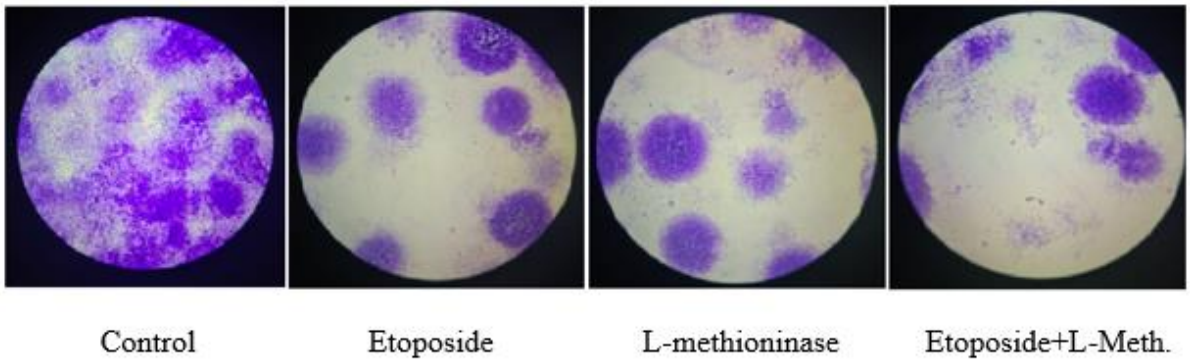


**Figure 4.21.** Colonies of U87MG cells at the end of 21 days.

L-methioninase efficiently inhibited the proliferation of U87MG cells, as evidenced by the significant reduction in colony formation following incubation with the enzyme. This decrease in colony growth demonstrated the suppressive effect of L-methioninase on the proliferative capacity and survival of these cells. Figure 4.22 illustrates the impact of L-methioninase and etoposide on the colony count of U87MG cells.

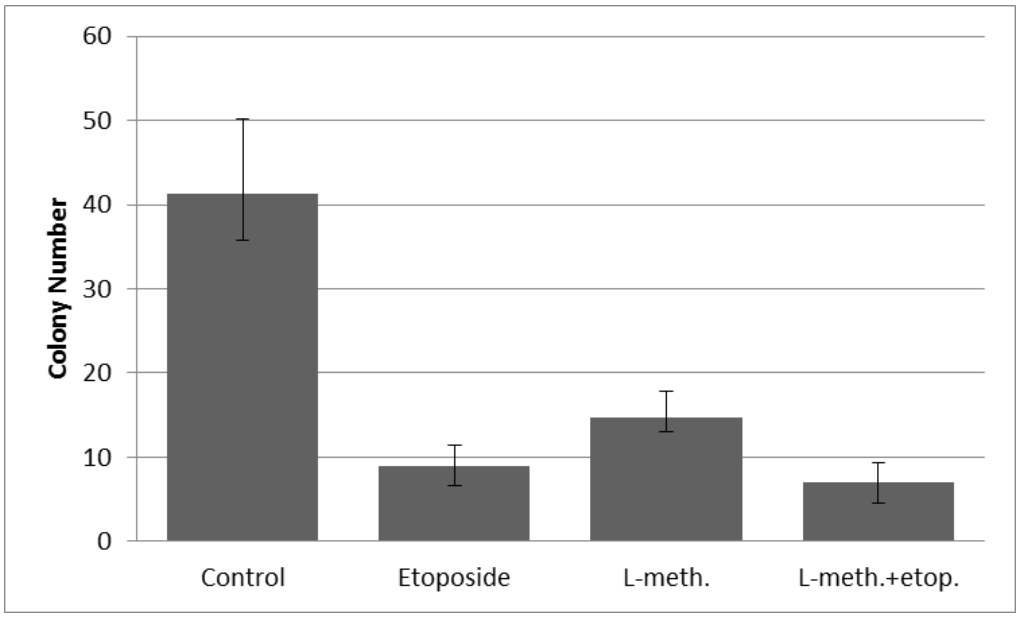


**Figure 4.22.** Colony number of U87MG cells at the end of 21 days.

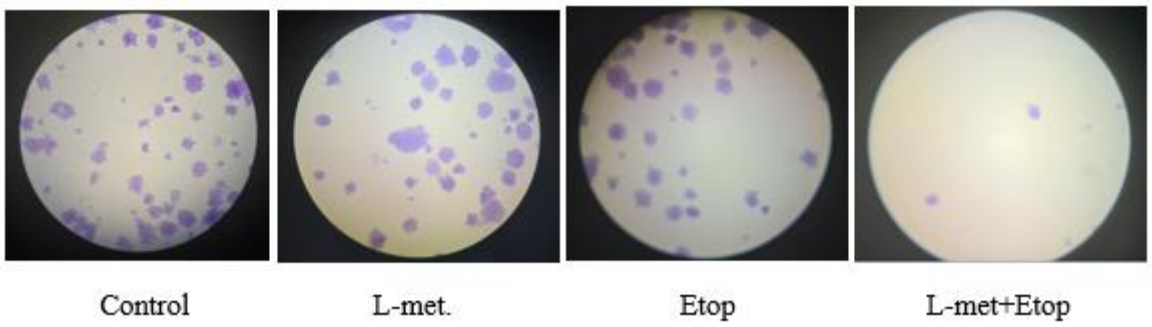


**Figure 4.23.** Colonies of T98G cells at the end of 21 days.

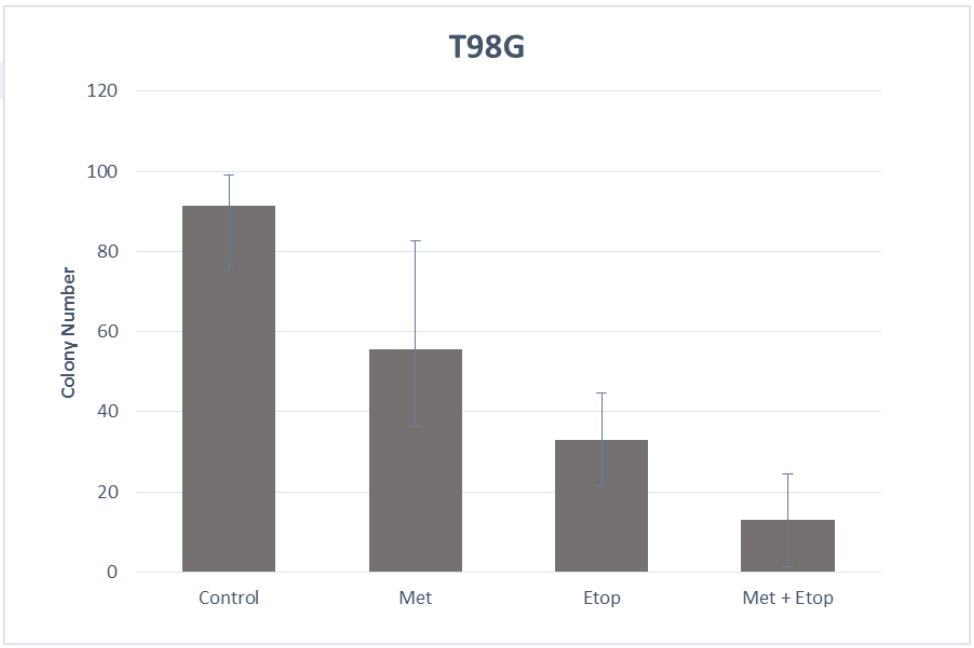


**Figure 4.24.** Colony number of T98G cells.

L-methioninase and etoposide effectively suppressed colony formation by T98G cells, as shown in Figure 4.23. Control cells produced 92 colonies, whereas the combined administration of L-methioninase and etoposide reduced colony formation to 15. When L-methioninase was administered alone, colony numbers were reduced to 56, and etoposide reduced them to 32, as shown in Figure 4.24. L-methioninase efficiently inhibited T98G cell proliferation, resulting in a significant reduction in colony formation. This reduction in colony growth indicates a suppressive effect of L-methioninase on the proliferative capacity and survival of these cells.

There is a lack of studies in the literature regarding colony formation of Glioblastoma cells under the influence of L-methioninase and etoposide. These data provide supplementary insights into the effect of L-methioninase and etoposide on the tumorization behavior of Glioblastoma cells.

### 4.10. RT-qPCR Results

RT-qPCR was used to assess the expression levels of survivin, c-Myc, and caspase 3 genes in U87MG and T98G cells treated with etoposide, L-methioninase, or a combination of both.

When exposed to L-methioninase, etoposide, and the combination treatment, Figure 4.25a demonstrates a significant decrease in survivin expression. Notably, within one day of culture, it was found that the combination of L-methioninase, etoposide, and their combination led to the complete inhibition of c-Myc expression in both U87MG and T98G cells (Figure 4.25b).

The oncogene c-Myc is a pivotal regulator of cell proliferation and is frequently overexpressed in various human carcinomas, including glioblastoma (Jamerson et al., 2004; Cadoret et al., 2005; Liu et al., 2006). Its overexpression often leads to the deregulation of critical cellular processes such as transcription, translation, and protein stability, contributing to the development of malignancies (McEwan et al., 2012; Rehman et al., 2022). Decreased c-Myc expression has been associated with the induction of apoptosis, suppression of cellular proliferation, and cell cycle arrest (Thompson, 1998). In this study, the use of L-methioninase, etoposide, and their combination resulted in complete suppression of c-Myc expression in both U87MG and T98G cells during a 24-hour culture period (Figure 25b). This suggests that the investigated therapeutic interventions influence signaling pathways related to cell growth and division, potentially leading to cell cycle arrest and reduced proliferation rates (Xu et al., 2010).

Survivin, also known as BIRC5 (baculoviral inhibitor of apoptosis repeat-containing 5), is an anti-apoptotic protein that is highly expressed in cancer cells, such as glioblastoma, where it plays a critical role in their survival and resistance to cell death (Mobahat, Narendran, & Riabowol, 2014; Tong et al., 2019). Survivin is involved in the regulation of cell cycle progression, inhibition of apoptosis, and induction of chromosomal instability (Conde et al.,

2017; Sheng et al., 2018). It suppresses the activity of Caspase 3 and 7, key enzymes involved in apoptosis (Shin et al., 2001; Chiou, Jones, & Tarnawski, 2003). Decreased survivin expression is associated with cytotoxic conditions, making it an attractive target for cancer therapies (Khaw et al., 2013; Han et al., 2018; Ozdemir & Göktürk, 2019). Assessment of mRNA expression in U87MG and T98G cells after a 24-hour culture with L-methioninase and etoposide revealed a substantial reduction in survivin expression. Combination therapy with L-methioninase and etoposide nearly completely suppressed survivin expression after 24 h of incubation (Figure 4.25a). This downregulation of survivin expression indicates that these interventions effectively affect the anti-apoptotic pathway, potentially enhancing apoptosis and reducing cell viability.

These results suggest that the combined treatment of L-methioninase and etoposide has a synergistic effect, leading to a significant reduction in the expression levels of c-Myc and survivin. This reduction may contribute to decreased cell proliferation and increased apoptosis in both U87MG and T98G cells, highlighting the therapeutic potential of this combination in targeting the key biochemical pathways involved in cancer cell growth and survival.

Caspase-3 expression level analysis provides insights into the apoptotic response and effectiveness of apoptosis-inducing treatments. In this study, we examined the effects of etoposide, L-methioninase, and their combination on Caspase-3 expression were examined. Notably, when comparing the combination treatment with the individual treatments, we observed an increase in Caspase-3 expression (Figure 4.25c). These findings, which include the downregulation of survivin and C-myc expression, along with the induction of Caspase-3 expression, suggest that the combined treatment of L-methioninase and etoposide has significant potential to induce apoptosis, inhibit survival, and impede the proliferation of glioblastoma cells. These results provide robust support for the therapeutic potential of L-methioninase and its combination therapy strategy in oncology.

The results of RT-qPCR analysis demonstrated that L-methioninase not only exhibits fundamental cytotoxicity against Glioblastoma cells but also exerts cytotoxic effects by downregulating vital genes for cancer cell viability, such as survivin and c-Myc, while upregulating Caspase-3, a gene essential for apoptosis.

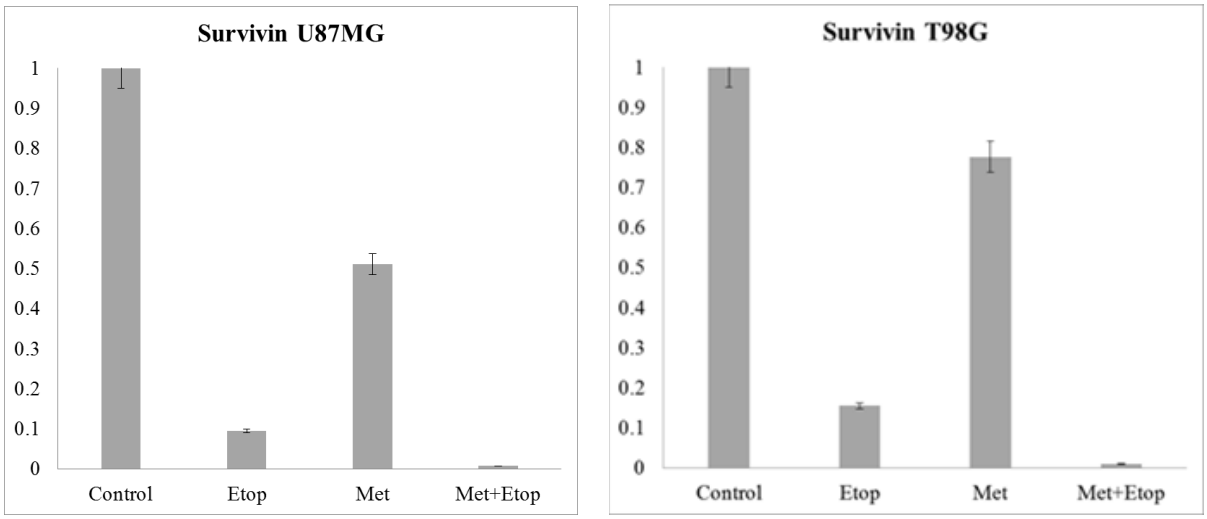


(**a**)

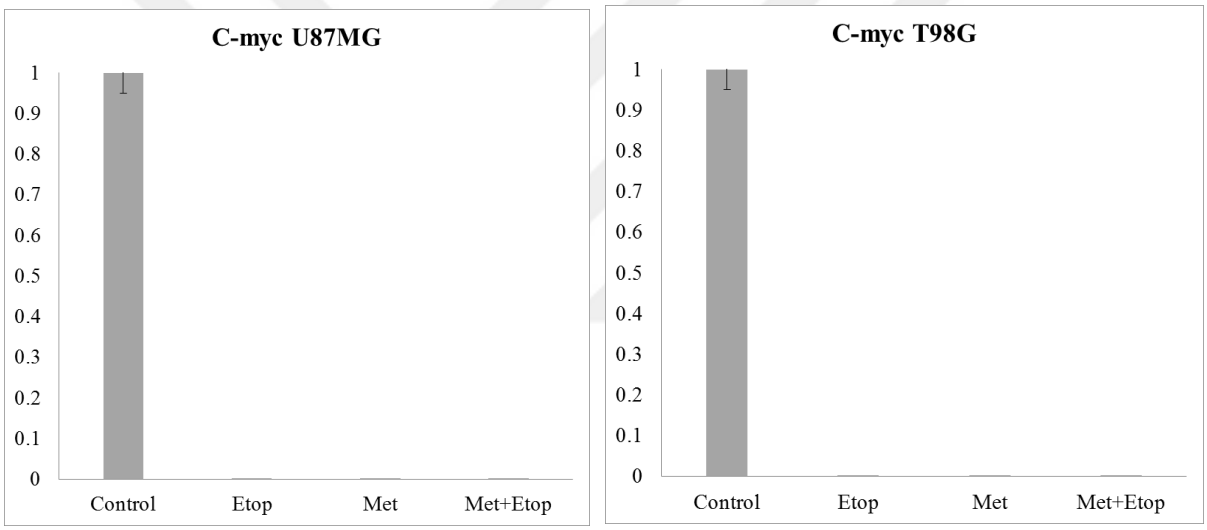


(**b**)

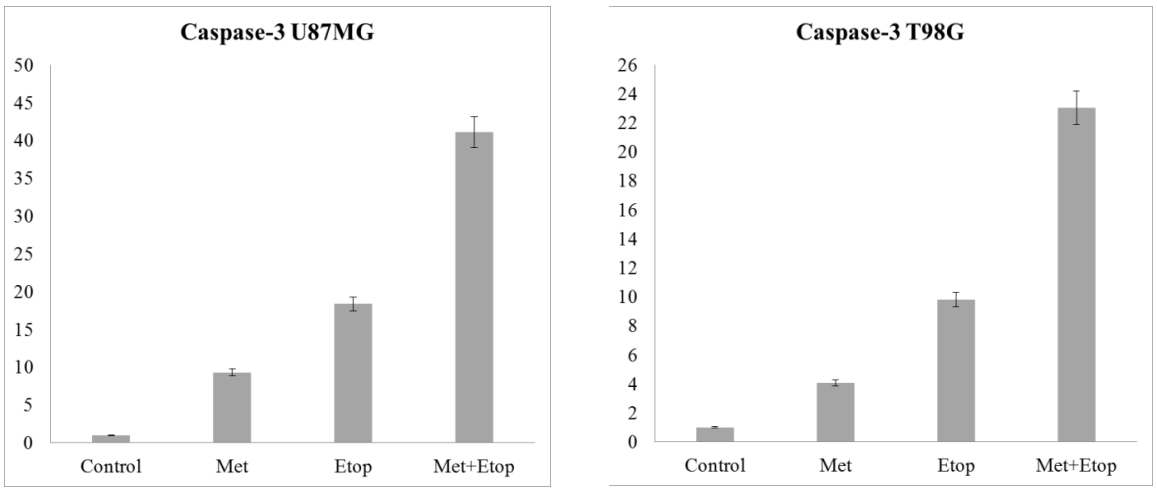


(**c**)

**Figure 4.25.** The relative expression of Survivin (**a**), C-myc (**b**), Caspase-3 (**c**).

L-methioninase shows promise as a potential therapeutic agent for glioblastoma; however, its effectiveness can be influenced by the complexity of glioblastoma tumors and tumor microenvironment. Challenges include the blood-brain barrier, which hinders the delivery of therapeutic agents and may lead to immune system interference that can degrade or neutralize enzymes. Tumor heterogeneity further complicates matters, resulting in varying responses to treatment. Overcoming these obstacles necessitates a comprehensive understanding of glioblastoma biology, its microenvironment, and the interactions between tumor cells and their surroundings. Innovations in drug delivery methods are crucial to improving drug delivery as they enable more effective delivery of L-methioninase and other treatments to the tumor site.Previous studies have documented glioblastoma cells as methionine-dependent (Kawaguchi et al., 2018; Hoffman, 2017; Guo et al., 1993) andvarious cancer studies have mainly used recombinant L-methioninase from *Pseudomonas putida*; the current study emphasizes the effectiveness of L-methioninase from *Brevibacterium linens* on Glioblastoma cells Importantly, the utilization of food-grade bacterium-derived L-methioninase in this study holds promise for its future application as a safe and readily available therapeutic agent on Glioblastoma cells.

This study revealed that L-methioninase exhibited cytotoxic effects on Glioblastoma cells and significantlyprevented etoposide-induced cytotoxicity in both human and mouse cells. In a study conducted by Machover et al. (2019), recombinant methioninase from *Brevibacterium linens* demonstrated potent cytotoxicity against 33 of 35 cancer cell lines, including those associated with colorectal carcinoma, hepatocellular carcinoma, acute promyelocytic leukemia, ovarian adenocarcinoma, and lung adenocarcinoma. These findings suggest that L-methioninase has the potential to be utilized in the treatment of various cancer types and could be considered as a promising candidate for cancer therapy.

## 4.11. Results for evaluation of the effect of the use of L-Methioninase from *Brevibacterium linens* BL2 on microbial community shift and volatile sulfur compound development in raw milk Cheddar cheese slurries

### *4.11.1. Evaluation of total viable bacterial count and total lactic acid bacterial count*

Total viable bacterial count and total lactic acid bacteria count analyses were conducted to assess changes in microbial numbers over a nine-day period. The results of these counts are illustrated in Figure 4.26 and Figure 4.27. Notably, the populations of viable and lactic acid bacteria appeared to stabilize after approximately 3-4 days of fermentation.

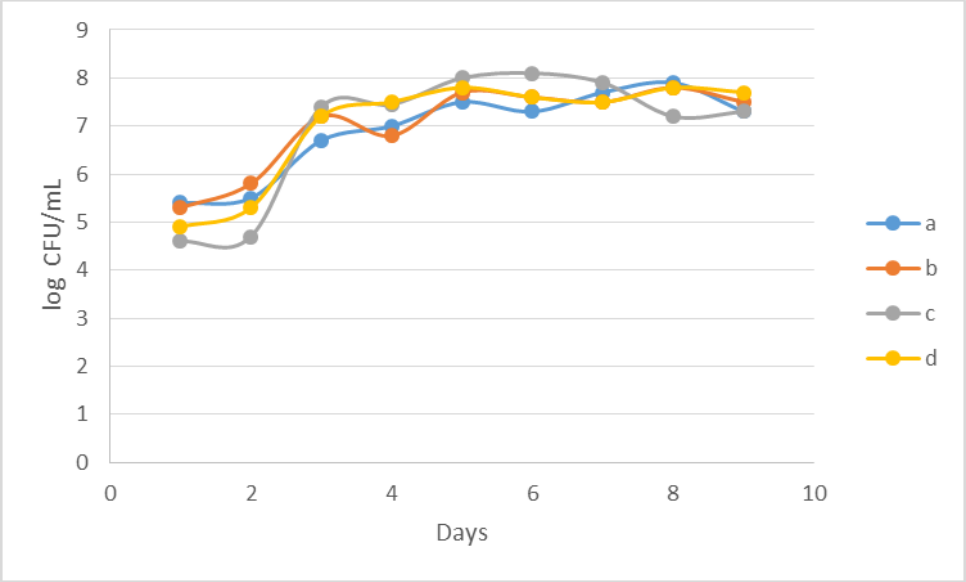


**Figure 4.26.** Total Viable Bacteria Count in Cheddar Cheese Slurries during nine days fermentation. Values on the graph are the mean of triplicate measurements.

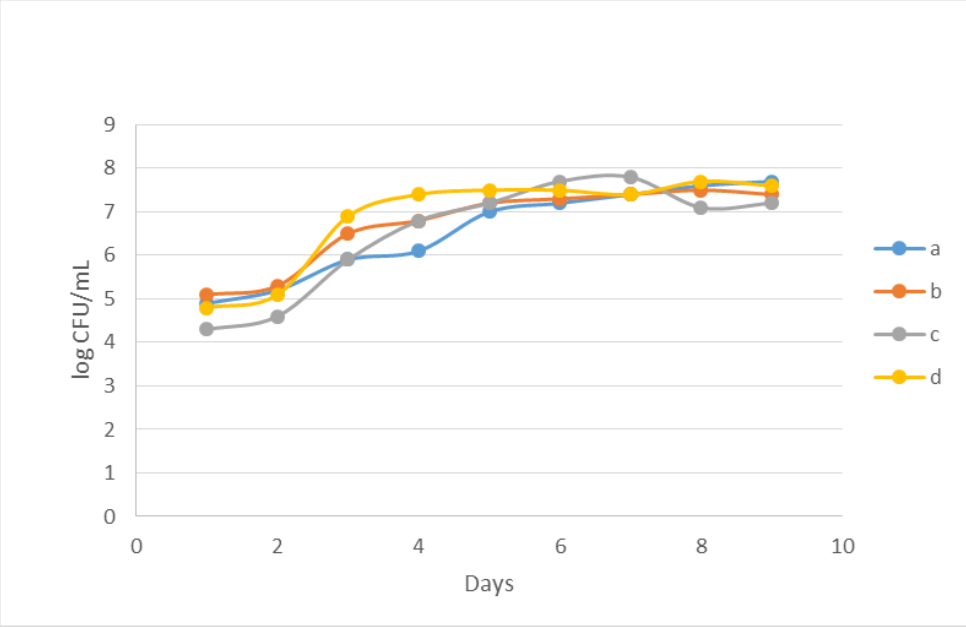


**Figure 4.27.** Lactic Acid Bacteria Count in Cheddar Cheese Slurries during nine days fermentation. Values on the graph are the mean of triplicate measurements.

### 4.11.2. PCR and Gel Electrophoresis

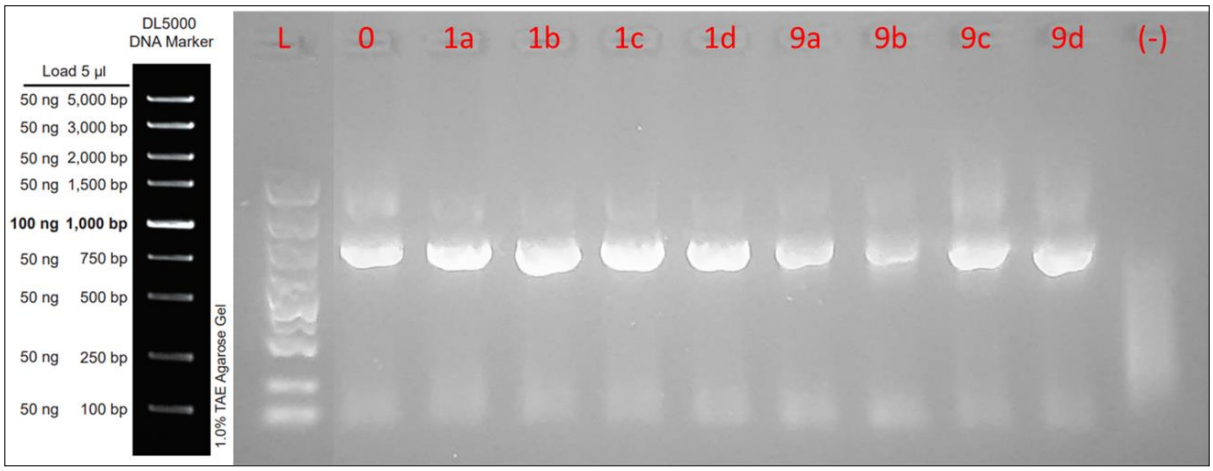


**Figure 4.28.** Electrophoresis image. The running amplicons from cheese slurry samples, which appear as intense bands. L: ladder, 0:sample at zero day, a is control, b is control plus methionine, c is methionine plus *Brevibacterium linens*, and d is methionine plus L-methioninase. 1 and 9 stand for one and nine days of incubation. For electrophoresis, the DL5000 DNA Marker (catalog number: MD102) was employed**.**

DNA fragments isolated from the cheddar cheese slurry samples were confirmed by PCR and Gel Electrophoresis. The running amplicons are shown in Figure 4.28. The presence of intense bands indicated the successful completion of the DNA isolation process.

### 4.11.3. Next Generation Sequences Analyses

In this section, the samples labeled a, b, c, and d were evaluated in terms of bacterial abundance based on the results obtained from next-generation sequencing. Sample a represents the control slurry, sample b contains only methionine in the slurry, sample c contains methionine along with *Brevibacterium linens* BL2 in the slurry, and sample d contains methionine combined with L-methioninase enzyme in the slurry. Moreover, the samples were compared on days 1 and 9 to assess changes in the microbial community. Figure 4.29 visually represents the percentage distribution of bacteria in the samples. Lactococcus appeared to have an approximately equal distribution across each sample. However, the distribution of the other bacteria varied among the samples. Figure 4.30 displays a bar graph, where each bar represents a sample, showing the distribution of bacteria

for each sample. Streptococcus spp. experienced a significant decrease after one day of incubation. This graph illustrates the changes in bacterial distribution over time in different samples.

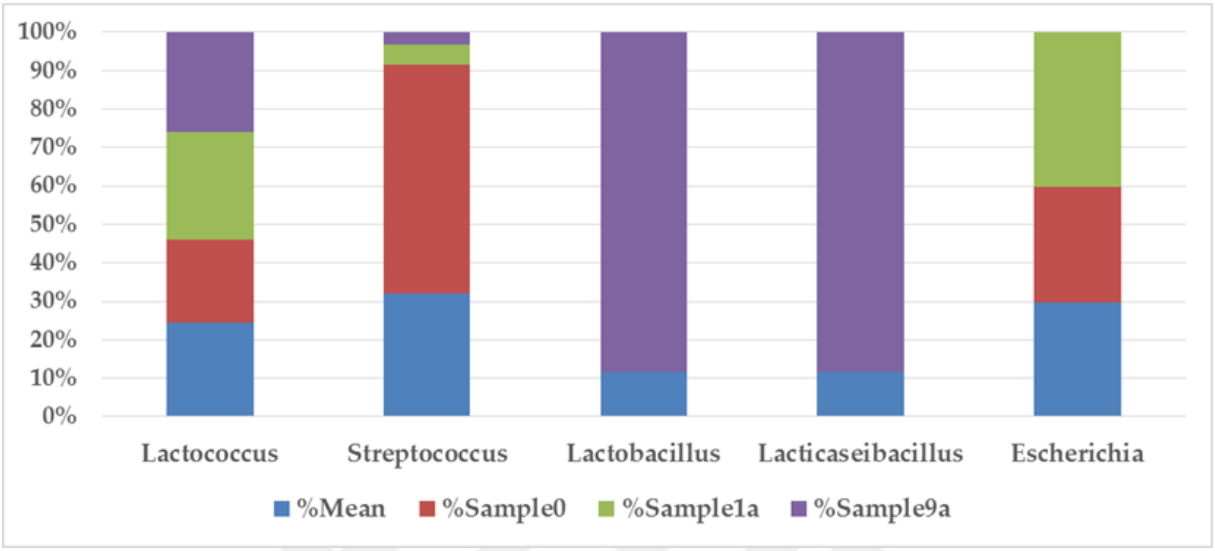


**Figure 4.29.** Percent abundance comparison of Bacteria species between samples for sample a.

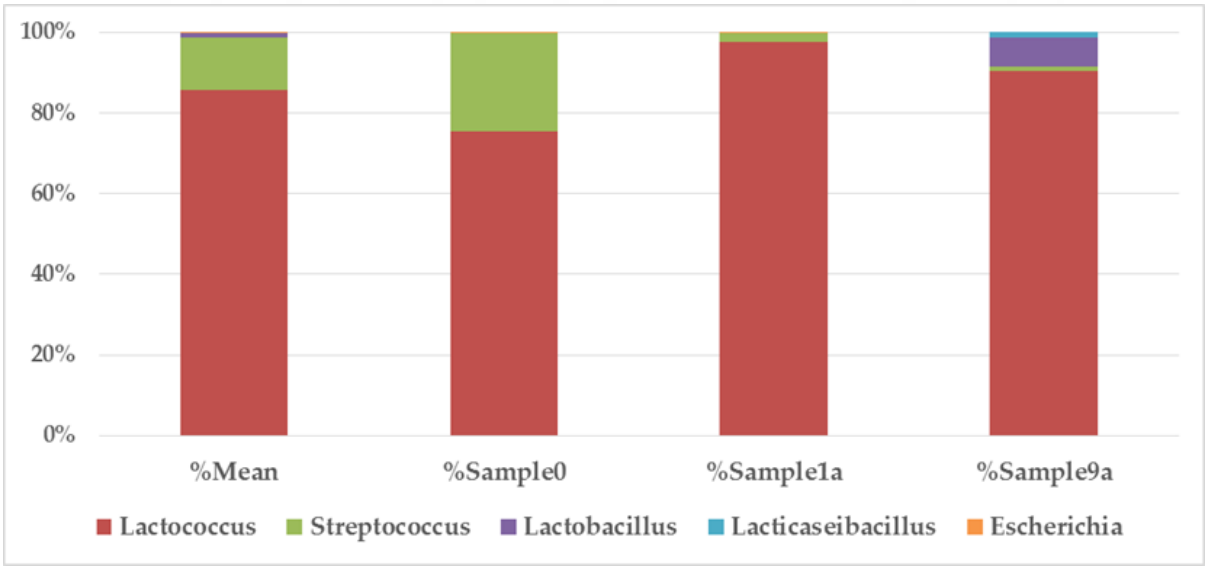


**Figure 4.30.** Variation in the bacterial population distribution over time in sample a.

Cheddar cheese slurry was prepared from raw milk. Therefore, a number of different bacteria have begun to grow in cheese slurries during fermentation. This is important because it reveals the true time span in which the L-methioninase enzyme can be applied to develop

volatile sulfur compounds for industrial purposes. As the fermentation process progresses, the microbial composition of cheese samples can change significantly, influenced by factors such as the quality of raw milk and the presence of other nutrients.

Figures 4.31 and 4.32 provide insights into the changes observed in sample b. It is evident that the addition of methionine dramatically increased the diversity of the microbiota after 9 days of incubation. At zero and one day of incubation, the characteristics were similar to those of sample a. However, by the ninth day, a considerable number of different bacteria had emerged, including *Lacticaseibacillus*, *Limosilactobacillus*, *Enterococcus*, and undesired bacteria such as *Listeria*. This suggests that the application of L-methioninase should occur in the early stages of cheddar fermentation, as prolonged incubation can lead to the growth of various bacteria, including undesirable bacteria. Similar patterns are observed for samples c and d. The bacterial distribution of sample c is shown in Figures 4.33 and 4.34. Although *B. linens* was detected in this sample, its growth was limited despite the addition of methionine. This limitation might be due to the acidic environment of the cheddar cheese slurry, which is not conducive to the growth of *B. linens* (Fox et al., 2017). The bacterial diversity of sample d can be seen in Figures 4.35 and 4.36. The diversity on day is similar to that of sample c. The most diverse microbial community was detected on the ninth day in sample b.

The addition of methionine might have accelerated the growth of a more diverse bacterial population, whereas *B. linens* and L-methioninase could have suppressed this formation. These findings underscore the importance of timing when L-methioninase is applied during cheddar cheese fermentation.

Several bacteria can originate from the cow's skin or other body parts, as well as from the farm environment. The main goal of this study was to develop an optimal L-methioninase application without harming the natural microbiota of raw milk. In Sample a (control slurry), *Lactococcus* and *Streptococcus* were the dominant lactic acid bacteria throughout the 9 day fermentation. On the nineth day, *Lactibacillus* and *Escherichia* species were identified. *Lacticaseibacillus* is a probiotic bacterium found in several types (Barzideh et al., 2022; Mohamed et al., 2023).

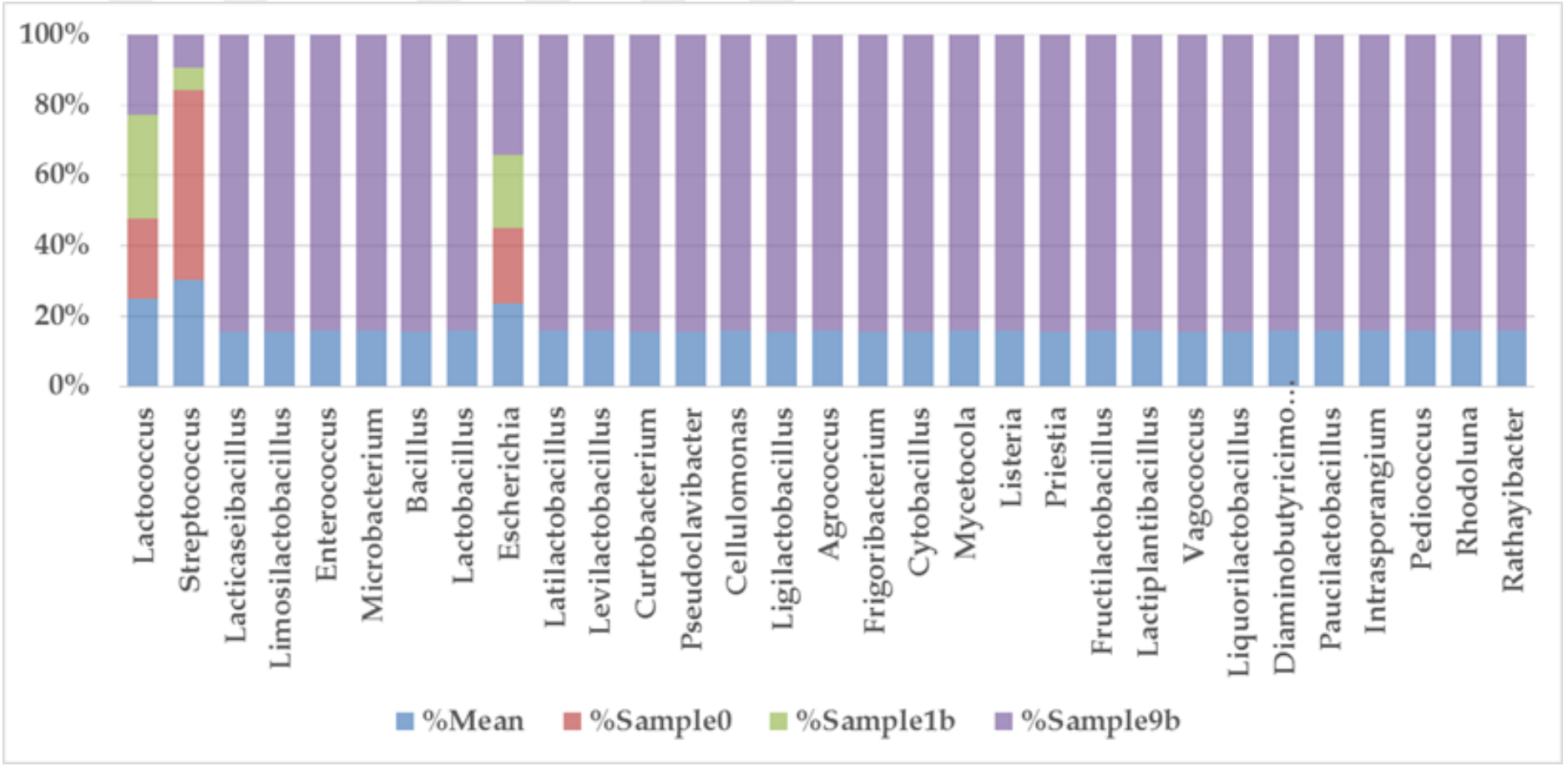


**Figure 4.31.** Percent abundance comparison of Bacteria species at different days for sample b.

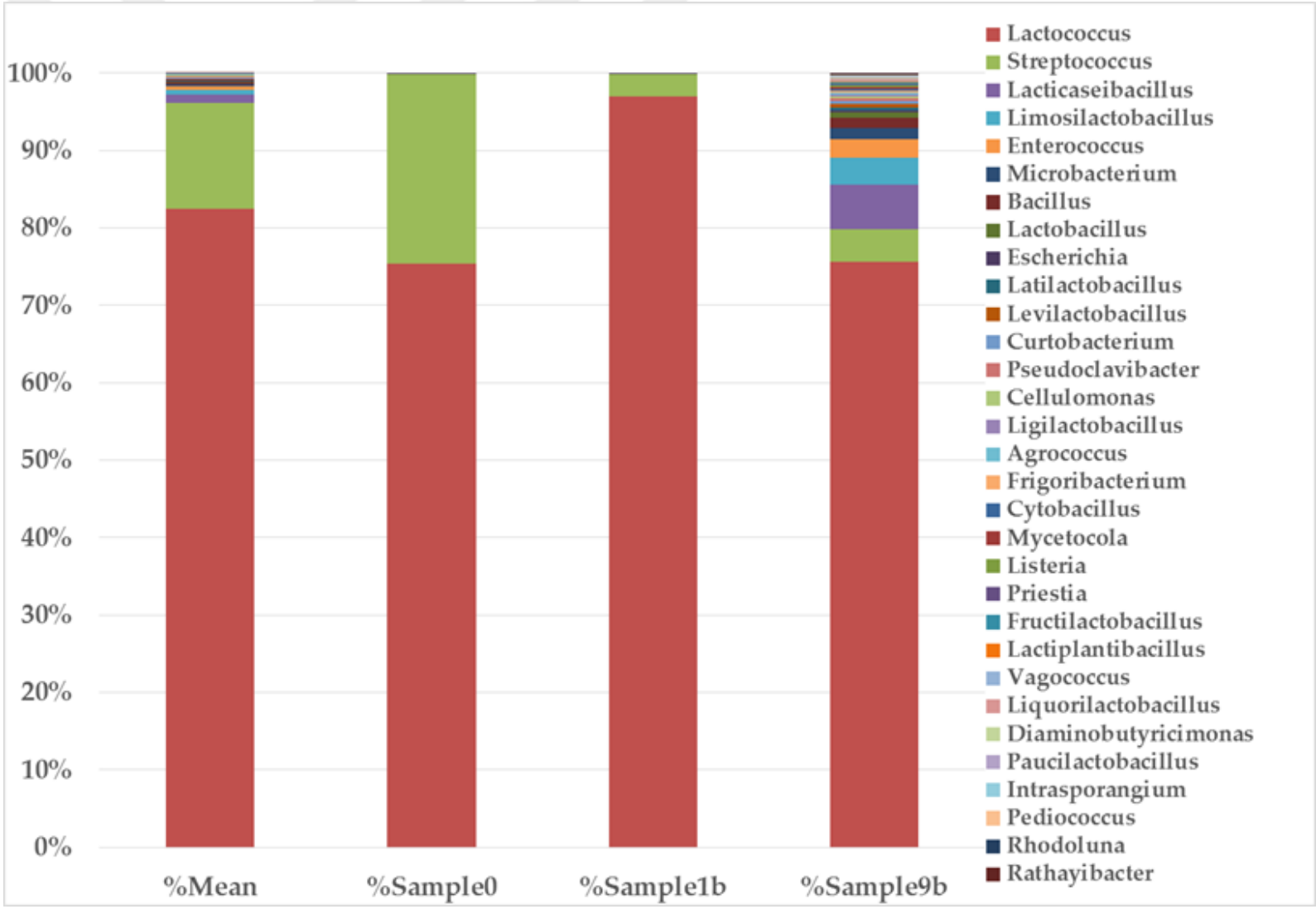


**Figure 4.32.** Variation in the bacterial population distribution over time in sample b.

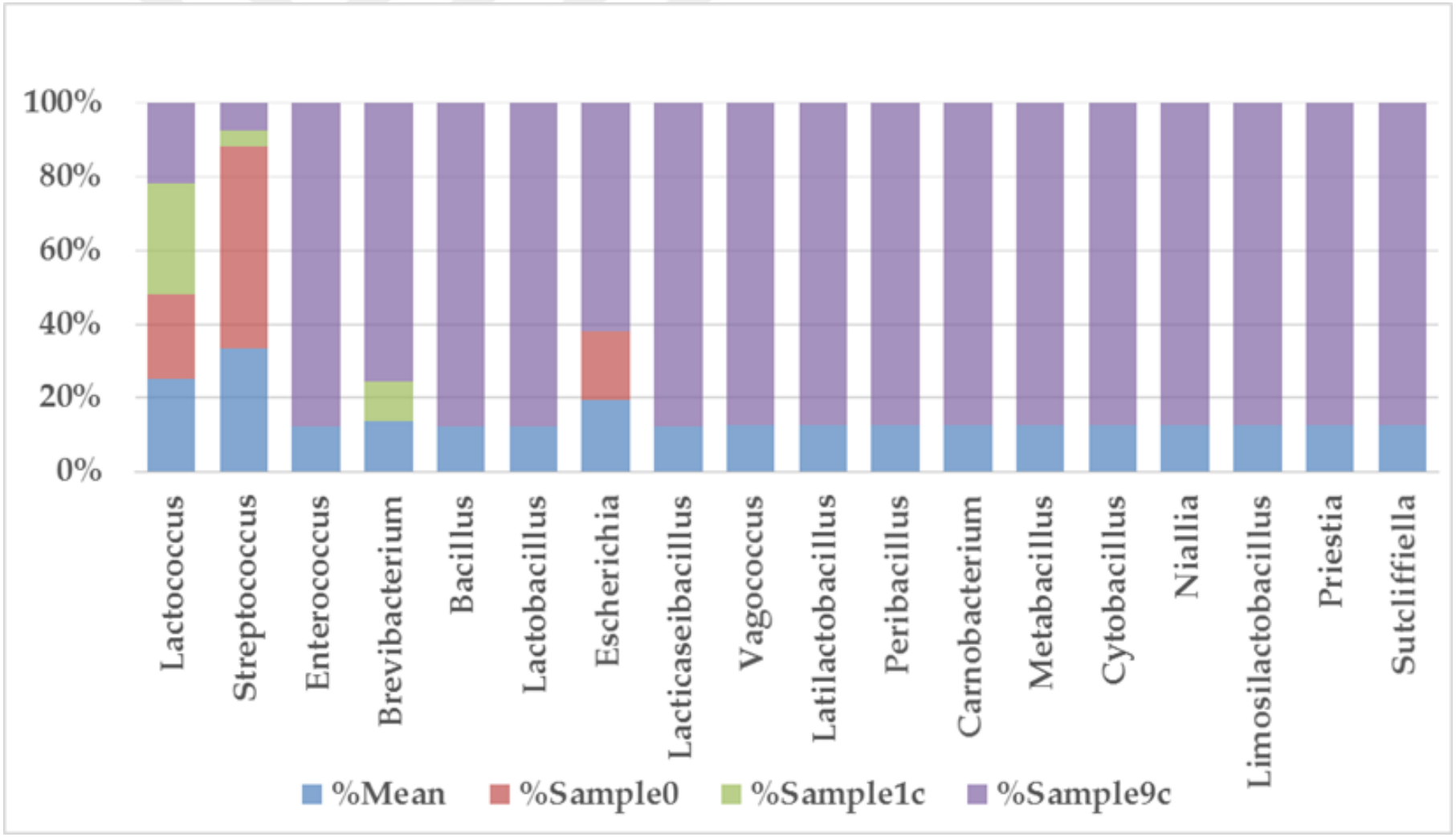


**Figure 4.33.** Percent abundance comparison of Bacteria species at different days for sample c.

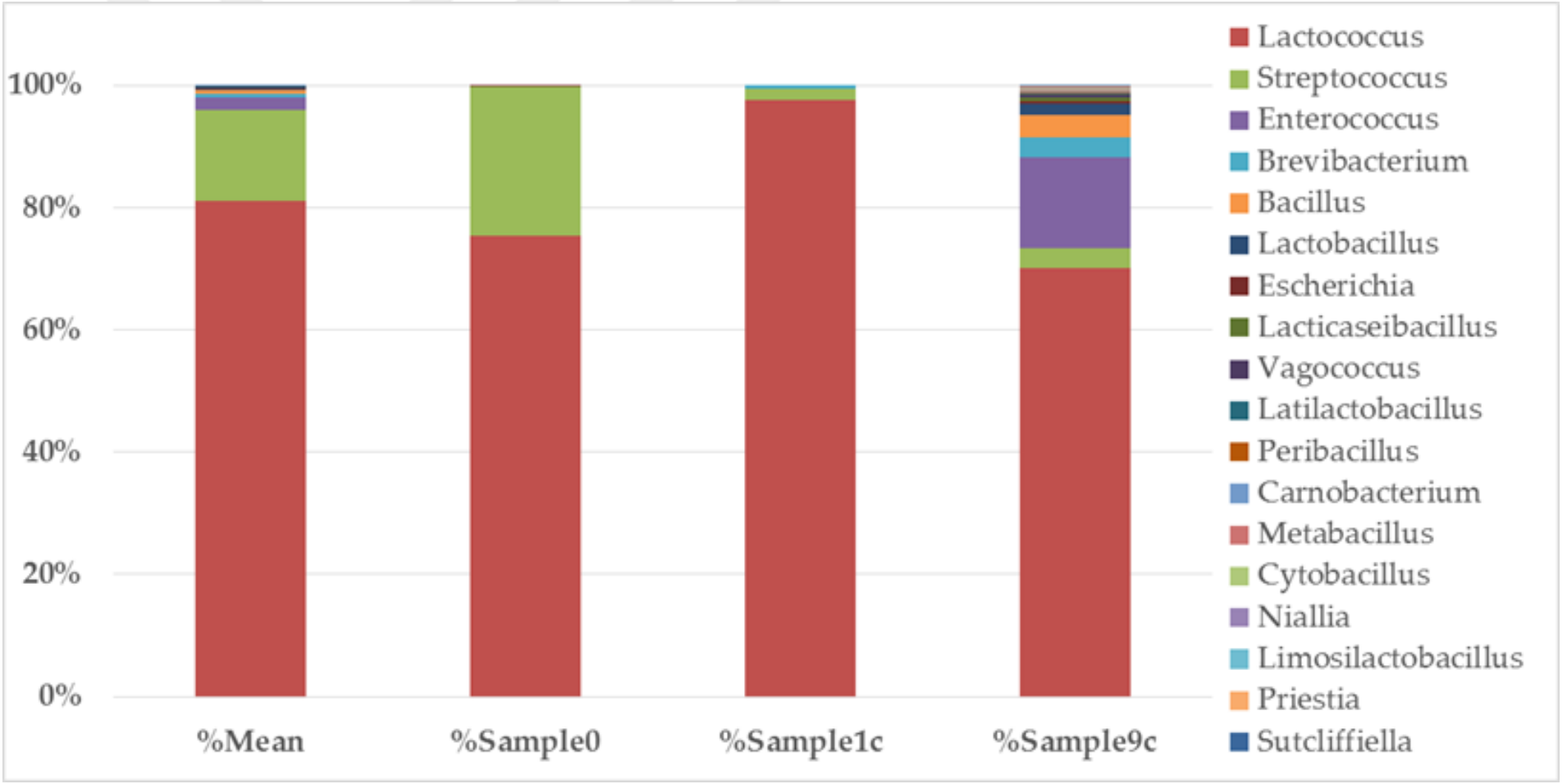


**Figure 4.34.** Variation in the bacterial population distribution over time in sample c.

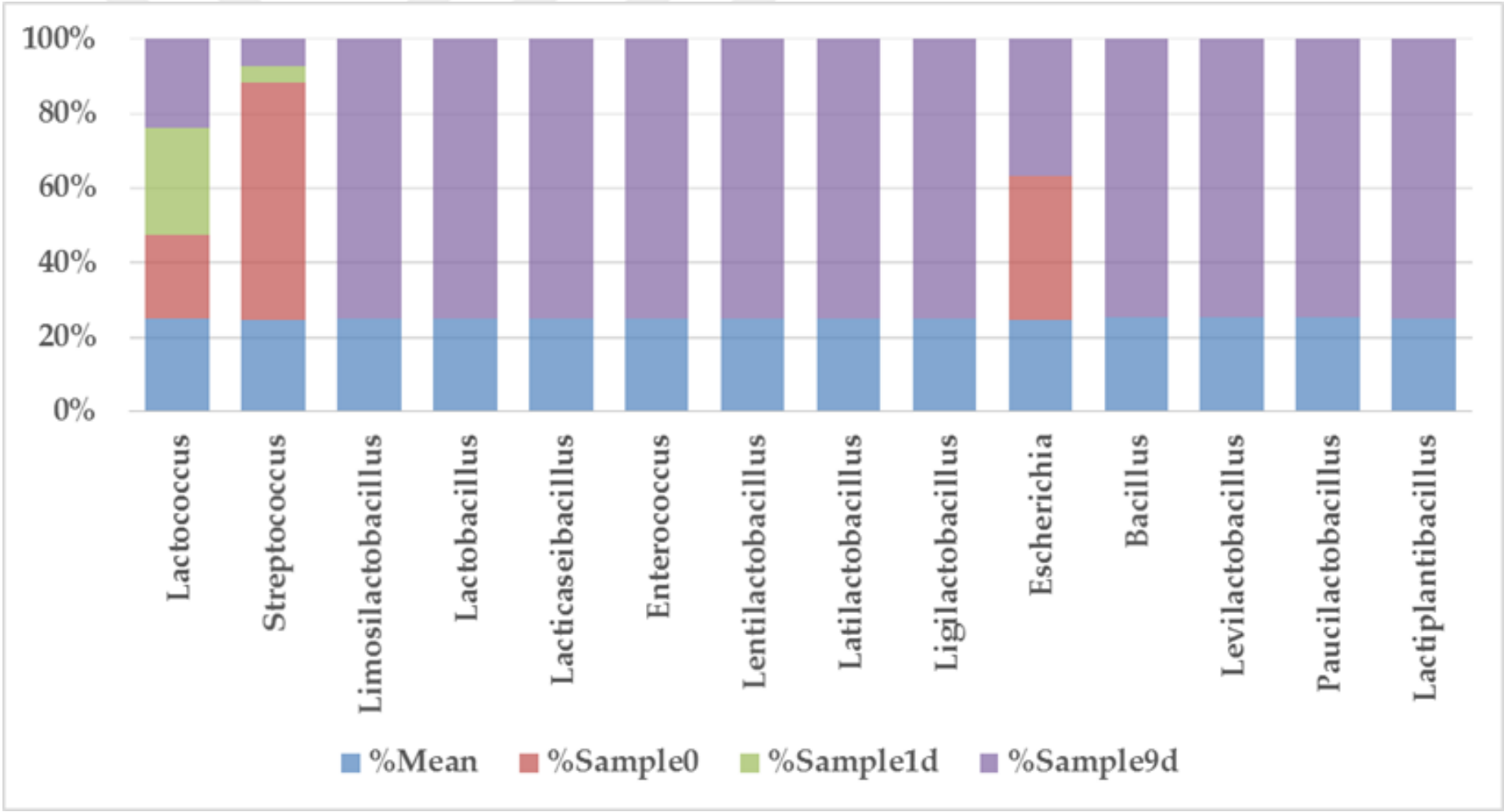


**Figure 4.35.** Percent abundance comparison of Bacteria species at different days for sample d.

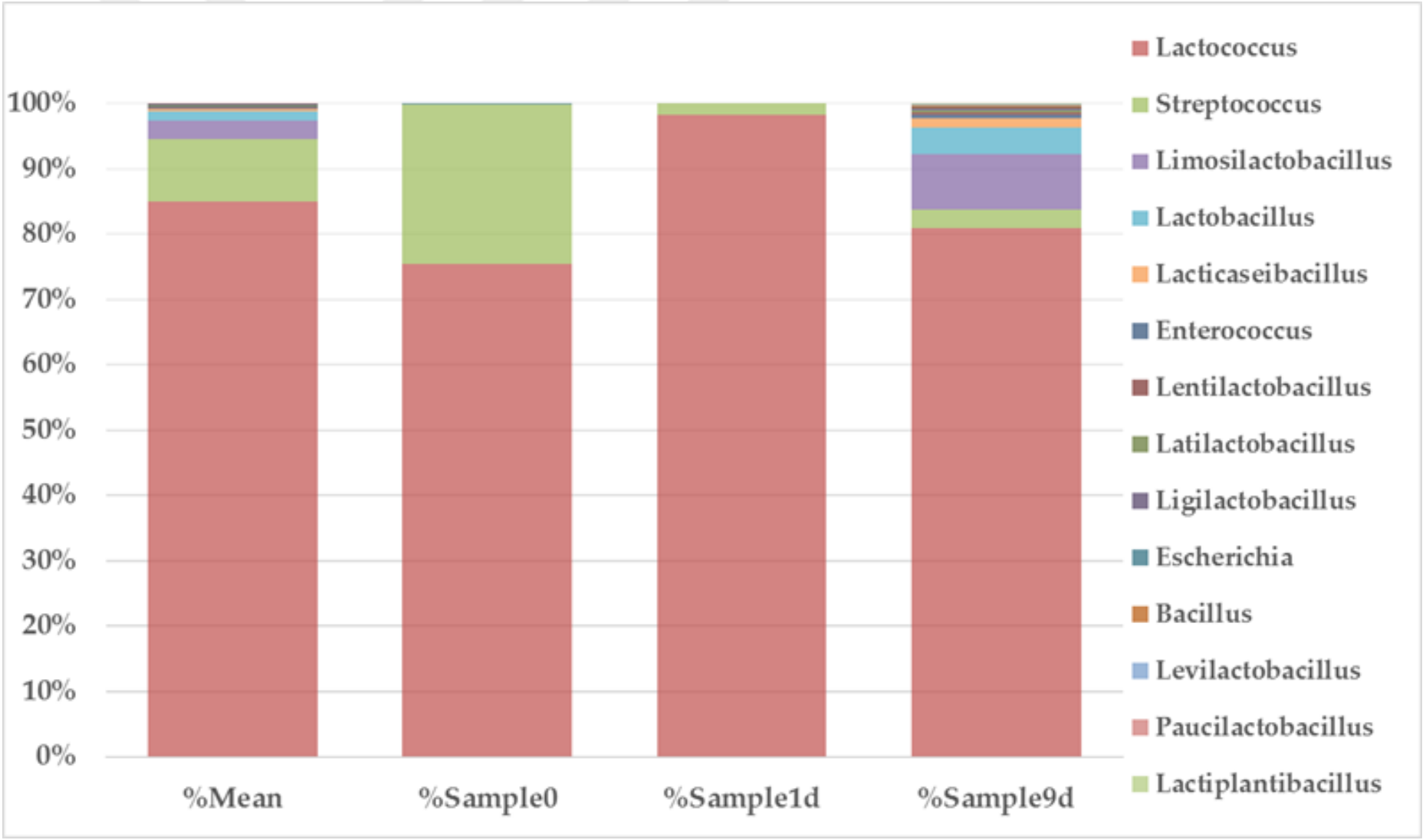


**Figure 4.36.** Variation in the bacterial population distribution over time in sample d.

A normal distribution of lactic acid bacteria was observed in the zero sample of sample b (control slurry + methionine) and on the first day of sample b. However, on the ninth day, various bacteria were observed. This might stem from the addition of methionine to sample b. *Limosilactobacillus fermentum* is a lactic acid generally found in fermented milk products with high textural and sensory qualities (Pakroo et al., 2022).

Sample c (control slurry + methionine + *Br. linens*) had a similar bacterial population distribution at zero and 1 d of fermentation with samples a and b. Less bacterial diversity was observed on the ninth day compared to sample b. This might be because *Brevibacterium linens* BL2 limited the growth of some bacterial populations. Sample d (control slurry + methionine + L-methioninase) showed a similar pattern as sample c. L-methioninase degraded methionine in the medium; thus, some bacterial types could be affected by methionine deprivation.

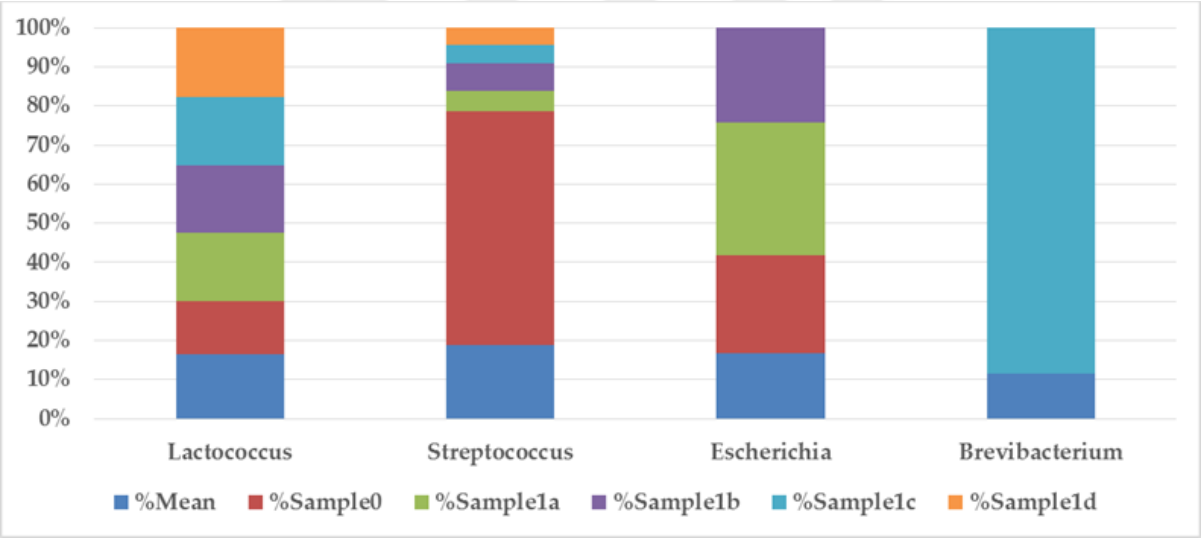


**Figure 4.37.** Percent abundance comparison of Bacteria species at day 1.

Zero-day (control) samples and samples a,b,c, and d at 1 d are compared in Figures 4.37 and 4.38. In general, *Lactococcus*, *Streptococcus*, and *Brevibacterium* (intentionally added to sample C) were dominant in all types. *Escherichia* was detected in very low amounts in some of the samples. Therefore, 1 day fermentation can be considered as a limited diversity of bacterial populations in cheddar cheese slurries. Contrary to the 1 day fermentation, 9 days of

fermentation resulted in a wide range of bacterial populations in all samples. The degree of diversity can be observed in Figures 4.39 and 4.40.

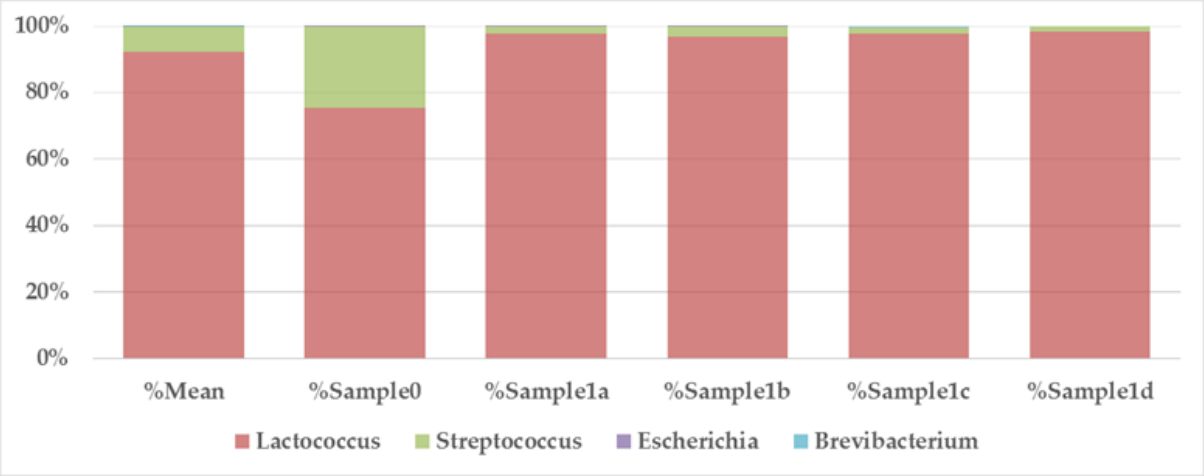


**Figure 4.38.** Variation in the bacterial population distribution over time in samples at day 1.

Previous studies have employed next-generation sequencing to evaluate alterations in the microbiota of cheddar cheese during its maturation phases (Choi et al., 2020; Overbeck, 2021). In that study, the microbial community was monitored across ripening periods to elucidate how lactic acid bacteria changes during the ripening process of cheddar cheese. Nevertheless, the comprehensive next-generation sequencing data presented in this thesis concerning the impact of L-methioninase on Cheddar cheese slurries represent a first-of-its-kind study. These data provide valuable insights into the optimal timing for the application of L-methioninase enzyme in cheddar cheese production, preventing an excessive microbiota shift within the cheese matrix.

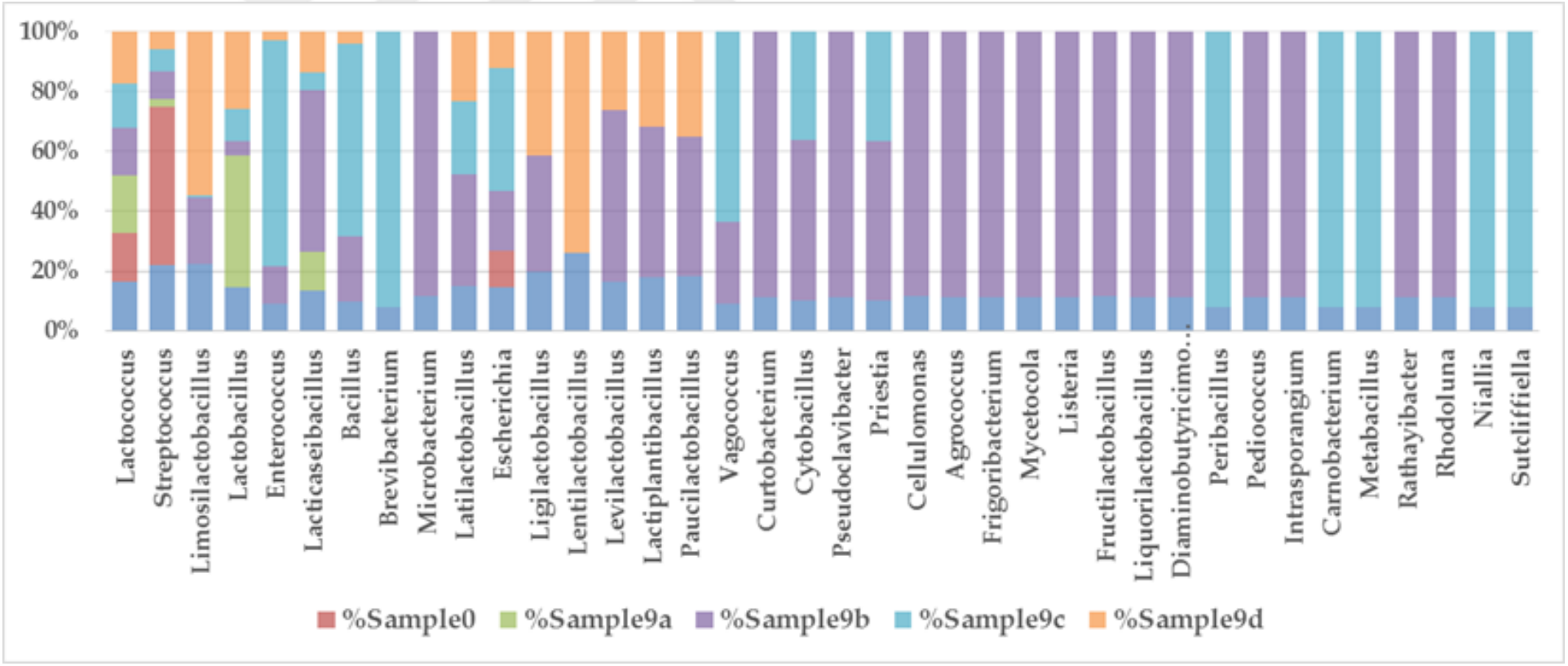


**Figure 4.39.** Percent abundance comparison of Bacteria species at day 9.

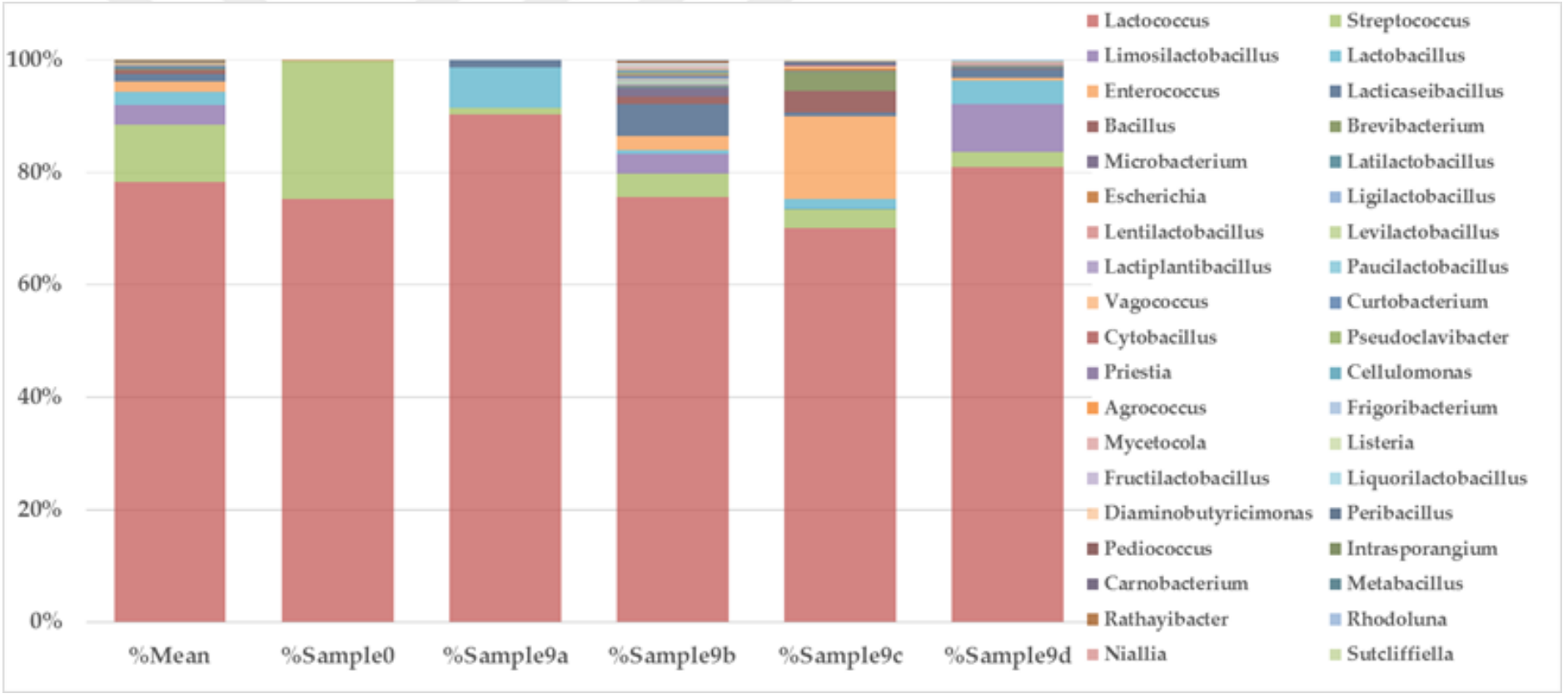


**Figure 4.40.** Variation in the bacterial population distribution over time in samples at day 9.

### 4.11.4. Principal Component Analysis (PCA) assessment of 1st day and 9th day of fermentations between samples

Principal Component analysis (PCA) demonstrated the similarity between two or more genetic species. To identify the association between variables in multidimensional data, Principal Component Analysis (PCA) analysis relies on the dimensionality reduction method to find the highest variance. To observe the patterns within the data, the analysis reduces the data to 2 or 3 dimensional planes. The basic characteristic of PCA is the exposure of the variance with minimum variance. To observe the pattern that will emerge in this analysis, the data and the groups to which the data belong were analyzed in three dimensions. In the figures below, for this purpose, basic component analysis of the samples was carried out at all levels and only at the genus level. PCA graphs can be seen in two dimensions in Figures 4.41 and 4.42, and in three dimensions in Figures 4.43 and 4.44. The graph illustrates a rapid shift in diversity across various dimensions during the 9-day fermentation period in samples b, c, and d.

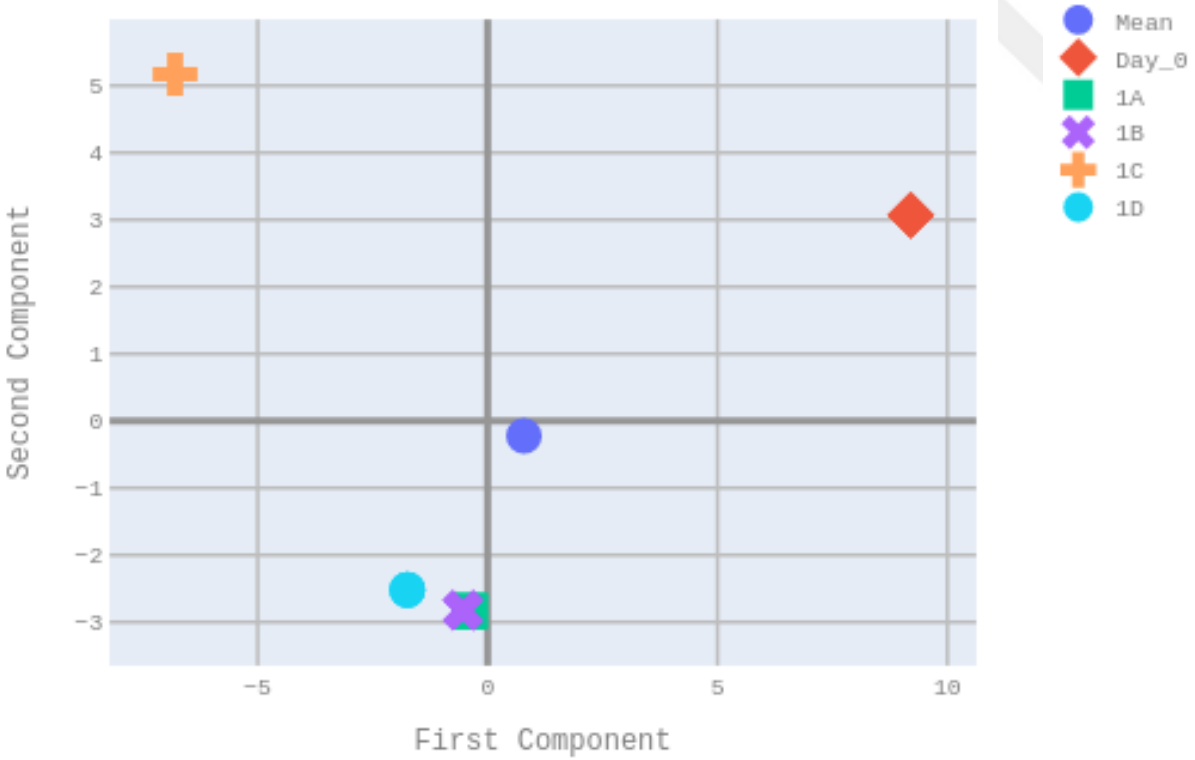


**Figure 4.41.** 2-Dimension PCA analysis of samples by all data at 1st day.

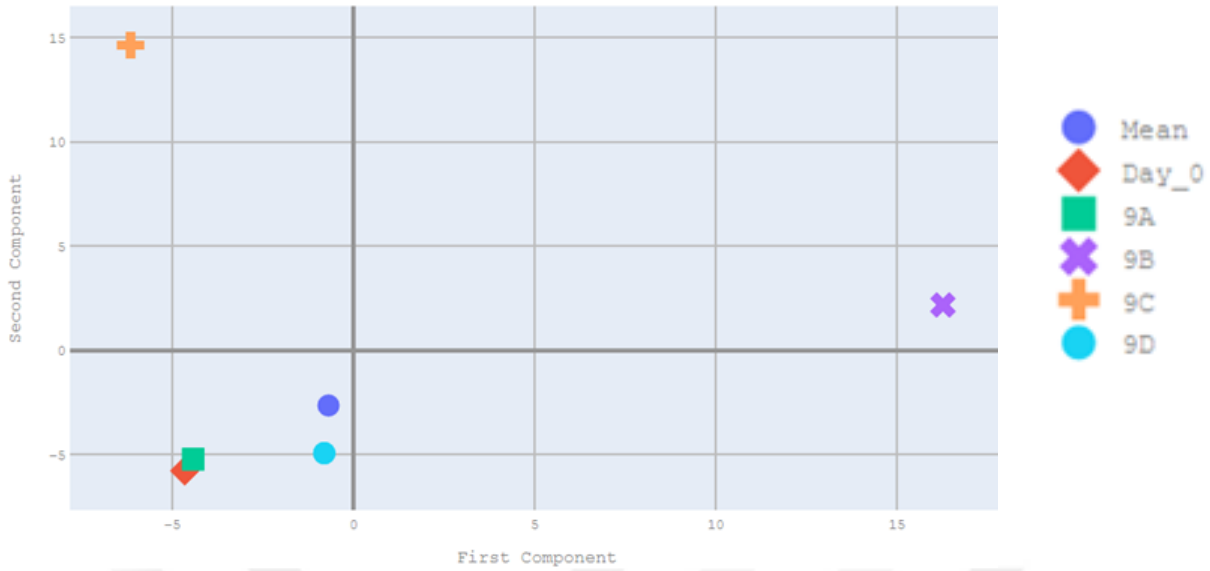


**Figure 4.42.** 2-Dimension PCA analysis of samples by all data at 9th day.

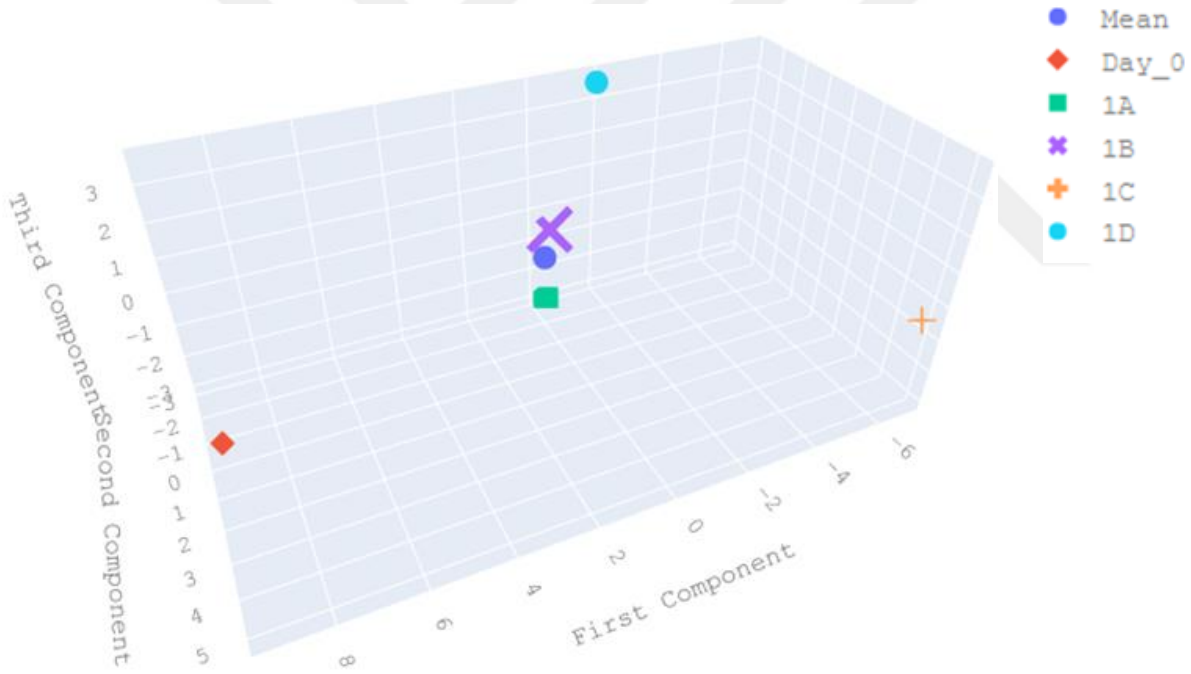


**Figure 4.43.** 3-Dimension PCA analysis of samples by all data at 1st day.

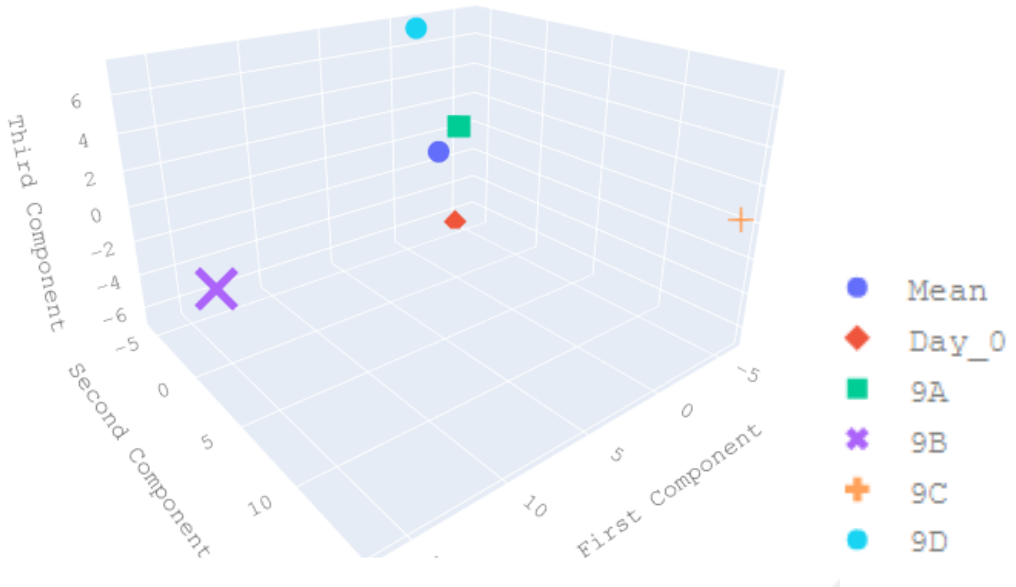


**Figure 4.44.** 3-Dimension PCA analysis of samples by all data at 9th day.

### 4.11.5. Principal Coordinate Analysis (PcoA) Assessment of Samples with Weighted Unifrac Analysis and Bray-Curtis Analysis (Beta Diversity)

Principal Coordinates Analysis (PCoA) shares similarities with Principal Component Analysis (PCA) as it focuses on illustrating the distances between samples. More precisely, its objective is to optimize the linear correspondence between the distances recorded in the distance matrix and the distances observed in a reduced-dimensional space that is frequently composed of only two or three selected axes. By comparing samples within and between groups, the principal goal of beta diversity analysis was to observe the structural relationships between groups or samples. For this purpose, since it was aimed at comparing the samples with the bacteria they contained, Principal Coordinate Analysis (PCoA), that is, principal coordinate analysis, was performed. PCoA analyses, unlike PCA analyses, also considered the distances between the bacteria in the samples. In addition, the metagroups in which the samples were found constituted another leg of this analysis. For PCoA analyses, the graphs below were constructed using weighted UniFrac and Bray-Curtis analyses. Bray-Curtis PCoA was constructed using a statistic whose analysis accounts for the presence of common shared bacteria, taking into account the proportions of bacteria in the samples. The genomic sequences of the bacteria present in the samples were used to build a phylogenetic tree, which was then used to determine the distance using weighted UniFrac. Prevalence refers to the relative number of individuals within a group that exhibit favorable results at a certain

moment in time. This measurement assesses the current overall condition of the population, particularly in terms of positive outcomes. By contrast, incidence is related to the rate at which new cases are reported (Marshall, 2005). This analysis also considered the prevalence rates of bacteria. Unifrac and Bray-Curtis analyses after 1 and 9 days of fermentation are shown in Figure 4.45.

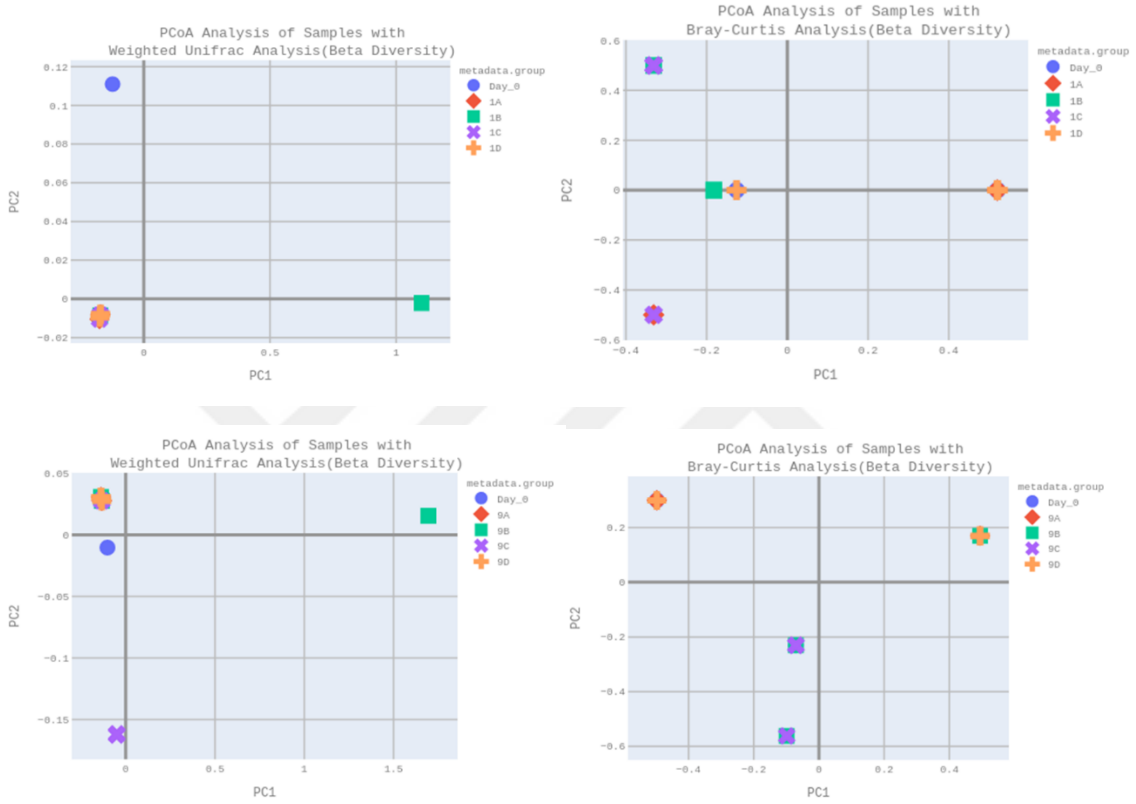


**Figure 4.45.** Beta diversity of 1 and 9 days of fermentation with Weighted Unifrac and Bray-Curtis Analysis.

### 4.11.6. Similarity Analysis Using Dendrogram

When DNA sequences display pronounced similarities, they tend to group together within a single branch of the dendrogram, which does not pose a significant challenge. However, in cases where similarity is low, DNA patterns form distinct clusters in separate branches. Determining the degree of similarity between DNA patterns in different branches solely from a dendrogram can be difficult or even impossible. In practice, a dendrogram is constructed by iteratively removing elements from a similarity matrix (Dijkshoorn et al., 2001).

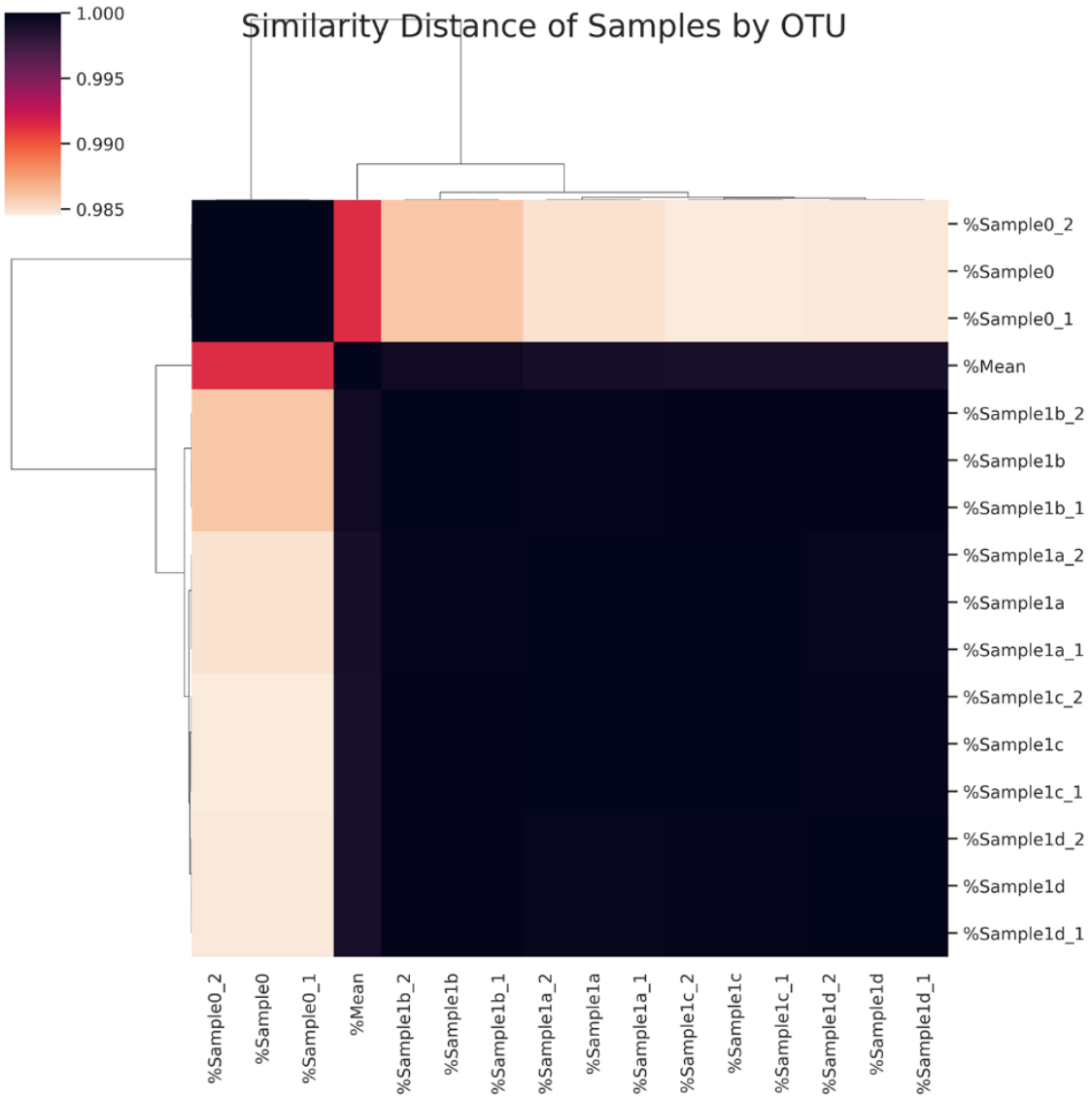


**Figure 4.46.** Similarity distance of samples by OTU at 1 day of fermentation. Dark color is dominant in most areas, thus the similarity of bacteria in all samples is high.

The dendrogram shown in Figures 4.46 and 4.47 was created by analyzing the proximity of the samples to each other according to their diversity and quantity. “Pearson” similarity method and Single-linkage hierarchy clustering method were used for closeness calculation. As seen in Figures 4.46 and 4.47, one of the examples is specified as “mean.” This sample was created by averaging all otuses, expressed as a percentage, and added to represent the average diversity. The samples on the horizontal and vertical axes of the graph are colored such that their similarity ratio with other samples is between 0 and 1. As the similarity ratio increased, the color darkened, approaching 1. In the opposite case, the samples moved farther

away from each other. When performing this analysis, all taxonomic levels of the samples were considered. Each sample of triplicates was considered in the graphs. The results suggest that diversity was initially quite similar across all samples on day 1. However, diversity shifts became evident on the 9th day of fermentation, as depicted in the heatmap.

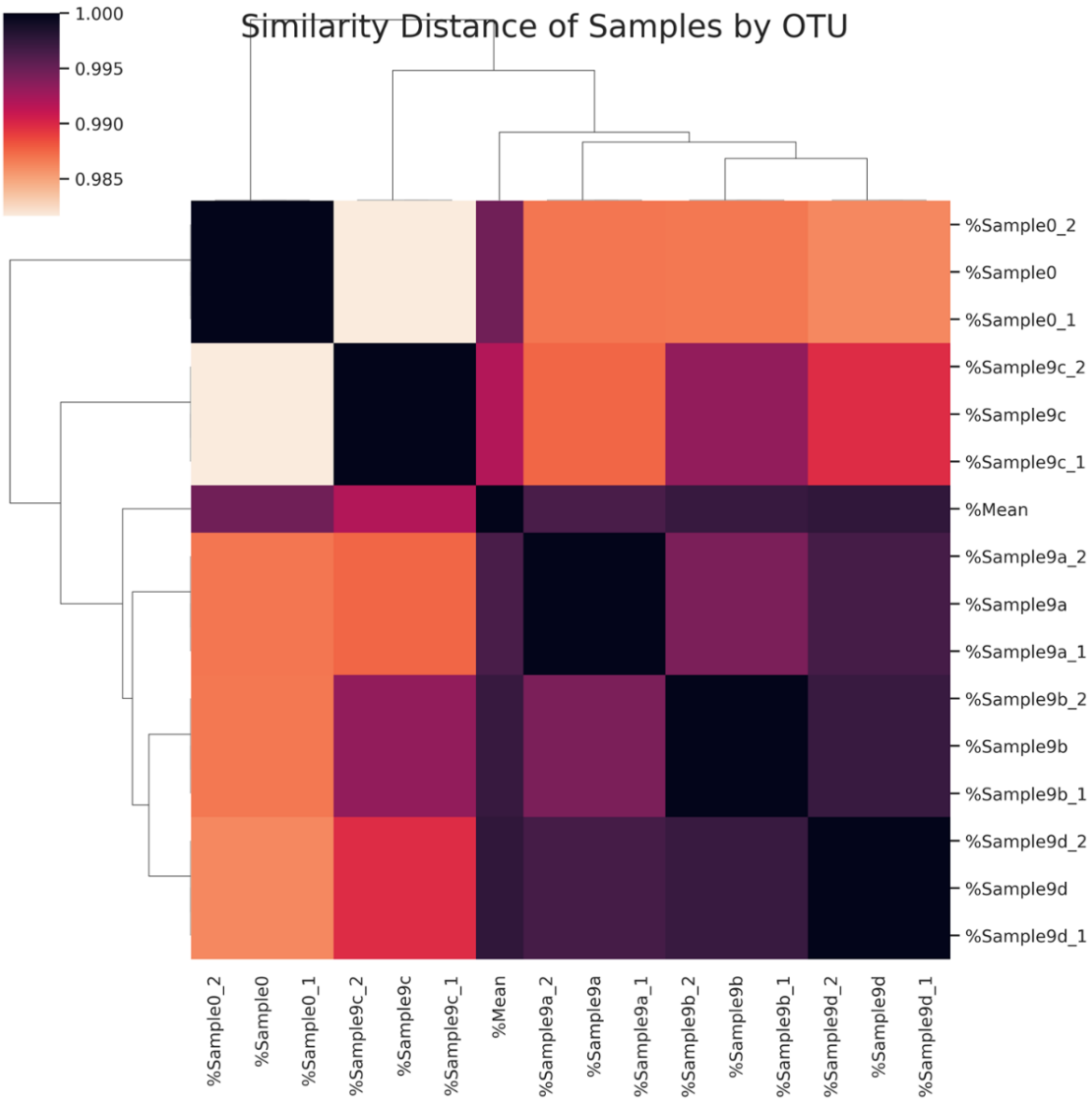


**Figure 4.47.** Similarity distance of samples by OUT at 9 days of fermentation. At the 9$^{th}$ day, the diversity of bacteria was higher than 1$^{st}$ day of fermentation. Thus, the extent of diversity can be seen in this graph.

### 4.11.7. Cladogram of Genus for 1 and 9 Days of Fermentation Between Samples

A cladogram is a type of branching diagram used in biology to depict evolutionary relationships or ancestry between different species or groups of organisms. It is a visual representation of a phylogenetic tree that illustrates the common ancestors and points of divergence among various species. Cladograms are essential tools in evolutionary biology and systematics as they help scientists understand the evolutionary history and relatedness of different organisms. By analyzing the branching patterns in a cladogram, researchers can infer information about the shared ancestry and evolutionary changes that have occurred over time (Nelson and Platnick, 1981; Brower, 2016).

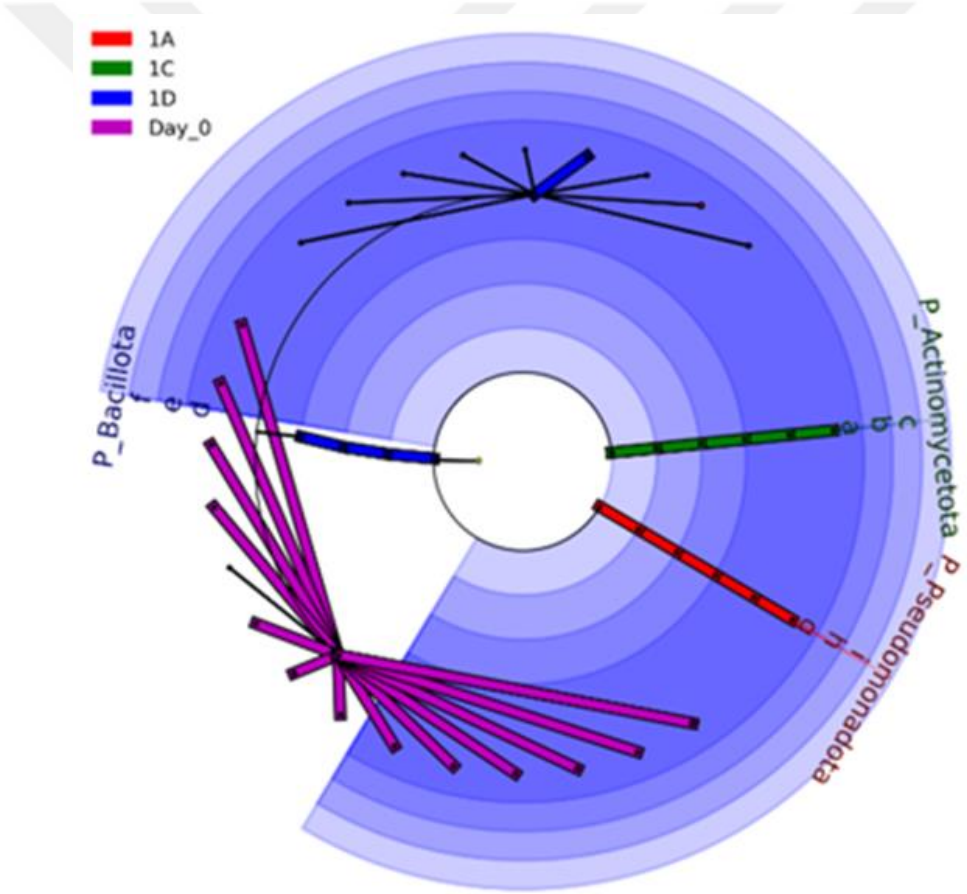


**Figure 4.48.** Genus Cladogram of 1 day of fermentation of samples.

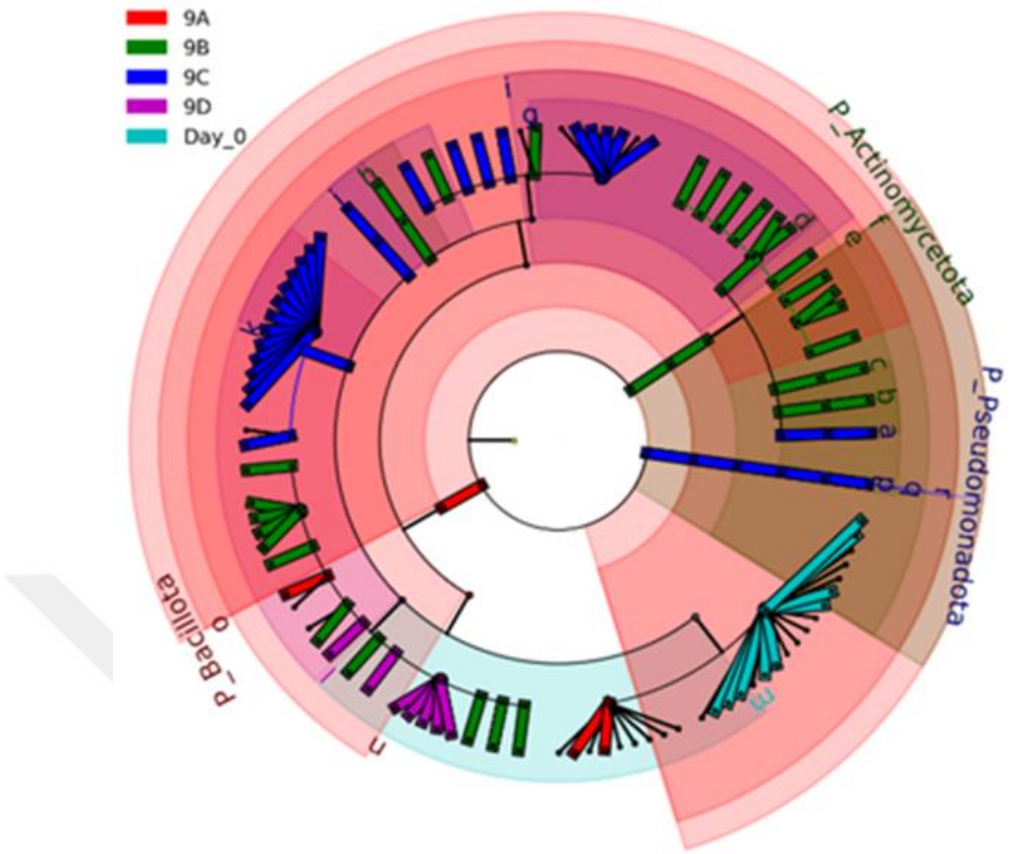


**Figure 4.49.** Genus Cladogram of 9 day of fermentation of samples.

Cladograms of samples at 1 and 9 days of fermentation are shown in Figures 4.48 and 4.49. Cladograms help to visualize distributive and quantitative shifts in microbial populations (Zhang et al., 2021). This visualization helps to understand the core microbiome and how species are associated in a phylogenetic tree. As shown in Figures 4.48 and 4.49, the diversity of bacterial species shifted significantly (diversity of species increased) on day 9.

### 4.11.8.Taxonomy, LDA score and Cladogram of Sample a (control slurry)

Linear Discriminant Analysis (LDA) is employed to maximize the component axes for the separation of classes. A detailed list of the bacterial species in the sample after 9 days of incubation is shown in Table 4.1. Linear Discriminant Analysis (LDA) is shown in Figure 4.50. The genus cladogram is shown in Figure 4.51. All these data show the percentage population of species and their statistical significance. The results demonstrated that, in the control slurry, only starter cultures dominated at all stages of fermentation.

**Table 4.1.** Bacterial population distribution of Sample a at 1 day and 9 day with control sample.

| **Taxon** | **Taxonomy** | **%Mean** | **%Sample0** | **%Sample1a** | **%Sample9a** |
|---|---|---|---|---|---|
| *Bacteria* | Domain | 100 | 100 | 100 | 100 |
| *Bacilli* | Class | 99.874 | 99.873 | 99.83 | 100 |
| *Lactobacillales* | Order | 99.874 | 99.873 | 99.83 | 100 |
| *Bacillota* | Phylum | 99.874 | 99.873 | 99.83 | 100 |
| *Streptococcaceae* | Family | 98.776 | 99.873 | 99.83 | 91.566 |
| *Lactococcus* | Genus | 85.612 | 75.364 | 97.691 | 90.272 |
| *Lactococcus lactis* | Species | 50.173 | 44.866 | 55.202 | 56.09 |
| *Lactococcus cremoris* | Species | 32.117 | 25.718 | 40.431 | 32.821 |
| *Streptococcus* | Genus | 13.164 | 24.509 | 2.139 | 1.293 |
| *Streptococcus thermophilus* | Species | 10.134 | 18.81 | 1.673 | 1.145 |
| *Streptococcus equinus* | Species | 1.464 | 2.702 | 0.32 | 0 |
| *Lactococcus piscium* | Species | 1.122 | 1.747 | 0.57 | 0.31 |
| *Lactobacillaceae* | Family | 1.098 | 0 | 0 | 8.434 |
| *Lactococcus allomyrinae* | Species | 1.043 | 1.511 | 0.65 | 0.377 |
| *Lactobacillus delbrueckii* | Species | 0.919 | 0 | 0 | 7.06 |
| *Lactobacillus* | Genus | 0.919 | 0 | 0 | 7.06 |
| *Streptococcus sp. LPB0220* | Species | 0.575 | 1.046 | 0.146 | 0 |
| *Lactococcus protaetiae* | Species | 0.391 | 0.535 | 0.335 | 0 |
| *Lactococcus garvieae* | Species | 0.305 | 0.395 | 0.226 | 0.189 |
| *Streptococcus salivarius* | Species | 0.298 | 0.599 | 0 | 0 |
| *Lactococcus raffinolactis* | Species | 0.209 | 0.24 | 0.118 | 0.35 |
| *Lacticaseibacillus* | Genus | 0.179 | 0 | 0 | 1.374 |
| *Lactococcus taiwanensis* | Species | 0.175 | 0.197 | 0.16 | 0.135 |
| *Enterobacterales* | Order | 0.126 | 0.127 | 0.17 | 0 |

**Table 4.1. (Continued)**

| | | | | | |
|---|---|---|---|---|---|
| *Gammaproteobacteria* | Class | 0.126 | 0.127 | 0.17 | 0 |
| *Pseudomonadota* | Phylum | 0.126 | 0.127 | 0.17 | 0 |
| *Enterobacteriaceae* | Family | 0.126 | 0.127 | 0.17 | 0 |
| *Escherichia* | Genus | 0.126 | 0.127 | 0.17 | 0 |
| *Escherichia coli* | Species | 0.126 | 0.127 | 0.17 | 0 |
| *Lacticaseibacillus rhamnosus* | Species | 0.112 | 0 | 0 | 0.862 |
| *Streptococcus cristatus* | Species | 0.096 | 0.194 | 0 | 0 |
| *Streptococcus suis* | Species | 0.093 | 0.187 | 0 | 0 |
| *Streptococcus pyogenes* | Species | 0.091 | 0.183 | 0 | 0 |
| *Streptococcus iniae* | Species | 0.081 | 0.162 | 0 | 0 |
| *Lactococcus petauri* | Species | 0.077 | 0.155 | 0 | 0 |
| *Streptococcus equi* | Species | 0.074 | 0.148 | 0 | 0 |
| *Lacticaseibacillus paracasei* | Species | 0.067 | 0 | 0 | 0.512 |
| *Streptococcus oralis* | Species | 0.065 | 0.13 | 0 | 0 |
| *Streptococcus australis* | Species | 0.061 | 0.123 | 0 | 0 |
| *Streptococcus agalactiae* | Species | 0.06 | 0.12 | 0 | 0 |
| *Streptococcus anginosus* | Species | 0.053 | 0.106 | 0 | 0 |
| *Streptococcus dysgalactiae* | Species | 0.019 | 0 | 0 | 0.148 |

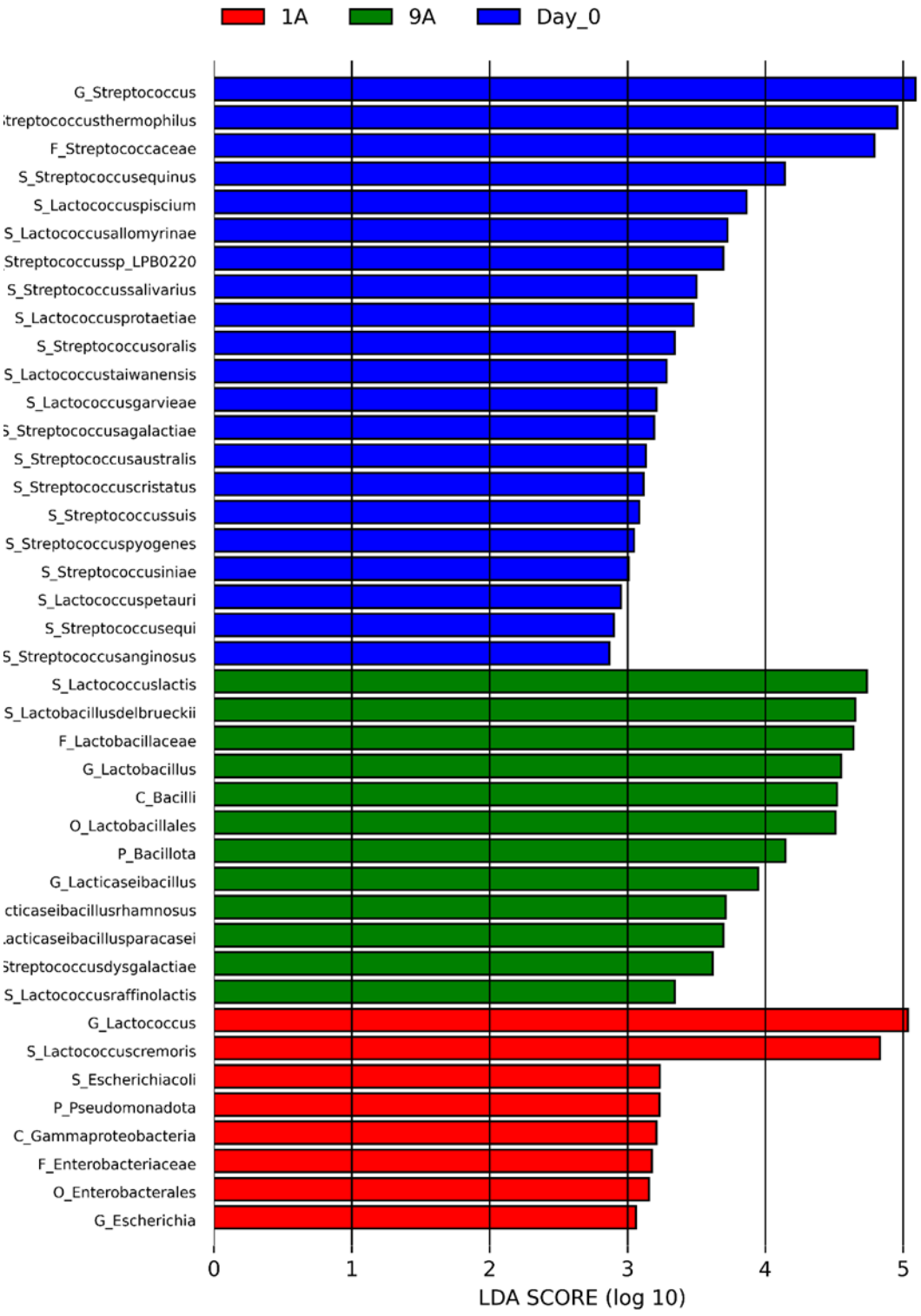


**Figure 4.50.** LDA score of genus in sample a (control slurry).

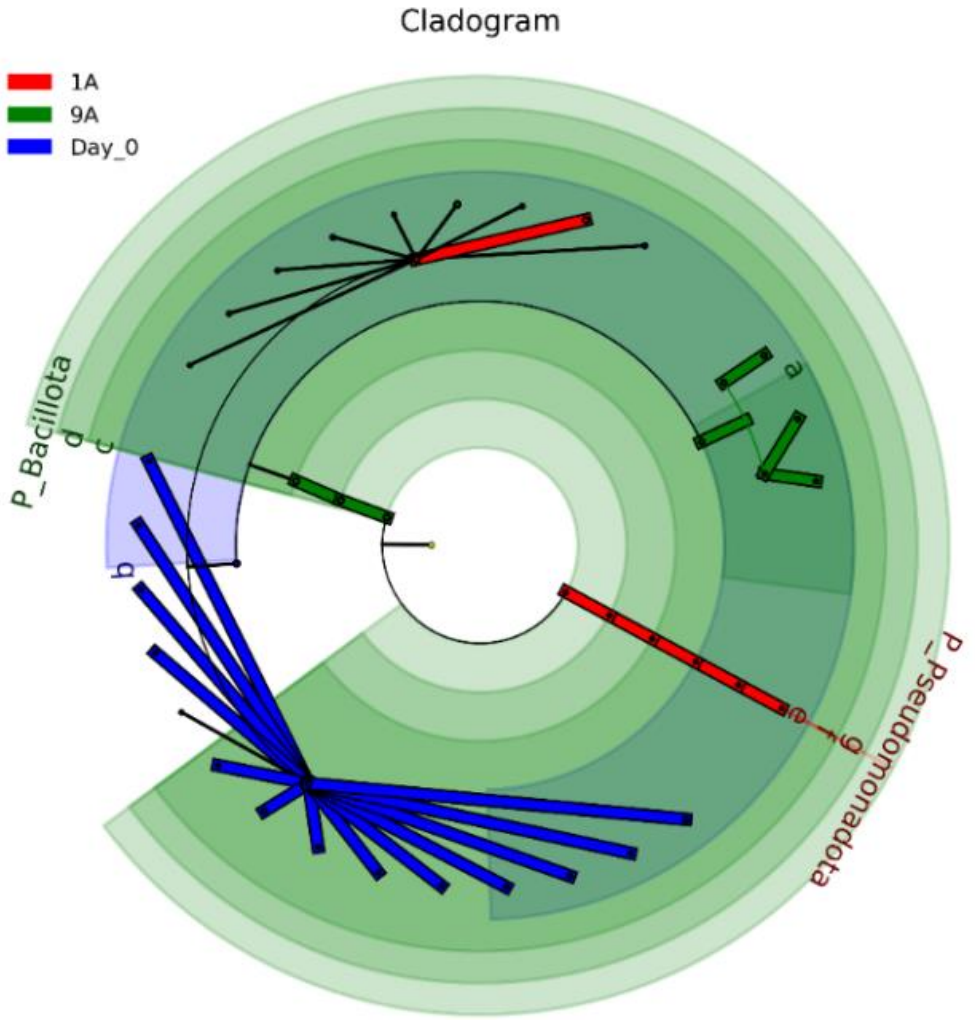


**Figure 4. 51.** Genus cladogram of genus in sample a (control slurry).

### 4.11.9.Taxonomy, LDA score and Cladogram of Sample b (control slurry and methionine)

A detailed list of the bacterial species in sample b after 9 days of incubation is shown in Table 4.2. Linear Discriminant Analysis (LDA) is shown in Figure 4.53. The genus cladogram is shown in Figure 4.52. All these data show the percentage population of species and their statistical significance. In the bacterial percentages, cladogram, and LDA scores, it was evident that the most significant increase in diversity occurred in the control and methionine groups. This change could potentially be attributed to methionine as certain bacteria may exhibit variations in methionine metabolism.

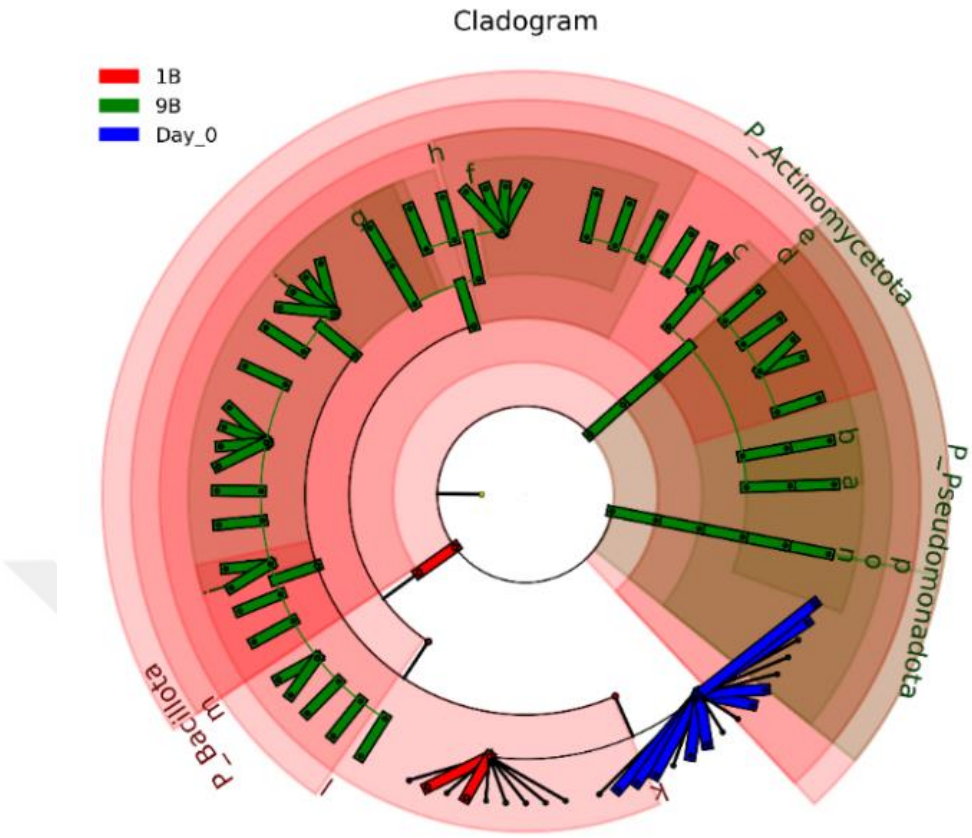


**Figure 4.52.** Genus cladogram of genus in sample b (control slurry and methionine).

### 4.11.10.Taxonomy, LDA score and Cladogram of Sample c (control slurry + methionine + *Br. linens* BL2)

A detailed list of bacterial species in sample C over 9 days of incubation is shown in Table 4.3. Linear Discriminant Analysis (LDA) is shown in Figure 4.55. The genus cladogram is shown in Figure 4.54. All these data show the percentage population of species and their statistical significance. The percentages of bacterial species, cladogram, and LDA scores all indicate that methionine induced a notable increase in diversity, while starter cultures continued to maintain their dominance.

**Table 4.2.** Detailed information of microbial community of sample b.

| Taxon | Taxonomy | %Mean | %Sample0 | %Sample1b | %Sample9b |
|---|---|---|---|---|---|
| *Bacteria* | Domain | 100 | 100 | 100 | 100 |
| *Bacillota* | Phylum | 99.192 | 99.873 | 99.878 | 96.21 |
| *Bacilli* | Class | 99.192 | 99.873 | 99.878 | 96.21 |
| *Lactobacillales* | Order | 98.835 | 99.873 | 99.878 | 94.297 |
| *Streptococcaceae* | Family | 96.142 | 99.873 | 99.878 | 79.85 |
| *Lactococcus* | Genus | 82.412 | 75.364 | 96.956 | 75.598 |
| *Lactococcus lactis* | Species | 47.663 | 44.866 | 57.19 | 38.423 |
| *Lactococcus cremoris* | Species | 30.919 | 25.718 | 37.737 | 32.702 |
| *Streptococcus* | Genus | 13.73 | 24.509 | 2.922 | 4.252 |
| *Streptococcus thermophilus* | Species | 10.02 | 18.81 | 2.343 | 0.314 |
| *Lactobacillaceae* | Family | 2.2 | 0 | 0 | 11.803 |
| *Streptococcus equinus* | Species | 1.499 | 2.702 | 0.43 | 0.203 |
| *Lactococcus piscium* | Species | 1.384 | 1.747 | 0.552 | 1.876 |
| *Lacticaseibacillus* | Genus | 1.063 | 0 | 0 | 5.703 |
| *Lactococcus allomyrinae* | Species | 1.048 | 1.511 | 0.606 | 0.601 |
| *Streptococcus sp. LPB0220* | Species | 0.806 | 1.046 | 0.149 | 1.322 |
| *Lacticaseibacillus rhamnosus* | Species | 0.775 | 0 | 0 | 4.159 |
| *Micrococcales* | Order | 0.669 | 0 | 0 | 3.586 |
| *Actinomycetota* | Phylum | 0.669 | 0 | 0 | 3.586 |
| *Actinomycetes* | Class | 0.669 | 0 | 0 | 3.586 |
| *Limosilactobacillus* | Genus | 0.644 | 0 | 0 | 3.457 |
| *Microbacteriaceae* | Family | 0.593 | 0 | 0 | 3.18 |
| *Limosilactobacillus fermentum* | Species | 0.586 | 0 | 0 | 3.143 |
| *Enterococcaceae* | Family | 0.493 | 0 | 0 | 2.643 |
| *Enterococcus* | Genus | 0.464 | 0 | 0 | 2.486 |

**Table 4.2. (Continued)**

| | | | | | |
|---|---|---|---|---|---|
| *Lactococcus protaetiae* | Species | 0.388 | 0.535 | 0.239 | 0.259 |
| *Bacillales* | Order | 0.357 | 0 | 0 | 1.913 |
| *Lactococcus garvieae* | Species | 0.353 | 0.395 | 0.17 | 0.564 |
| *Bacillaceae* | Family | 0.319 | 0 | 0 | 1.71 |
| *Streptococcus salivarius* | Species | 0.293 | 0.599 | 0 | 0 |
| *Microbacterium* | Genus | 0.264 | 0 | 0 | 1.414 |
| *Enterococcus faecium* | Species | 0.252 | 0 | 0 | 1.349 |
| *Lactococcus taiwanensis* | Species | 0.25 | 0.197 | 0.186 | 0.499 |
| *Lactococcus raffinolactis* | Species | 0.25 | 0.24 | 0.138 | 0.471 |
| *Bacillus* | Genus | 0.241 | 0 | 0 | 1.294 |
| *Microbacterium sp. No. 7* | Species | 0.226 | 0 | 0 | 1.211 |
| *Lacticaseibacillus paracasei* | Species | 0.217 | 0 | 0 | 1.165 |
| *Bacillus cytotoxicus* | Species | 0.167 | 0 | 0 | 0.897 |
| *Lactococcus petauri* | Species | 0.159 | 0.155 | 0.138 | 0.203 |
| *Streptococcus agalactiae* | Species | 0.152 | 0.12 | 0 | 0.499 |
| *Gammaproteobacteria* | Class | 0.14 | 0.127 | 0.122 | 0.203 |
| *Lactobacillus delbrueckii* | Species | 0.14 | 0 | 0 | 0.749 |
| *Enterobacterales* | Order | 0.14 | 0.127 | 0.122 | 0.203 |
| *Enterobacteriaceae* | Family | 0.14 | 0.127 | 0.122 | 0.203 |
| *Escherichia* | Genus | 0.14 | 0.127 | 0.122 | 0.203 |
| *Pseudomonadota* | Phylum | 0.14 | 0.127 | 0.122 | 0.203 |
| *Lactobacillus* | Genus | 0.14 | 0 | 0 | 0.749 |
| *Escherichia coli* | Species | 0.14 | 0.127 | 0.122 | 0.203 |
| *Streptococcus iniae* | Species | 0.133 | 0.162 | 0 | 0.287 |
| *Streptococcus oralis* | Species | 0.128 | 0.13 | 0 | 0.342 |
| *Enterococcus saigonensis* | Species | 0.112 | 0 | 0 | 0.601 |
| *Streptococcus dysgalactiae* | Species | 0.109 | 0 | 0 | 0.582 |

**Table 4.2. (Continued)**

| | | | | | |
|---|---|---|---|---|---|
| *Streptococcus cristatus* | Species | 0.095 | 0.194 | 0 | 0 |
| *Streptococcus suis* | Species | 0.091 | 0.187 | 0 | 0 |
| *Streptococcus pyogenes* | Species | 0.09 | 0.183 | 0 | 0 |
| *Streptococcus sp. FDAARGOS_522* | Species | 0.088 | 0 | 0 | 0.471 |
| *Latilactobacillus* | Genus | 0.081 | 0 | 0 | 0.434 |
| *Enterococcus casseliflavus* | Species | 0.079 | 0 | 0 | 0.425 |
| *Levilactobacillus suantsaii* | Species | 0.078 | 0 | 0 | 0.416 |
| *Levilactobacillus* | Genus | 0.078 | 0 | 0 | 0.416 |
| *Streptococcus equi* | Species | 0.072 | 0.148 | 0 | 0 |
| *Curtobacterium* | Genus | 0.072 | 0 | 0 | 0.388 |
| *Streptococcus australis* | Species | 0.06 | 0.123 | 0 | 0 |
| *Pseudoclavibacter* | Genus | 0.06 | 0 | 0 | 0.324 |
| *Pseudoclavibacter sp. Marseille-Q3772* | Species | 0.06 | 0 | 0 | 0.324 |
| *Limosilactobacillus reuteri* | Species | 0.059 | 0 | 0 | 0.314 |
| *Streptococcus anginosus* | Species | 0.052 | 0.106 | 0 | 0 |
| *Latilactobacillus curvatus* | Species | 0.052 | 0 | 0 | 0.277 |
| *Cellulomonas sp. C5510* | Species | 0.05 | 0 | 0 | 0.268 |
| *Cellulomonas* | Genus | 0.05 | 0 | 0 | 0.268 |
| *Cellulomonadaceae* | Family | 0.05 | 0 | 0 | 0.268 |
| *Curtobacterium pusillum* | Species | 0.05 | 0 | 0 | 0.268 |
| *Lacticaseibacillus casei* | Species | 0.048 | 0 | 0 | 0.259 |
| *Ligilactobacillus* | Genus | 0.048 | 0 | 0 | 0.259 |
| *Ligilactobacillus saerimneri* | Species | 0.048 | 0 | 0 | 0.259 |
| *Agrococcus sp. Marseille-Q4369* | Species | 0.047 | 0 | 0 | 0.25 |
| *Agrococcus* | Genus | 0.047 | 0 | 0 | 0.25 |
| *Frigoribacterium* | Genus | 0.043 | 0 | 0 | 0.231 |
| *Frigoribacterium sp. NBH87* | Species | 0.043 | 0 | 0 | 0.231 |

**Table 4.2. (Continued)**

| | | | | | |
|---|---|---|---|---|---|
| *Cytobacillus* | Genus | 0.043 | 0 | 0 | 0.231 |
| *Streptococcus sp. FDAARGOS_520* | Species | 0.043 | 0 | 0 | 0.231 |
| *Cytobacillus gottheilii* | Species | 0.043 | 0 | 0 | 0.231 |
| *Listeria* | Genus | 0.038 | 0 | 0 | 0.203 |
| *Listeriaceae* | Family | 0.038 | 0 | 0 | 0.203 |
| *Listeria monocytogenes* | Species | 0.038 | 0 | 0 | 0.203 |
| *Microbacterium sp. YJN-G* | Species | 0.038 | 0 | 0 | 0.203 |
| *Mycetocola* | Genus | 0.038 | 0 | 0 | 0.203 |
| *Mycetocola sp. JXN-3* | Species | 0.038 | 0 | 0 | 0.203 |
| *Priestia* | Genus | 0.034 | 0 | 0 | 0.185 |
| *Priestia megaterium* | Species | 0.034 | 0 | 0 | 0.185 |
| *Fructilactobacillus* | Genus | 0.033 | 0 | 0 | 0.176 |
| *Fructilactobacillus lindneri* | Species | 0.033 | 0 | 0 | 0.176 |
| *Lactiplantibacillus* | Genus | 0.031 | 0 | 0 | 0.166 |
| *Lactiplantibacillus plantarum* | Species | 0.031 | 0 | 0 | 0.166 |
| *Liquorilactobacillus* | Genus | 0.029 | 0 | 0 | 0.157 |
| *Latilactobacillus sakei* | Species | 0.029 | 0 | 0 | 0.157 |
| *Vagococcus penaei* | Species | 0.029 | 0 | 0 | 0.157 |
| *Vagococcus* | Genus | 0.029 | 0 | 0 | 0.157 |
| *Liquorilactobacillus hordei* | Species | 0.029 | 0 | 0 | 0.157 |
| *Diaminobutyricimonas sp. LJ205* | Species | 0.028 | 0 | 0 | 0.148 |
| *Paucilactobacillus nenjiangensis* | Species | 0.028 | 0 | 0 | 0.148 |
| *Paucilactobacillus* | Genus | 0.028 | 0 | 0 | 0.148 |
| *Diaminobutyricimonas* | Genus | 0.028 | 0 | 0 | 0.148 |
| *Bacillus cereus* | Species | 0.028 | 0 | 0 | 0.148 |
| *Pediococcus pentosaceus* | Species | 0.026 | 0 | 0 | 0.139 |
| *Intrasporangiaceae* | Family | 0.026 | 0 | 0 | 0.139 |

**Table 4.2. (Continued)**

| | | | | | |
|---|---|---|---|---|---|
| *Intrasporangium* | Genus | 0.026 | 0 | 0 | 0.139 |
| *Intrasporangium calvum* | Species | 0.026 | 0 | 0 | 0.139 |
| *Pediococcus* | Genus | 0.026 | 0 | 0 | 0.139 |
| *Bacillus anthracis* | Species | 0.024 | 0 | 0 | 0.129 |
| *Bacillus velezensis* | Species | 0.022 | 0 | 0 | 0.12 |
| *Lacticaseibacillus manihotivorans* | Species | 0.022 | 0 | 0 | 0.12 |
| *Curtobacterium flaccumfaciens* | Species | 0.022 | 0 | 0 | 0.12 |
| *Rathayibacter* | Genus | 0.021 | 0 | 0 | 0.111 |
| *Rathayibacter sp. VKM Ac-2759* | Species | 0.021 | 0 | 0 | 0.111 |
| *Rhodoluna* | Genus | 0.021 | 0 | 0 | 0.111 |
| *Rhodoluna limnophila* | Species | 0.021 | 0 | 0 | 0.111 |
| *Enterococcus durans* | Species | 0.021 | 0 | 0 | 0.111 |

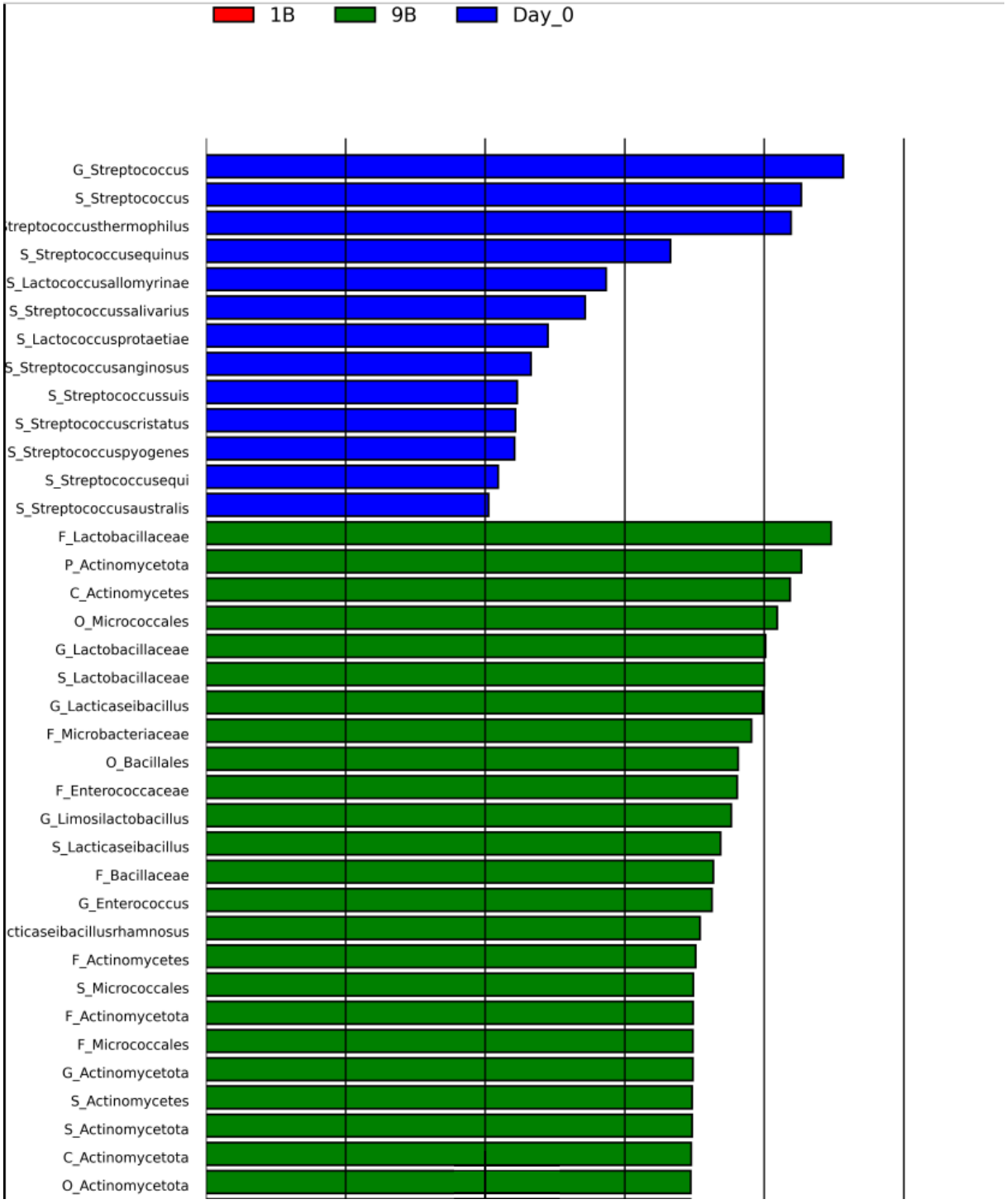


**Figure 4.53a.** Detailed information of sample b (control slurry and methionine).

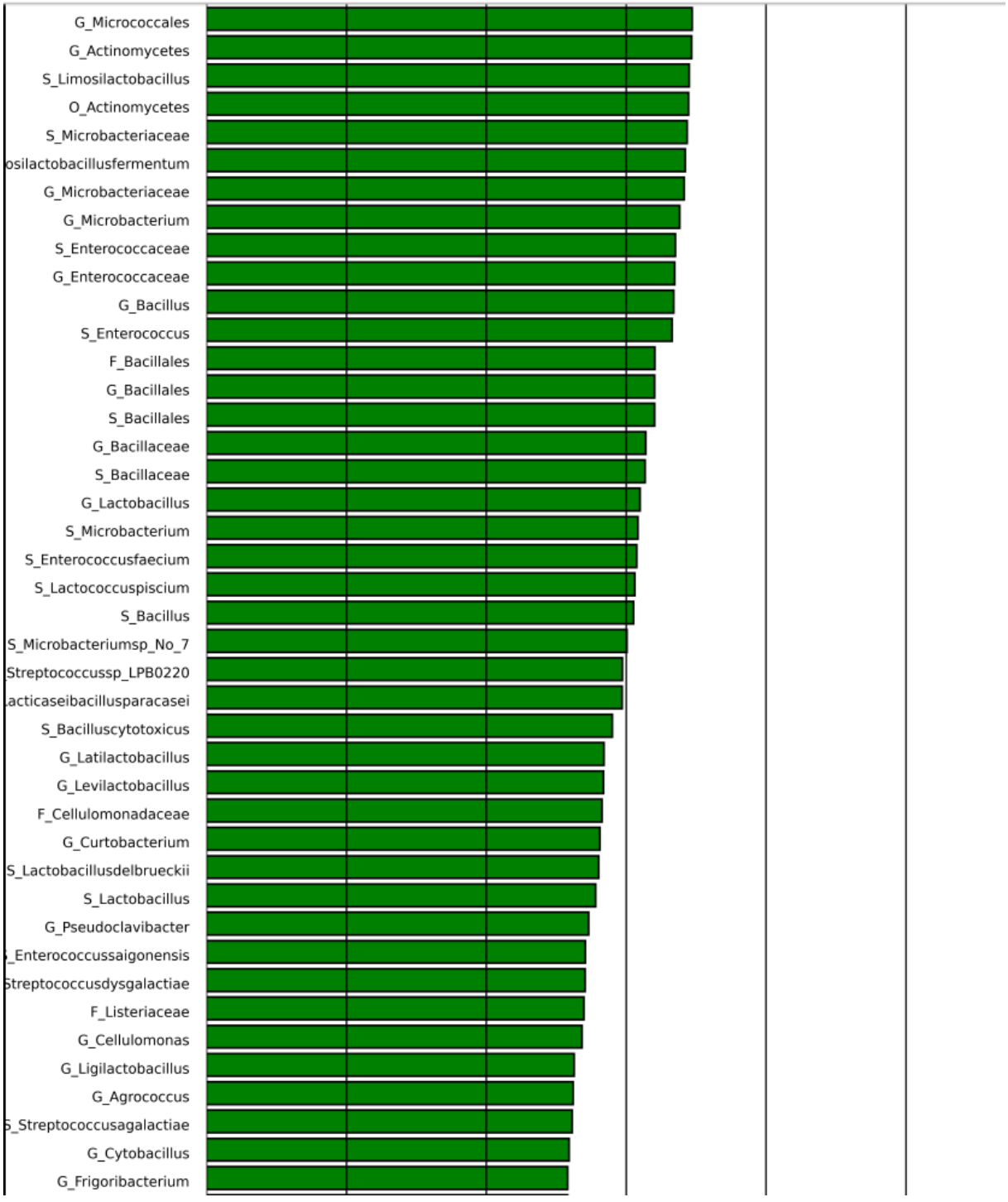


**Figure 4.53b.** Detailed information of sample b (control slurry and methionine).

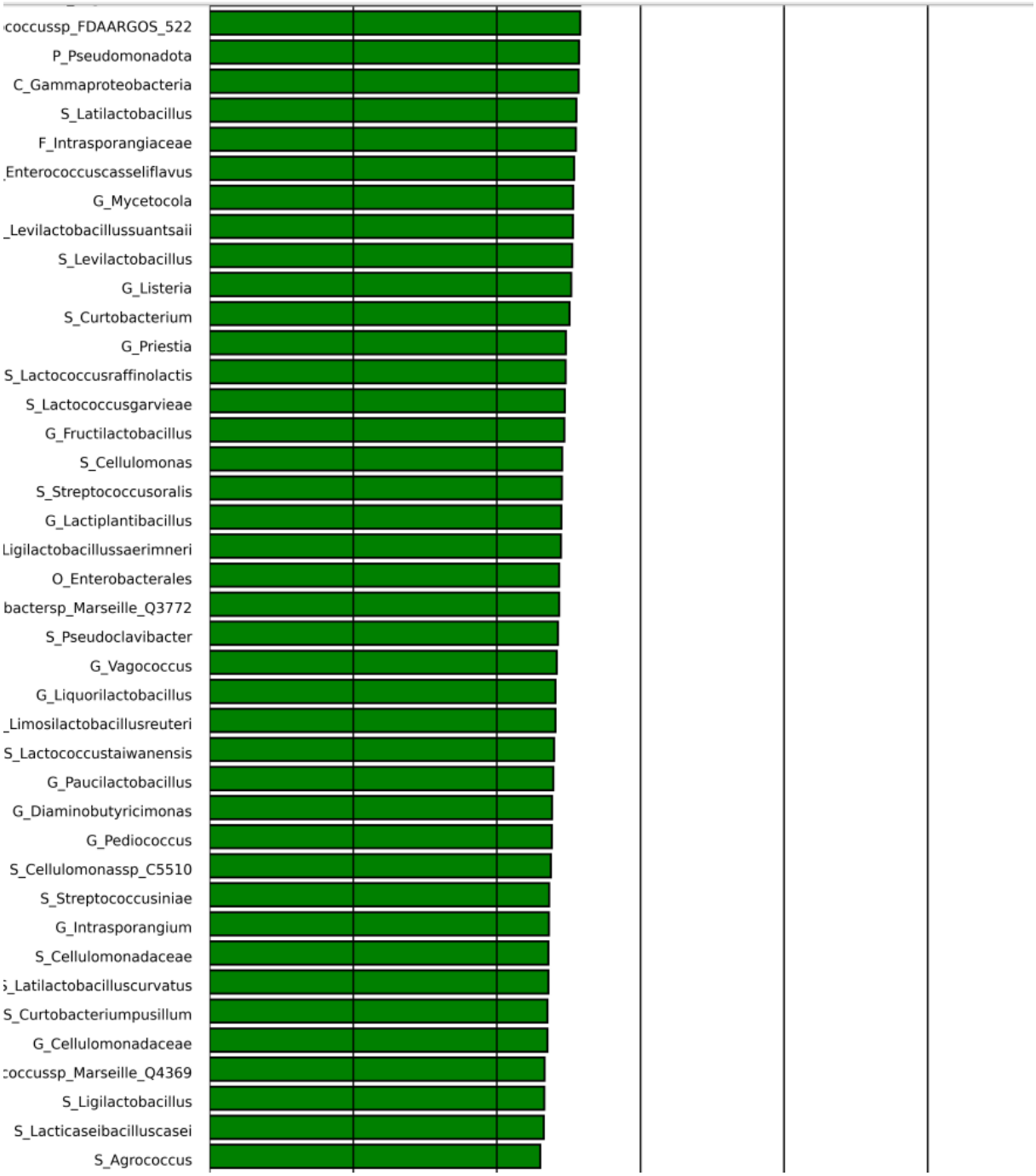


**Figure 4.53c.** Detailed information of sample b (control slurry and methionine).

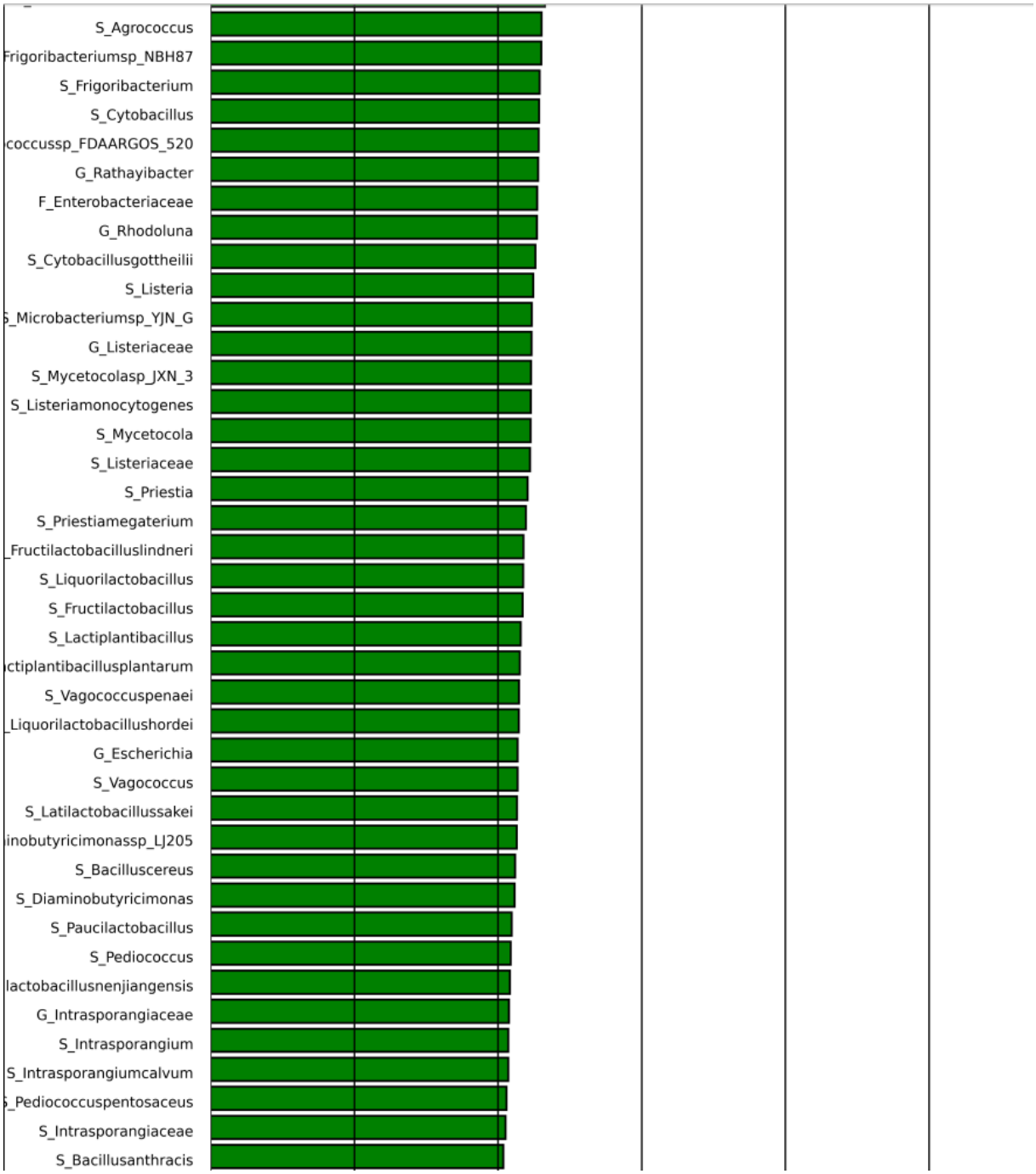


**Figure 4.53d.** Detailed information of sample b (control slurry and methionine).

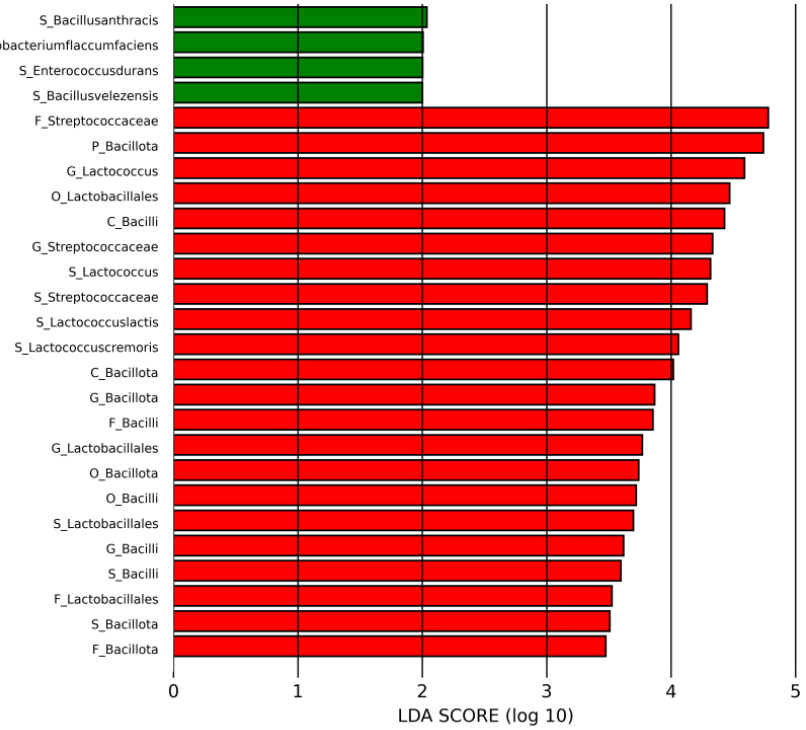


**Figure 4.53e.** Detailed information of sample b (control slurry and methionine).

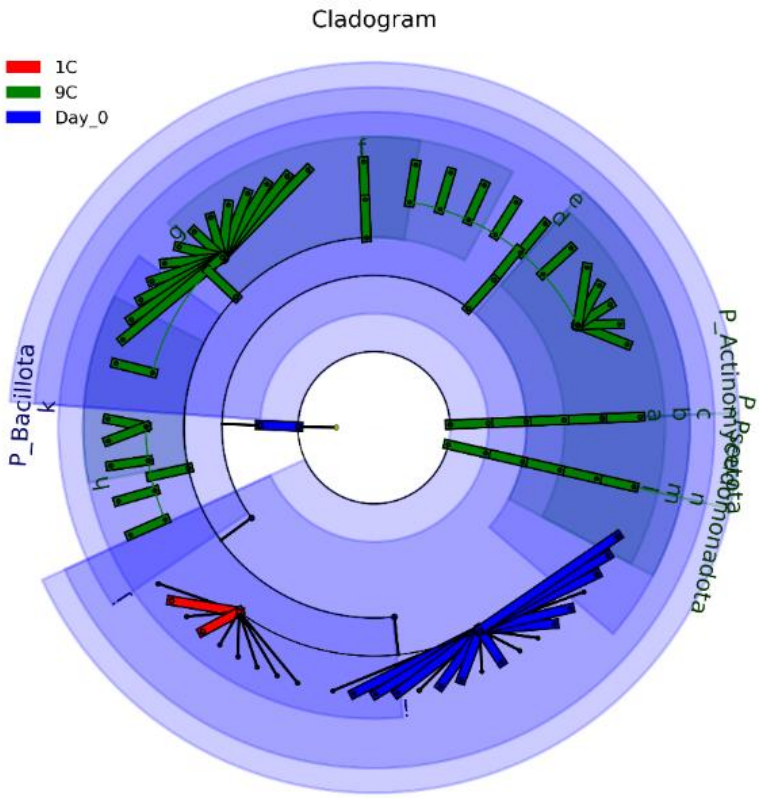


**Figure 4.54.** Genus cladogram of sample c (control slurry + methionine + Br. linens BL2).

**Table 4.3.** Species in sample c detected by next generation sequencing.

| Taxon | Taxonomy | %Mean | %Sample0 | %Sample1c | %Sample9c |
|---|---|---|---|---|---|
| *Bacteria* | Domain | 100 | 100 | 100 | 100 |
| *Bacillota* | Phylum | 99.274 | 99.873 | 99.543 | 96.325 |
| *Bacilli* | Class | 99.274 | 99.873 | 99.543 | 96.325 |
| *Lactobacillales* | Order | 98.597 | 99.873 | 99.543 | 91.543 |
| *Streptococcaceae* | Family | 96.03 | 99.873 | 99.543 | 73.394 |
| *Lactococcus* | Genus | 81.182 | 75.364 | 97.621 | 70.042 |
| *Lactococcus lactis* | Species | 47.699 | 44.866 | 56.888 | 39.804 |
| *Lactococcus cremoris* | Species | 30.088 | 25.718 | 39.758 | 27.307 |
| *Streptococcus* | Genus | 14.848 | 24.509 | 1.922 | 3.352 |
| *Streptococcus thermophilus* | Species | 11.131 | 18.81 | 1.559 | 0.533 |
| *Enterococcaceae* | Family | 2.149 | 0 | 0 | 15.189 |
| *Enterococcus* | Genus | 2.097 | 0 | 0 | 14.825 |
| *Streptococcus equinus* | Species | 1.627 | 2.702 | 0.262 | 0.196 |
| *Lactococcus piscium* | Species | 1.125 | 1.747 | 0.161 | 0.659 |
| *Lactococcus allomyrinae* | Species | 1.085 | 1.511 | 0.652 | 0.295 |
| *Bacillales* | Order | 0.677 | 0 | 0 | 4.783 |
| *Bacillaceae* | Family | 0.677 | 0 | 0 | 4.783 |
| *Streptococcus sp. LPB0220* | Species | 0.653 | 1.046 | 0 | 0.449 |
| *Brevibacterium* | Genus | 0.595 | 0 | 0.457 | 3.254 |
| *Actinomycetes* | Class | 0.595 | 0 | 0.457 | 3.254 |
| *Actinomycetota* | Phylum | 0.595 | 0 | 0.457 | 3.254 |
| *Brevibacterium aurantiacum* | Species | 0.595 | 0 | 0.457 | 3.254 |
| *Micrococcales* | Order | 0.595 | 0 | 0.457 | 3.254 |
| *Brevibacteriaceae* | Family | 0.595 | 0 | 0.457 | 3.254 |
| *Bacillus* | Genus | 0.542 | 0 | 0 | 3.829 |
| *Enterococcus faecium* | Species | 0.54 | 0 | 0 | 3.815 |

**Table 4.3. (Continued)**

| | | | | | |
|---|---|---|---|---|---|
| *Enterococcus gilvus* | Species | 0.484 | 0 | 0 | 3.422 |
| *Bacillus cytotoxicus* | Species | 0.419 | 0 | 0 | 2.959 |
| *Lactobacillaceae* | Family | 0.391 | 0 | 0 | 2.763 |
| *Lactococcus protaetiae* | Species | 0.379 | 0.535 | 0.161 | 0.21 |
| *Streptococcus salivarius* | Species | 0.337 | 0.599 | 0 | 0 |
| *Lactococcus raffinolactis* | Species | 0.25 | 0.24 | 0 | 0.813 |
| *Lactococcus garvieae* | Species | 0.248 | 0.395 | 0 | 0.182 |
| *Lactobacillus* | Genus | 0.244 | 0 | 0 | 1.725 |
| *Lactobacillus delbrueckii* | Species | 0.244 | 0 | 0 | 1.725 |
| *Enterococcus raffinosus* | Species | 0.238 | 0 | 0 | 1.683 |
| *Enterococcus casseliflavus* | Species | 0.236 | 0 | 0 | 1.669 |
| *Streptococcus dysgalactiae* | Species | 0.228 | 0 | 0.101 | 1.403 |
| *Lactococcus taiwanensis* | Species | 0.22 | 0.197 | 0 | 0.771 |
| *Enterococcus gallinarum* | Species | 0.187 | 0 | 0 | 1.318 |
| *Pseudomonadota* | Phylum | 0.131 | 0.127 | 0 | 0.421 |
| *Gammaproteobacteria* | Class | 0.131 | 0.127 | 0 | 0.421 |
| *Enterobacterales* | Order | 0.131 | 0.127 | 0 | 0.421 |
| *Enterobacteriaceae* | Family | 0.131 | 0.127 | 0 | 0.421 |
| *Escherichia* | Genus | 0.131 | 0.127 | 0 | 0.421 |
| *Escherichia coli* | Species | 0.131 | 0.127 | 0 | 0.421 |
| *Enterococcus saigonensis* | Species | 0.121 | 0 | 0 | 0.856 |
| *Streptococcus cristatus* | Species | 0.109 | 0.194 | 0 | 0 |
| *Streptococcus suis* | Species | 0.105 | 0.187 | 0 | 0 |
| *Streptococcus pyogenes* | Species | 0.103 | 0.183 | 0 | 0 |
| *Streptococcus oralis* | Species | 0.101 | 0.13 | 0 | 0.196 |
| *Streptococcus agalactiae* | Species | 0.093 | 0.12 | 0 | 0.182 |
| *Streptococcus iniae* | Species | 0.091 | 0.162 | 0 | 0 |

**Table 4.3. (Continued)**

| | | | | | |
|---|---|---|---|---|---|
| *Lacticaseibacillus* | Genus | 0.087 | 0 | 0 | 0.617 |
| *Lactococcus petauri* | Species | 0.087 | 0.155 | 0 | 0 |
| *Streptococcus equi* | Species | 0.083 | 0.148 | 0 | 0 |
| *Enterococcus avium* | Species | 0.083 | 0 | 0 | 0.589 |
| *Streptococcus australis* | Species | 0.069 | 0.123 | 0 | 0 |
| *Lacticaseibacillus rhamnosus* | Species | 0.06 | 0 | 0 | 0.421 |
| *Streptococcus anginosus* | Species | 0.06 | 0.106 | 0 | 0 |
| *Enterococcus sp. FDAARGOS_375* | Species | 0.054 | 0 | 0 | 0.379 |
| *Vagococcus zengguangii* | Species | 0.052 | 0 | 0 | 0.365 |
| *Vagococcus* | Genus | 0.052 | 0 | 0 | 0.365 |
| *Bacillus cereus* | Species | 0.046 | 0 | 0 | 0.323 |
| *Enterococcus thailandicus* | Species | 0.042 | 0 | 0 | 0.295 |
| *Latilactobacillus* | Genus | 0.04 | 0 | 0 | 0.281 |
| *Latilactobacillus curvatus* | Species | 0.04 | 0 | 0 | 0.281 |
| *Enterococcus cecorum* | Species | 0.032 | 0 | 0 | 0.224 |
| *Bacillus altitudinis* | Species | 0.032 | 0 | 0 | 0.224 |
| *Bacillus pumilus* | Species | 0.03 | 0 | 0 | 0.21 |
| *Enterococcus durans* | Species | 0.03 | 0 | 0 | 0.21 |
| *Peribacillus asahii* | Species | 0.03 | 0 | 0 | 0.21 |
| *Peribacillus* | Genus | 0.03 | 0 | 0 | 0.21 |
| *Carnobacterium inhibens* | Species | 0.028 | 0 | 0 | 0.196 |
| *Carnobacteriaceae* | Family | 0.028 | 0 | 0 | 0.196 |
| *Enterococcus hirae* | Species | 0.028 | 0 | 0 | 0.196 |
| *Lacticaseibacillus paracasei* | Species | 0.028 | 0 | 0 | 0.196 |
| *Metabacillus* | Genus | 0.028 | 0 | 0 | 0.196 |
| *Carnobacterium* | Genus | 0.028 | 0 | 0 | 0.196 |
| *Metabacillus sp. B2-18* | Species | 0.028 | 0 | 0 | 0.196 |

**Table 4.3. (Continued)**

| | | | | | |
|---|---|---|---|---|---|
| *Enterococcus faecalis* | Species | 0.024 | 0 | 0 | 0.168 |
| *Streptococcus sp. FDAARGOS_522* | Species | 0.022 | 0 | 0 | 0.154 |
| *Cytobacillus kochii* | Species | 0.022 | 0 | 0 | 0.154 |
| *Cytobacillus* | Genus | 0.022 | 0 | 0 | 0.154 |
| *Niallia* | Genus | 0.02 | 0 | 0 | 0.14 |
| *Niallia circulans* | Species | 0.02 | 0 | 0 | 0.14 |
| *Limosilactobacillus* | Genus | 0.02 | 0 | 0 | 0.14 |
| *Limosilactobacillus fermentum* | Species | 0.02 | 0 | 0 | 0.14 |
| *Priestia* | Genus | 0.018 | 0 | 0 | 0.126 |
| *Streptococcus parasanguinis* | Species | 0.018 | 0 | 0 | 0.126 |
| *Priestia megaterium* | Species | 0.018 | 0 | 0 | 0.126 |
| *Sutcliffiella* | Genus | 0.018 | 0 | 0 | 0.126 |
| *Sutcliffiella horikoshii* | Species | 0.018 | 0 | 0 | 0.126 |
| *Streptococcus gallolyticus* | Species | 0.016 | 0 | 0 | 0.112 |
| *Bacillus thuringiensis* | Species | 0.016 | 0 | 0 | 0.112 |

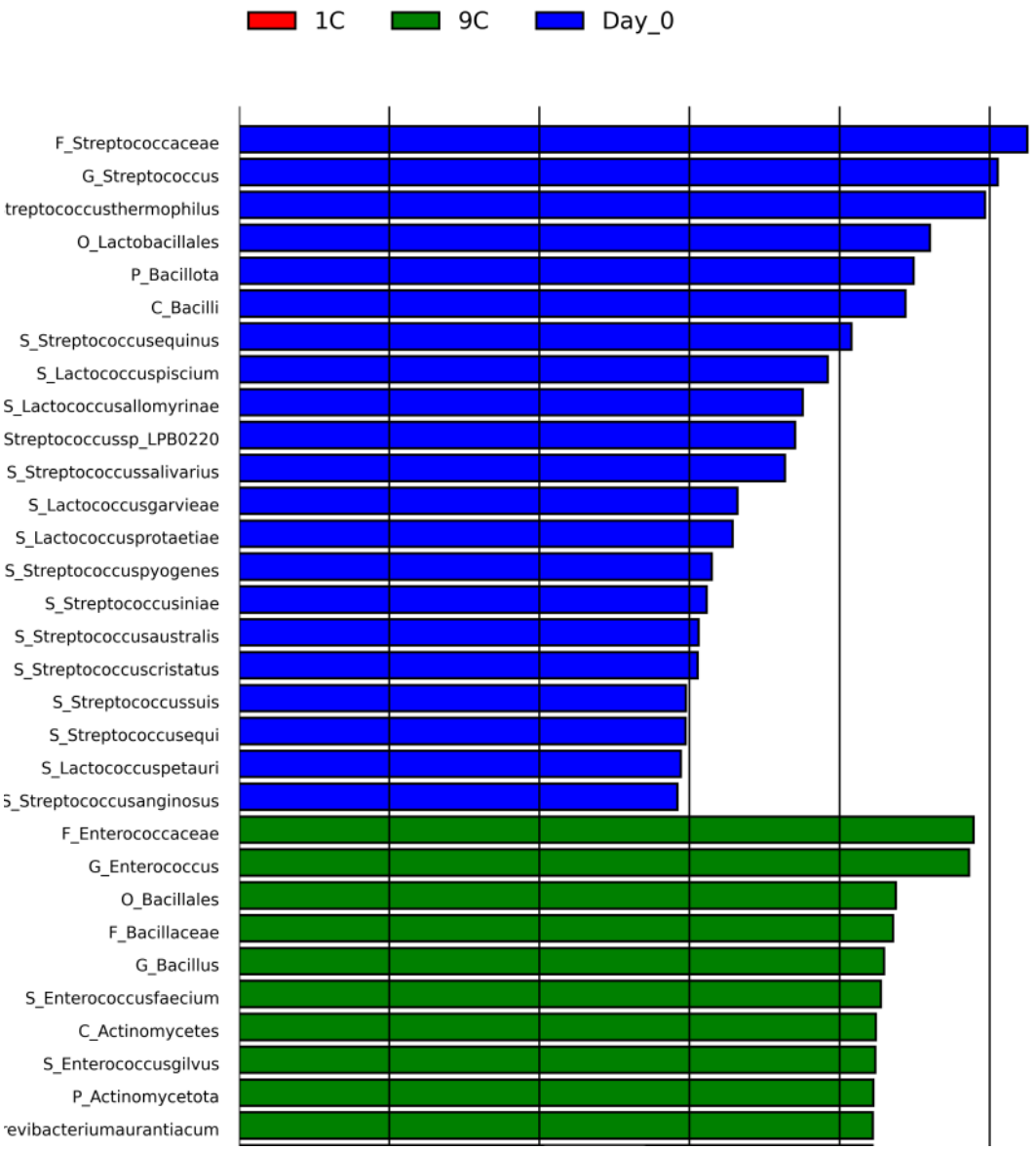


**Figure 4.55a.** LDA score of sample c (control slurry + methionine + *Br. linens* BL2).

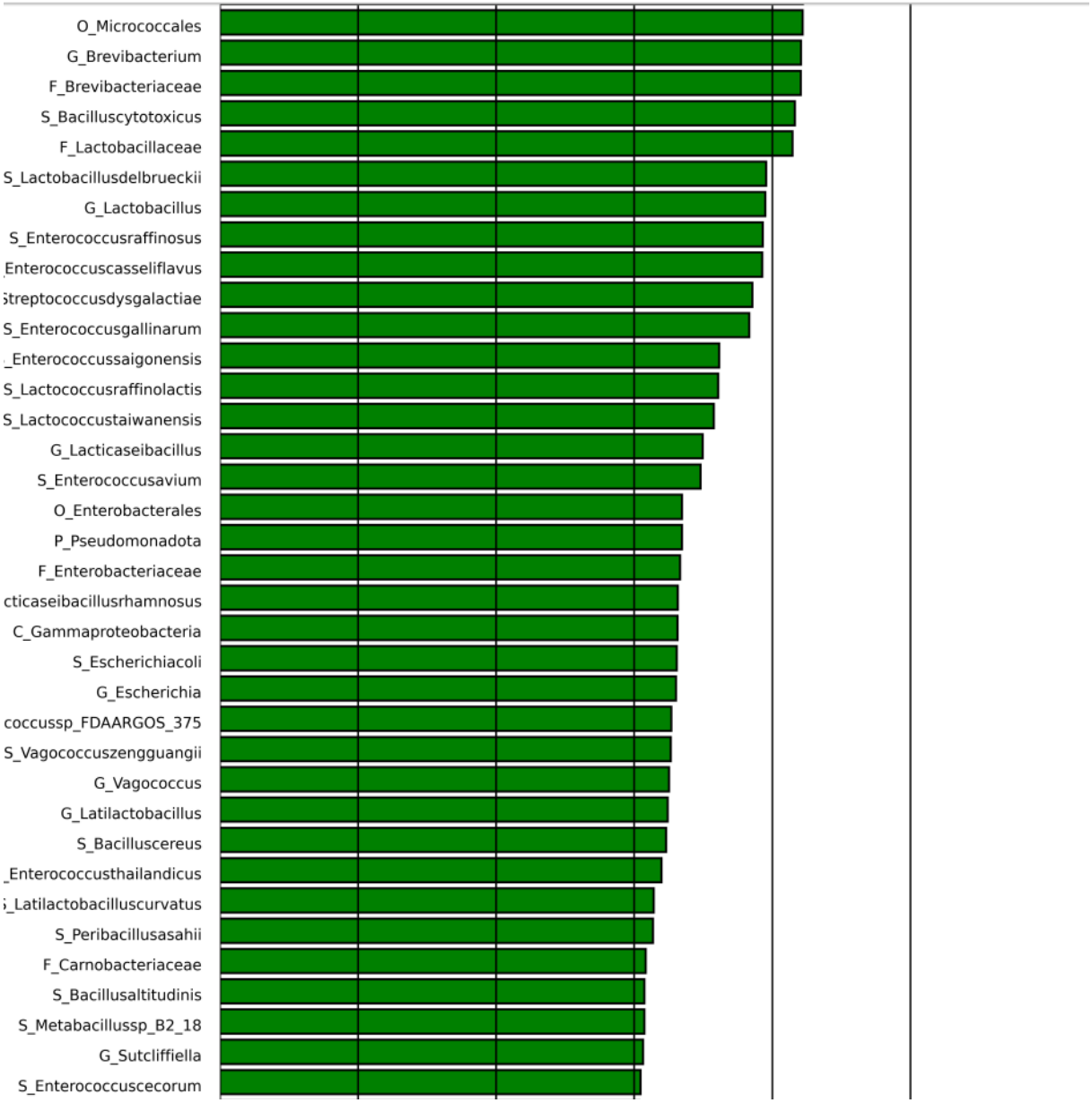


**Figure 4.55b.** LDA score of sample c (control slurry + methionine + *Br. linens* BL2).

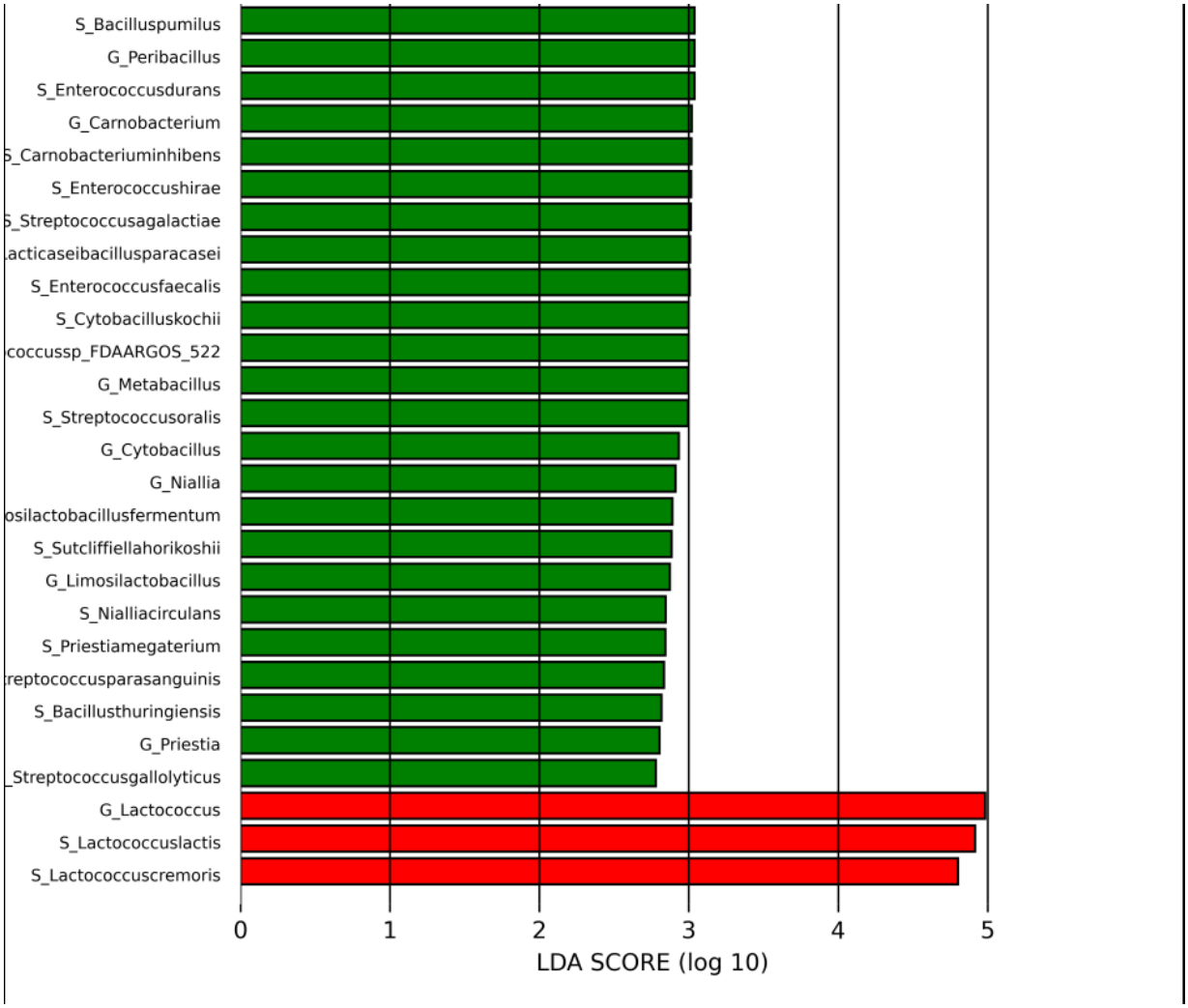


**Figure 4.55c.** LDA score of sample c (control slurry + methionine + *Br. linens* BL2).

### 4.11.11.Taxonomy, LDA score and Cladogram of Sample d (control slurry + methionine + L-methioninase)

A detailed list of bacterial species in sample D over 9 days of incubation is shown in Table 4.4. Linear Discriminant Analysis (LDA) is shown in Figure 4.56. The genus cladogram is shown in Figure 4.57. All these data show the percentage population of species and their statistical significance. Since methionine was catabolized by L-methioninase, the diversity shift was less pronounced than that of sample b, while the starter cultures maintained their dominance.

**Table 4.4.** Species in sample d detected by next generation sequencing.

| Taxon | Taxonomy | %Mean | %Sample0 | %Sample1d | %Sample9d_1 |
|---|---|---|---|---|---|
| *Bacteria* | Domain | 100 | 100 | 100 | 100 |
| *Bacilli* | Class | 99.918 | 99.873 | 100 | 99.878 |
| *Bacillota* | Phylum | 99.918 | 99.873 | 100 | 99.878 |
| *Lactobacillales* | Order | 99.837 | 99.873 | 100 | 99.637 |
| *Streptococcaceae* | Family | 94.504 | 99.873 | 100 | 83.71 |
| *Lactococcus* | Genus | 85.053 | 75.364 | 98.191 | 80.954 |
| *Lactococcus lactis* | Species | 50.749 | 44.866 | 59.331 | 47.641 |
| *Lactococcus cremoris* | Species | 30.457 | 25.718 | 37.035 | 28.296 |
| *Streptococcus* | Genus | 9.451 | 24.509 | 1.809 | 2.756 |
| *Streptococcus thermophilus* | Species | 6.606 | 18.81 | 1.45 | 0.119 |
| *Lactobacillaceae* | Family | 5.15 | 0 | 0 | 15.38 |
| *Limosilactobacillus* | Genus | 2.839 | 0 | 0 | 8.479 |
| *Limosilactobacillus fermentum* | Species | 2.437 | 0 | 0 | 7.278 |
| *Lactobacillus* | Genus | 1.393 | 0 | 0 | 4.162 |
| *Lactococcus piscium* | Species | 1.378 | 1.747 | 0.458 | 1.962 |
| *Lactobacillus delbrueckii* | Species | 1.355 | 0 | 0 | 4.046 |
| *Streptococcus equinus* | Species | 1 | 2.702 | 0.252 | 0.126 |
| *Lactococcus allomyrinae* | Species | 0.866 | 1.511 | 0.508 | 0.611 |
| *Streptococcus sp. LPB0220* | Species | 0.514 | 1.046 | 0.106 | 0.418 |
| *Lactococcus taiwanensis* | Species | 0.493 | 0.197 | 0.183 | 1.096 |
| *Lacticaseibacillus* | Genus | 0.482 | 0 | 0 | 1.439 |
| *Lactococcus garvieae* | Species | 0.374 | 0.395 | 0.192 | 0.54 |
| *Lacticaseibacillus rhamnosus* | Species | 0.335 | 0 | 0 | 1.001 |
| *Lactococcus protaetiae* | Species | 0.333 | 0.535 | 0.252 | 0.221 |
| *Streptococcus sp. FDAARGOS_522* | Species | 0.296 | 0 | 0 | 0.883 |

**Table 4.4. (Continued)**

| | | | | | |
|---|---|---|---|---|---|
| *Lactococcus raffinolactis* | Species | 0.251 | 0.24 | 0.119 | 0.397 |
| *Limosilactobacillus reuteri* | Species | 0.25 | 0 | 0 | 0.747 |
| *Streptococcus salivarius* | Species | 0.193 | 0.599 | 0 | 0 |
| *Enterococcus* | Genus | 0.183 | 0 | 0 | 0.547 |
| *Enterococcaceae* | Family | 0.183 | 0 | 0 | 0.547 |
| *Streptococcus agalactiae* | Species | 0.17 | 0.12 | 0 | 0.394 |
| *Lactococcus petauri* | Species | 0.152 | 0.155 | 0.113 | 0.19 |
| *Lacticaseibacillus paracasei* | Species | 0.147 | 0 | 0 | 0.438 |
| *Enterococcus faecium* | Species | 0.132 | 0 | 0 | 0.394 |
| *Streptococcus oralis* | Species | 0.126 | 0.13 | 0 | 0.251 |
| *Lentilactobacillus* | Genus | 0.117 | 0 | 0 | 0.35 |
| *Lentilactobacillus buchneri* | Species | 0.117 | 0 | 0 | 0.35 |
| *Streptococcus dysgalactiae* | Species | 0.097 | 0 | 0 | 0.289 |
| *Streptococcus iniae* | Species | 0.093 | 0.162 | 0 | 0.122 |
| *Ligilactobacillus saerimneri* | Species | 0.091 | 0 | 0 | 0.272 |
| *Latilactobacillus* | Genus | 0.091 | 0 | 0 | 0.272 |
| *Latilactobacillus curvatus* | Species | 0.091 | 0 | 0 | 0.272 |
| *Ligilactobacillus* | Genus | 0.091 | 0 | 0 | 0.272 |
| *Gammaproteobacteria* | Class | 0.082 | 0.127 | 0 | 0.122 |
| *Enterobacterales* | Order | 0.082 | 0.127 | 0 | 0.122 |
| *Enterobacteriaceae* | Family | 0.082 | 0.127 | 0 | 0.122 |
| *Pseudomonadota* | Phylum | 0.082 | 0.127 | 0 | 0.122 |
| *Escherichia* | Genus | 0.082 | 0.127 | 0 | 0.122 |
| *Escherichia coli* | Species | 0.082 | 0.127 | 0 | 0.122 |
| *Bacillus* | Genus | 0.081 | 0 | 0 | 0.241 |
| *Bacillaceae* | Family | 0.081 | 0 | 0 | 0.241 |
| *Bacillales* | Order | 0.081 | 0 | 0 | 0.241 |

**Table 4.4. (Continued)**

| | | | | | |
|---|---|---|---|---|---|
| *Bacillus cytotoxicus* | Species | 0.081 | 0 | 0 | 0.241 |
| *Limosilactobacillus mucosae* | Species | 0.066 | 0 | 0 | 0.197 |
| *Levilactobacillus suantsaii* | Species | 0.064 | 0 | 0 | 0.19 |
| *Levilactobacillus* | Genus | 0.064 | 0 | 0 | 0.19 |
| *Streptococcus cristatus* | Species | 0.063 | 0.194 | 0 | 0 |
| *Streptococcus suis* | Species | 0.06 | 0.187 | 0 | 0 |
| *Streptococcus pyogenes* | Species | 0.059 | 0.183 | 0 | 0 |
| *Streptococcus sp. FDAARGOS_520* | Species | 0.052 | 0 | 0 | 0.156 |
| *Enterococcus saigonensis* | Species | 0.051 | 0 | 0 | 0.153 |
| *Streptococcus equi* | Species | 0.048 | 0.148 | 0 | 0 |
| *Limosilactobacillus pontis* | Species | 0.048 | 0 | 0 | 0.143 |
| *Streptococcus australis* | Species | 0.04 | 0.123 | 0 | 0 |
| *Limosilactobacillus gastricus* | Species | 0.039 | 0 | 0 | 0.115 |
| *Lactobacillus sp. 3B* | Species | 0.039 | 0 | 0 | 0.115 |
| *Paucilactobacillus nenjiangensis* | Species | 0.038 | 0 | 0 | 0.112 |
| *Paucilactobacillus* | Genus | 0.038 | 0 | 0 | 0.112 |
| *Lactiplantibacillus* | Genus | 0.035 | 0 | 0 | 0.105 |
| *Lactiplantibacillus plantarum* | Species | 0.035 | 0 | 0 | 0.105 |
| *Streptococcus anginosus* | Species | 0.034 | 0.106 | 0 | 0 |

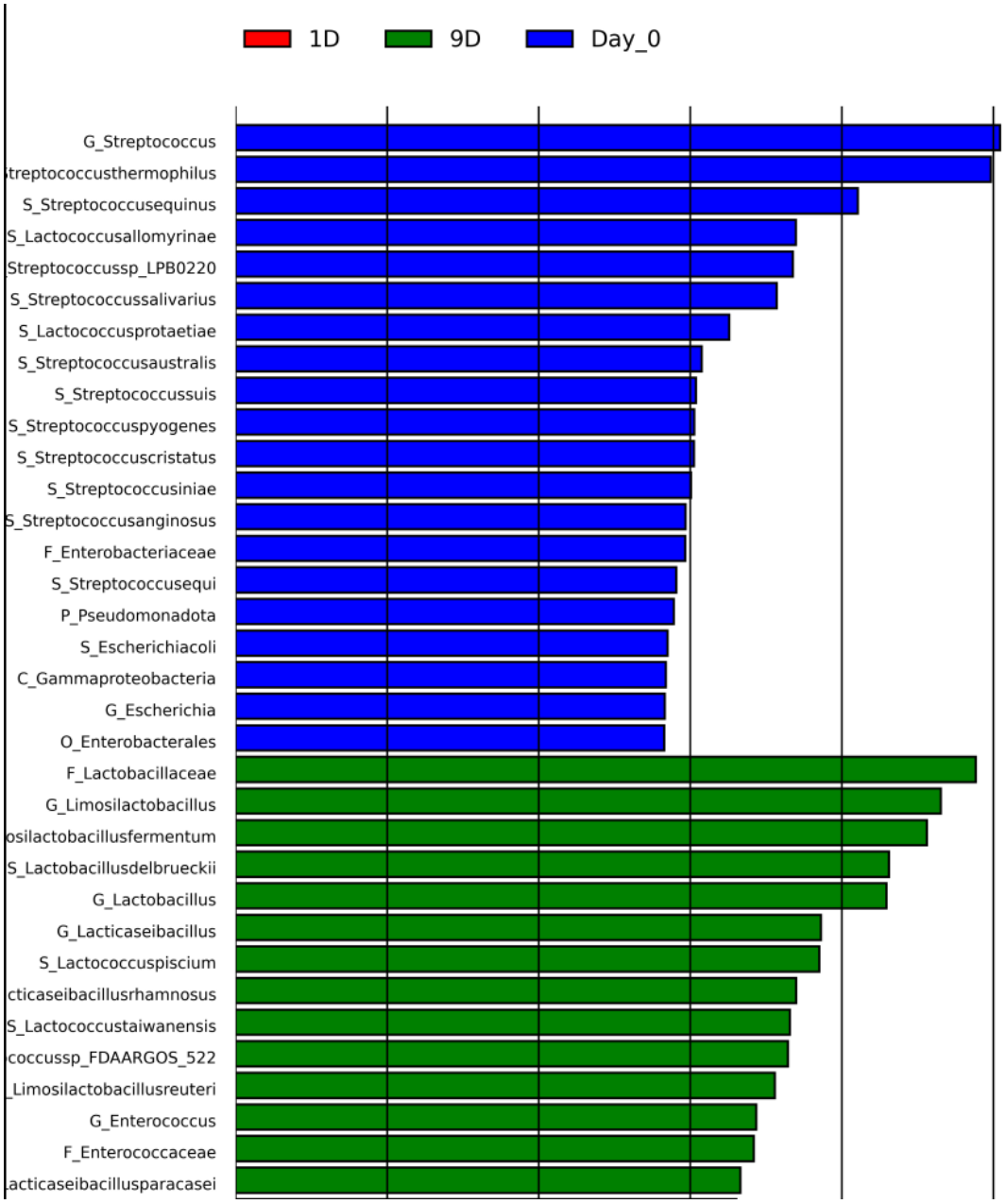


**Figure 4.56a.** LDA score of sample d (control slurry + methionine + L-methioninase).

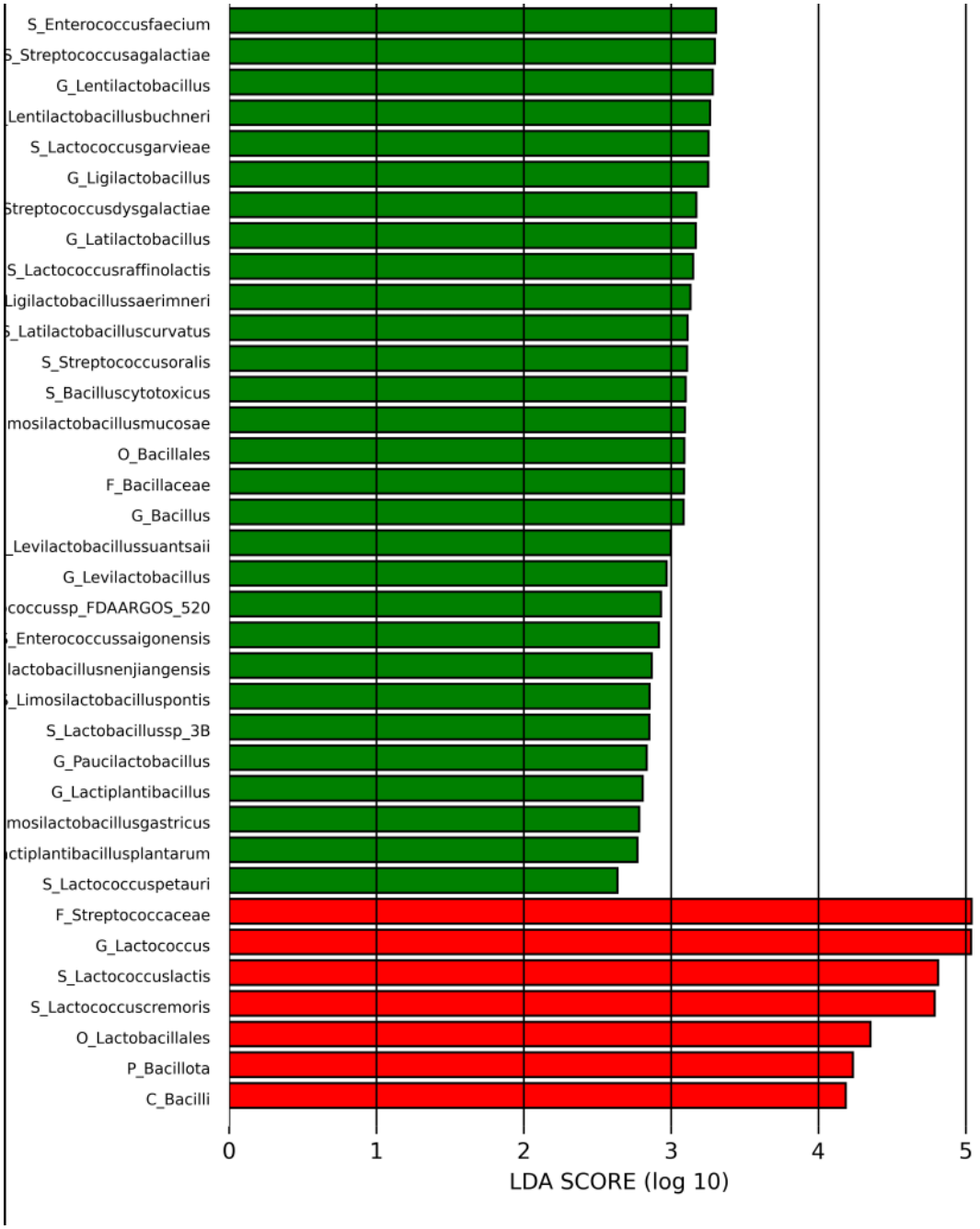


**Figure 4.56b.** LDA score of sample d (control slurry + methionine + L-methioninase).

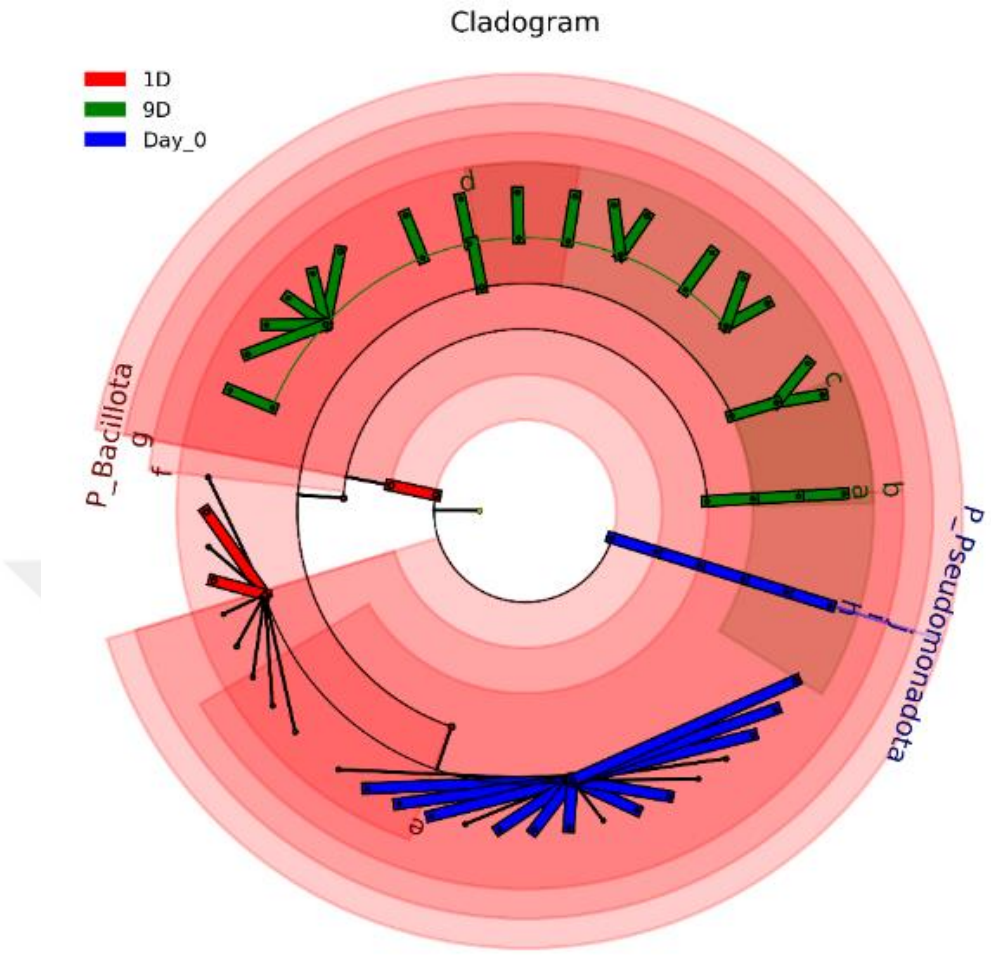


**Figure 4.57.** Genus cladogram of sample d (control slurry + methionine + L-methioninase).

### 4.11.12. GC-MS Analysis Results

Volatile compounds in the cheddar slurry samples were analyzed using SPME with GC-MS at four time points: zero (control), 1, 4, and 9 days of fermentation, across four distinct experimental sets.

The volatile compound profiles of cheddar cheese slurry are provided in the following tables:

Table 4.5: Volatile compound profile at zero time.
Table 4.6: Volatile compound profile at 1 day of incubation.
Table 4.7: Volatile compound profile at 4 days of incubation.
Table 4.8: Volatile compound profile at 9 days of incubation.

The changes in the amounts of methanethiol and dimethyl trisulfide over time in the samples are illustrated in Figure 4.58.

**Table 4.5.** Volatile compound profile of cheddar cheese slurry at time zero.

| Compound | LRI* | Control (Zero)** |
|---|---|---|
| **Methanethiol** | 670 | ND*** |
| **Toluene** | 1044 | 250.7±0.26 |
| **Limonene** | 1210 | 990.7±1.04 |
| **O-Cymene** | 1273 | 4480.9±4.69 |
| **Acetoin** | 1285 | 576.9±0.28 |
| **Dimethyl trisulfide** | 1387.5 | ND |
| **Acetic Acid** | 1445 | 722.5±0.76 |
| **Butanoic Acid** | 1630 | 330.3±0.35 |
| **Hexanoic Acid** | 1842.5 | 148.3±0.16 |
| **Phenol** | 1995.5 | 41.7±0.04 |
| **Octanoic Acid** | 2071.5 | 1370.5±1.43 |
| **Nonanoic Acid** | 2160.5 | 115.6±0.12 |
| **Benzoic Acid** | 2413 | 208.8±0.22 |
| **Dodecanoic Acid** | 2492 | 371.7±0.39 |

* Linear retention index calculated for the DVB/CAR/PDMS column.

**Volatile compound amounts are expressed in µg $kg^{-1}$ dry matter.

***Not determined. *(P* < 0.05).

Table 4.5 provides information about the volatile flavor compounds detected in cheddar cheese on day zero (control) of the experiment. No sulfur compounds were formed at this stage because neither methionine nor L-methioninase was added. The most prominent volatile compounds in the control samples were limonene and O-cymene. Limonene and O-cymene are aromatic compounds that are found in various foods and beverages. Limonene, in particular, is commonly associated with citrus fruits and has a fresh citrusy aroma. O-cymene is a monoterpene that is often found in the essential oils of aromatic plants and has a pleasant herbal scent.

**Table 4.6.** Volatile compound profile of cheddar cheese slurry at 1 day incubation.

| Compound | LRI* | a** | b** | c** | d** |
|---|---|---|---|---|---|
| **Methanethiol** | 670 | ND*** | ND | 1731.0 ± 1.09 | 1490.2 ± 1.31 |
| **Ethanol** | 923.5 | 9456.4±9.90 | 8356.2±2.54 | 6989±3.22 | 7935.4±4.99 |
| **2,3 Butanedione** | 980.5 | ND | ND | 1443.0±0.91 | 1520.2±0.96 |
| **Toluene** | 1044 | 2108.7 ± 2.21 | 389.7±0.24 | ND | ND |
| **Limonene** | 1210 | 538.8 ± 0.56 | 684.5±0.43 | 765.4±0.48 | 947.1±0.60 |
| **2-Heptanone** | 1175.5 | ND | ND | 54.5±0.03 | 947.1±0.60 |
| **O-Cymene** | 1273 | ND | 3595.9±2.26 | 4048.7±2.54 | 1507.6±0.95 |
| **Acetoin** | 1285 | 5693.6± 5.96 | 1970.9±1.24 | 1944.1±1.22 | 2181.1±1.37 |
| **Dimethyl Trisulfide** | 1387.5 | ND | ND | 52.4±0.01 | 65.8±0.04 |
| **Acetic Acid** | 1445 | 3370.2± 3.53 | 1679.5±1.06 | 1969.4±1.24 | 2111.4±1.33 |
| **Butanoic Acid** | 1630 | 556.8±0.58 | 351.5±0.22 | 243.7±0.15 | 1005.7±0.63 |
| **Pentanoic Acid** | 1730.5 | 21.5±0.02 | 117.1±0.07 | ND | ND |
| **Hexanoic Acid** | 1842.5 | 65.6±0.07 | 378.2±0.24 | 322.3±0.20 | 701.9±0.44 |
| **Dimethyl Sulfone** | 1907.5 | ND | ND | 539.8±0.34 | ND |
| **Phenol** | 1995.5 | 203.1±0.21 | 50.9±0.03 | 43.9±0.03 | 104.0±0.07 |
| **Octanoic Acid** | 2071.5 | 1723.2±1.80 | 908.6±0.57 | 972.1±0.61 | 1477.8±0.93 |
| **Nonanoic Acid** | 2160.5 | 154.4±0.16 | 67.8±0.04 | 56.2±0.04 | 111.9±0.07 |
| **9-Decenoic Acid** | 2337 | ND | ND | 121.3±0.08 | 264.2±0.17 |

| Table 4.6. (Continued) | | | | | |
|---|---|---|---|---|---|
| **Benzoic Acid** | 2413 | 454.0±0.48 | 271.2±0.17 | 226.6±0.14 | 500.2±0.31 |
| **Dodecanoic Acid** | 2492 | 707.7±0.74 | 397.2±0.25 | 329.2±0.21 | 989.3±0.62 |

* Linear retention index calculated for the DVB/CAR/PDMS column.

**Volatile compound amounts are expressed in µg $kg^{-1}$ dry matter.

***Not determined. ($P < 0.05$).

**Table 4.7.** Volatile compound profile of cheddar cheese slurry at 4 days incubation.

| Compound | LRI* | a** | b** | c** | d** |
|---|---|---|---|---|---|
| **Methanethiol** | 670 | ND*** | ND | 3589 ± 1.08 | 3884 ± 2.12 |
| **Ethyl Acetate** | 880 | 6645.4 ± 4.18 | 2662.9 ± 1.67 | 3462.9 ±1.58 | 5629.6 ± 3.54 |
| **Ethanol** | 923.5 | 16410.0 ± 10.31 | 11105.7 ± 6.98 | 9126.9 ± 5.73 | 13967.3 ± 8.78 |
| **2,3 Butanedione** | 980.5 | 1850.1 ± 0.54 | 1938.6 ± 1.04 | 5100.1 ± 2.06 | 4839.1 ± 3.04 |
| **Limonene** | 1210 | 1663.7 ± 1.05 | 1883.8 ± 1.36 | 828.7 ± 0.52 | 1832.9 ± 1.15 |
| **O-Cymene** | 1273 | 4606.4 ± 2.89 | 2882.2 ± 1.04 | 3883.4 ± 2.44 | 9838.4 ± 6.18 |
| **Acetoin** | 1285 | 4873.9 ± 3.06 | 2179.0 ± 1.37 | 4092.2±2.57 | 2199.4±1.54 |
| **Dimethyl Trisulfide** | 1387.5 | ND | ND | 498 ± 0.18 | 558 ± 0.31 |
| **Acetic Acid** | 1445 | 7490.1±4.71 | 5252.4±3.30 | 4914.8±3.09 | 10404.2±6.54 |
| **Benzaldehyde** | 1525 | 5068.4±3.18 | 1156.1±0.73 | 3980.1±1.25 | 2985.51.88 |
| **Propanoic Acid** | 1532.5 | 52.2±0.01 | 34.1±0.02 | 156.4±0.05 | 1847.2±1.16 |
| **Butanoic Acid** | 1630 | 2632.2±1.65 | 219.2±0.14 | 609.2±0.38 | 1192.7±0.75 |
| **Pentanoic Acid** | 1730.5 | 542.8±0.34 | 5182.6±3.26 | 120.9±0.08 | 456.8±1.2 |
| **Hexanoic Acid** | 1842.5 | 3279.5±2.60 | 1719.0±1.81 | 975.0±0.61 | 2420.2±1.52 |
| **Heptanoic Acid** | 1934 | 556.2±0.56 | 685.9±1.47 | 109.3±0.07 | 256.4±0.09 |
| **Phenol** | 1995.5 | 322.2±0.20 | 45.0±0.03 | 220.8±0.14 | 331.0±0.21 |
| **Octanoic Acid** | 2071.5 | 4241.0±2.66 | 3075.5±1.93 | 2513.8±1.58 | 4493.5±2.82 |
| **Nonanoic Acid** | 2160.5 | 360.9±0.23 | 302.6±0.14 | 246.8±0.16 | 336.3±0.21 |

| **Table 4.7. (Continued)** | | | | | |
|---|---|---|---|---|---|
| **9-Decenoic Acid** | 2337 | 1180.4±0.74 | 684.1±0.58 | 503.2±0.32 | 904.5±0.57 |
| **Benzoic Acid** | 2413 | 2101.4±1.32 | 187.0±0.12 | 900.9±0.57 | 1150.7±0.72 |
| **Indole** | 2428 | 1091.8 ± 0.69 | 289.4 ± 0.18 | 198.8 ± 0.09 | 152.9 ± 0.10 |
| **Dodecanoic Acid** | 2492 | 3541.5±2.23 | 1952.2±1.51 | 1051.2±0.66 | 2082.7±1.31 |
| **Tetradecanoic Acid** | 2690.5 | 1972.7 ± 5.01 | 1896.0±0.99 | 1164.0 ± 0.73 | 1507.9 ± 0.95 |

* Linear retention index calculated for the DVB/CAR/PDMS column.

**Volatile compound amounts are expressed in µg $kg^{-1}$ dry matter.

***Not determined. ($P < 0.05$).

**Table 4.8.** Volatile compound profile of cheddar cheese slurry at 9 days incubation.

| Compound | LRI* | a** | b** | c** | d** |
|---|---|---|---|---|---|
| **Methanethiol** | 670 | ND*** | ND | 9314.2±5.85 | 8654±2.14 |
| **Ethyl Acetate** | 880 | 3107.6±1.95 | 2187.2±1.84 | 3254.1±0.54 | 3085.3±1.05 |
| **Ethanol** | 923.5 | 6614.8±2.01 | 25658.6±16.12 | 8618.8±5.41 | 18583.1±11.68 |
| **2,3 Butanedione** | 980.5 | 998.2±0.12 | 1001.4±0.24 | 895.4± 0.84 | 1206.6±0.76 |
| **Limonene** | 1210 | 1259.6±0.79 | 4583.1±2.88 | 2924.1±1.84 | 344.5±0.22 |
| **O-Cymene** | 1273 | 7118.5±4.47 | 11923.7±7.49 | 8654.2±1.56 | 9377.0±5.89 |
| **Acetoin** | 1285 | 2245.3±1.41 | 8884.2±5.58 | 4215.8±2.22 | 4506.5±2.83 |
| **DimethylTrisulfide** | 1387.5 | ND | ND | 1223.3±1.53 | 954.2±0.21 |
| **Acetic Acid** | 1445 | 6432.9±4.04 | 3932.8±2.47 | 982.4±0.62 | 1169.7±0.35 |
| **Benzaldehyde** | 1525 | 3133.2± 1.69 | 7309.6± 4.59 | 896.7±0,23 | 288.8±0.18 |
| **Propanoic Acid** | 1532.5 | 1628.0±1.02 | 1898.0±1.08 | 4225.5±2.65 | 1999.0±1.75 |
| **Butanoic Acid** | 1630 | 1170.9±0.74 | 3070.1±1.29 | 2890.7±1.16 | 1174.7±0.74 |
| **Pentanoic Acid** | 1730.5 | 201.2±0.38 | 221.2±0.39 | 327.1±0.05 | 405.2±0.14 |
| **Hexanoic Acid** | 1842.5 | 26279.5±16.51 | 121858.4±76.56 | 89906.8±56.48 | 21810.5±13.70 |
| **Heptanoic Acid** | 1934 | 4970.2±2.01 | 7294.1±4.58 | 5470.8±3.44 | 6425.9±3.56 |
| **Phenol** | 1995.5 | 344.2±0.22 | 1577.2±0.99 | 1101.6±0.69 | 314.6±0.20 |
| **Octanoic Acid** | 2071.5 | 3558.0 ± 2.24 | 4560.4±5.87 | 4085.0±1.54 | 4598.2±2.89 |
| **Nonanoic Acid** | 2160.5 | 275.8±0.17 | 963.0±0.06 | 457.4±0.85 | 329.8±0.21 |

| **Table 4.8. (Continued)** | | | | | |
|---|---|---|---|---|---|
| **9-Decenoic Acid** | 2337 | 495.6±0.31 | 2140.9±1.45 | 1868.4±1.74 | 682.2±0.43 |
| **Benzoic Acid** | 2413 | 890.4±0.56 | 2302.2±1.45 | 2103.8±1.32 | 842.8±0.53 |
| **Indole** | 2428 | 573.7±0.36 | ND | 2006.9±1.26 | ND |
| **Dodecanoic Acid** | 2492 | 1442.6±0.91 | 4583.2±2.80 | 3292.3±2.68 | 2058.0±1.29 |
| **Tetradecanoic Acid** | 2690.5 | 438.2±0.28 | 2913.0±1.30 | 1622.0±1.19 | 642.6±0.40 |

* Linear retention index calculated for the DVB/CAR/PDMS column.

**Volatile compound amounts are expressed in µg $kg^{-1}$ dry matter.

***Not determined. ($P < 0.05$).

The absence of sulfur compounds at day zero was expected, as these compounds are typically formed during later stages of fermentation when methionine is available as a substrate for enzymatic reactions, such as those involving L-methioninase. The addition of methionine or L-methioninase later in the experiment likely led to the production of sulfur compounds, as indicated in previous descriptions. These sulfur compounds contribute to the characteristic aroma and flavor of cheddar cheese.

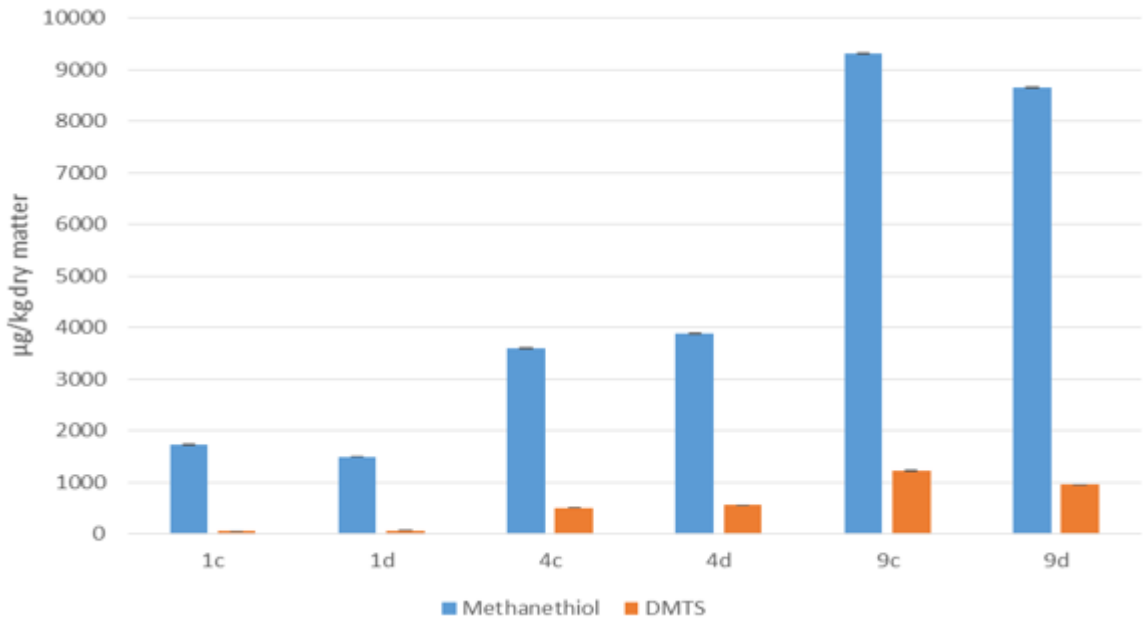


**Figure 4.58.** Methanethiol and dimethyl Trisulfide amount change in time between samples.

L-methioninase increased the levels of sulfur compounds (methanethiol and dimethyl trisulfide) after 9 days of incubation. Metahnethiol is considered an attractive flavor compound in cheddar cheese. Thus, L-methioninase obtained from *Brevibacterium linens* BL2 could be a potential food enzyme in cheddar cheese production to increase its economic value and sensory quality. Other volatile compounds, as depicted on the tables, which are important in cheddar cheese, were not profoundly affected by the addition of L-methioninase.

In the literature, methanethiol has been readily oxidized to dimethyl disulfide and dimethyl trisulfide (Dias and Weimer, 1999). However, Dimethyl Disulfide was not detected in the DVB/CAR/PDMS column in this study. The methanethiol content increased as the incubation period was extended, which is consistent with the findings of Dias and Weimer (1999). The formation of dimethyl trisulfide also increased, although not to the same extent as that of the

methanethiol. Other volatile compounds detected in cheddar cheese slurries at zeroth, first, fourth, and ninth days of incubation were consistent with the typical flavor characteristics of cheddar cheese, as documented in the literature (Wang et al., 2021).

Notably, no sulfur compounds were detected in the zero-day samples. However, after adding L-methioninase and *Brevibacterium linens* BL2, methanethiol and dimethyl trisulfide were formed, whereas no such formation was observed in the control samples. This indicated that L-methioninase from *Br. linens* BL2 remained stable under cheese production conditions. Notably, the addition of *Br. linens* or L-methioninase did not significantly disrupt the formation of other volatiles. Although methanethiol is a key compound contributing to cheddar cheese flavor, it does not provide a complete cheddar flavor profile, even in substantial amounts (Ashraf et al., 2023). Therefore, other specific volatiles essential for cheddar cheese flavor must also be generated.

The quantity of volatiles formed in cheddar cheese over nine days is detailed in Tables 4.5, 4.6, 4.7, and 4.8. A comparison of methanethiol and dimethyl trisulfide amounts can be seen in Figure 4.58, with methanethiol reaching its peak at 9314.2±5.85 µg kg-1 dry matter in sample 9c (control slurry + methionine + *Br. linens* BL2), where *Br. linens* BL2 were cultured.

Dias and Weimer (1999) explored the effect of L-methioninase from *Brevibacterium linens* BL2 on the production of sulfur compounds in cheddar cheese slurries. They used an SPB1-Sulphur column for sulfur compound detection, whereas a DVB-CAR-PDMS column was employed in this study. Notably, dimethyl sulfide and dimethyl disulfide were not detected in the DVB-CAR-PDMS column, in contrast with the SPB1-Sulphur column. A detailed microbial analysis was not conducted by Dias and Weimer, possibly because of concerns about significant microbial growth within 14 days of fermentation. This can be observed in the microbial diversity after 9 days of fermentation in this study. Lindsay and Rippe (1986) conducted another study on the production of sulfur compounds. In their study, L-methioninase from *Pseudomonas putida* was used to generate methanethiol, which was detected using a Carbopak BHT-100 column on a GC system. However, it is important to note that besides its methanethiol productivity, Pseudomonas putida has been reported as a

human pathogen (Fernández et al., 2015). Hence, it is crucial to conduct a comprehensive examination of food safety aspects related to L-methioninase from *Ps. putida* L-methioninase's relevance in different areas emphasizes the need for a thorough evaluation of its safety considerations to ensure its suitability for various uses.

# 5. CONCLUSION

This thesis describes the partial purification of L-methioninase from *Brevibacterium linens* BL2. This enzyme demonstrated significant potential as an effective anticancer treatment, particularly by showing cytotoxic effects against glioblastoma U87MG and T98G cells. It is worth noting that it exhibited a lower cytotoxic effect against MEF and HaCaT cells, indicating a certain level of selectivity in its action. Furthermore, L-methioninase effectively counteracted the cytotoxic effects of etoposide in HaCaT and MEF cells.

When combined with etoposide, L-methioninase showed increased cytotoxicity against glioblastoma U87MG and T98G cells compared to its individual effects. The expression levels of c-Myc and survivin, both well-known for their anti-apoptotic properties, were significantly downregulated when L-methioninase and etoposide were administered either individually or in combination. Furthermore, both L-methioninase and etoposide, whether used individually or together, upregulated the expression of Caspase-3, indicating enhanced activation of apoptotic pathways in cancer cells.

In addition to its application in cancer research, L-methioninase extracted from *Brevibacterium linens* BL2 can be utilized as a culture adjuvant, typically in smear cheeses. Although *Brevibacterium linens* BL2 is not commonly employed in cheddar cheese production because of the predominance of acidic conditions in the cheese-making process, we sought to investigate the use of L-methioninase from this bacterium to promote sulfur compound development in cheddar cheese slurries. Throughout the fermentation process, both *Brevibacterium linens* BL2 and L-methioninase demonstrated the ability to produce methanethiol and its oxidized form, Dimethyl Trisulfide. This indicates the potential of L-methioninase to accelerate flavor development in cheddar cheese production, thereby presenting economic advantages.

Furthermore, this study analyzed the microbiota of cheddar cheese slurries using next-generation sequencing. Prolonged fermentation periods resulted in uncontrolled shifts in bacterial populations within the raw milk cheddar cheese slurries. These findings could be instrumental in identifying the ideal timing for L-methionine incorporation of L-methioninase

in cheese production. Subsequent research could delve deeper into these aspects, with more comprehensive analyses of pasteurized milk cheddar cheese slurries.

# 6. RECOMMENDATIONS

Considering the data evaluated in this thesis, future studies should encompass the following areas:

First, experiments should be conducted with complete purification of L-methioninase. This is essential for demonstrating the full potential and effectiveness of this enzyme in various applications. Moreover, cancer experiments should be performed on different cell lines to evaluate the cytotoxic effects of L-methioninase. Therefore, it is crucial to explore its potential as a treatment option for various types of cancer. Detailed cell cycle analyses should be performed after L-methioninase treatment to understand its effect on cell division and proliferation. Additionally, Alternative forms of L-methioninase, such as oral or intravenous injection forms, should be investigated in vivo to optimize its delivery and efficacy.

Furthermore, the expanded use of L-methioninase in different types of cheeses should be investigated. Exploring how this enzyme influences the taste profiles and characteristics of different cheeses would broaden its application in the dairy industry. Additionally, it is essential to assess the physicochemical attributes of cheese, including texture, shelf life, and other quality parameters, to understand L-methioninase's impact of L-methionine. In this context, sensory analyses should be incorporated to evaluate the influence of enzymes on the taste, aroma, and overall sensory qualities of cheeses. Additionally, research efforts should be directed towards developing novel strategies for controlling microbial populations, potentially enhancing the quality and safety of fermented foods.

Finally, exploration and identification of novel microorganisms with the capacity to produce L-methioninase, particularly in food samples, may lead to the discovery of this enzyme. We believe that these research recommendations have the potential to expand the applications of L-methioninase in the fields of food science and cancer treatment.

# REFERENCES

Abozeid, A. A. (2023). Short review on microbial L-methioninase and its applications. Bulletin of Faculty of Science, Zagazig University, 2022(4), 107-139.

Abu-Tahon, M. A., & Isaac, G. S. (2016). Comparative study of a new alkaline L-methioninase production by Aspergillus ustus AUMC 10151 in submerged and solid-state fermentation. Brazilian Archives of Biology and Technology, 59, e16150484.

Adeoye, O., Olawumi, J., Opeyemi, A., & Christiania, O. (2018). Review on the role of glutathione on oxidative stress and infertility. JBRA Assisted Reproduction, 22(1), 61.

Afshari, R., Pillidge, C. J., Dias, D. A., Osborn, A. M., & Gill, H. (2020). Cheesomics: The future pathway to understanding cheese flavour and quality. Critical Reviews in Food Science and Nutrition, 60(1), 33-47.

Al-Khedhairy, A. A., & Wahab, R. (2022). Size-dependent cytotoxic and molecular study of the use of gold nanoparticles against liver cancer cells. Applied Sciences, 12(2), 901.

Al-Zahrani N.H., Bukhari K.A. (2019). Molecular identification, gene detection, and improving L-methioninase production of serratia sp. isolate. Pharmacophore,10(6), 14-25.

Amarita, F., Yvon, M., Nardi, M., Chambellon, E., Delettre, J., & Bonnarme, P. (2004). Identification and functional analysis of the gene encoding methionine-γ-lyase in *Brevibacterium linens*. Applied and Environmental Microbiology, 70(12), 7348-7354.

Anderson, M. E. (1998). Glutathione: an overview of biosynthesis and modulation. Chemico-Biological Interactions, 111, 1-14.

Ashraf, U., Sameen, A., Ashraf, J. Z., Tuseef, M., Khalid, R., Abbas, S. M. N., Sultan, M. M., Rafique, M., & Gull, T. (2023). Development and evaluation of processed cheese spread supplemented with ripened cheddar cheese. RADS Journal of Food Biosciences, 2(1), 1-9.

Aston, J. W. (1981). The production of volatile sulphur compounds in Cheddar cheese during accelerated ripening (Doctoral dissertation, Queensland University of Technology).

Baghdadi, A. M., & Danial, E. N. (2022). L-methioninase enzyme production by E. coli WSM2 using some organic by product residues. Egyptian Journal of Chemistry, 65(12), 275-281.

Barzideh, Z., Siddiqi, M., Mohamed, H. M., & LaPointe, G. (2022). Dynamics of starter and non-starter lactic acid bacteria populations in long-ripened cheddar cheese using propidium monoazide (PMA) treatment. Microorganisms, 10(8), 1669.

Behnan, J., Finocchiaro, G., & Hanna, G. (2019). The landscape of the mesenchymal signature in brain tumours. Brain, 142(4), 847–866.

Bolander-Gouaille, C., & Bottiglieri, T. (2003). Homocysteine: Related vitamins and neuropsychiatric disorders. Springen-Verlag, New York, LLC.

Borenfreund, E., & Puerner, J. A. (1985). Toxicity determined in vitro by morphological alterations and neutral red absorption. Toxicology Letters, 24(2-3), 119-124.

Bradford, M. M. (1976). A rapid and sensitive method for the quantitation of microgram quantities of protein utilizing the principle of protein-dye binding. Analytical Biochemistry, 72(1-2), 248-254.

Brower, A. V. (2016). What is a cladogram and what is not?. Cladistics, 32(5), 573-576.

Cadoret, A., Desbois-Mouthon, C., Wendum, D., Leneuve, P., Perret, C., Tronche, F., ... & Holzenberger, M. (2005). c-myc-induced hepatocarcinogenesis in the absence of IGF-I receptor. International Journal of Cancer, 114(4), 668-672.

Cavuoto, P., & Fenech, M. F. (2012). A review of methionine dependency and the role of methionine restriction in cancer growth control and life-span extension. Cancer Treatment Reviews, 38(6), 726-736.

Chaturvedi, S., & Bertino, J. R. (2019). Methods to study the role of methionine-restricted diet and methioninase in cancer growth control. Methionine Dependence of Cancer and Aging: Methods and Protocols, 1-12.

Chaturvedi, S., Hoffman, R. M., & Bertino, J. R. (2018). Exploiting methionine restriction for cancer treatment. Biochemical Pharmacology, 154, 170-173.

Chiou, S. K., Jones, M. K., & Tarnawski, A. S. (2003). Survivin–an anti-apoptosis protein: its biological roles and implications for cancer and beyond. Signature, 9(4), 47.

Choi, J., In Lee, S., Rackerby, B., Frojen, R., Goddik, L., Ha, S. D., & Park, S. H. (2020). Assessment of overall microbial community shift during Cheddar cheese production from raw milk to aging. Applied Microbiology and Biotechnology, 104, 6249-6260.

Conde, M., Michen, S., Wiedemuth, R., Klink, B., Schröck, E., Schackert, G., & Temme, A. (2017). Chromosomal instability induced by increased BIRC5/Survivin levels affects tumorigenicity of glioma cells. BMC Cancer, 17, 1-17.

Davidov, K., Iankelevich-Kounio, E., Yakovenko, I., Koucherov, Y., Rubin-Blum, M., & Oren, M. (2020). Identification of plastic-associated species in the Mediterranean Sea using DNA metabarcoding with Nanopore MinION. Scientific reports, 10(1), 17533.

D'Alessio, A., Proietti, G., Sica, G., & Scicchitano, B. M. (2019). Pathological and molecular features of glioblastoma and its peritumoral tissue. Cancers, 11(4), 469.

De Filippis, F., Genovese, A., Ferranti, P., Gilbert, J. A., & Ercolini, D. (2016). Metatranscriptomics reveals temperature-driven functional changes in microbiome impacting cheese maturation rate. Scientific Reports, 6(1), 21871.

De Vita, V., Hellman, S., & Rosenberg, S. (1993). Cancer: Principles and practice of oncology Lippincott. Philadelphia USA.

Di Filippo, L. D., Duarte, J. L., Luiz, M. T., de Araújo, J. T. C., & Chorilli, M. (2021). Drug delivery nanosystems in glioblastoma multiforme treatment: current state of the art. Current Neuropharmacology, 19(6), 787-812.

Dias, B., & Weimer, B. (1998). Conversion of methionine to thiols by lactococci, lactobacilli, and brevibacteria. Applied and Environmental Microbiology, 64(9), 3320-3326.

Dias, B. E. (1999). Methanethiol and Cheddar cheese flavor. Utah State University.

Dias, B., & Weimer, B. (1999). Production of volatile sulfur compounds in Cheddar cheese slurries. International Dairy Journal, 9(9), 605-611.

Dijkshoorn, L., Towner, K. J., & Struelens, M. (Eds.). (2001). New approaches for the generation and analysis of microbial typing data. Elsevier.

Dreier, M., Meola, M., Berthoud, H., Shani, N., Wechsler, D., & Junier, P. (2022). High-throughput qPCR and 16S rRNA gene amplicon sequencing as complementary methods for the investigation of the cheese microbiota. BMC Microbiology, 22(1), 48.

El-Sayed, A. S. (2009). L-methioninase production by Aspergillus flavipes under solid-state fermentation. Journal of Basic Microbiology, 49(4), 331-341.

El-Sayed, A. S. (2010). Microbial L-methioninase: production, molecular characterization, and therapeutic applications. Applied Microbiology and Biotechnology, 86, 445-467.

El-Sayed, A. S., Shouman, S. A., & Nassrat, H. M. (2012). Pharmacokinetics, immunogenicity and anticancer efficiency of Aspergillus flavipes L-methioninase. Enzyme and Microbial Technology, 51(4), 200-210.

Epner, D., Baxter, J., Kivi, J., Hards, R. (2003). U.S. Patent Application No. 10/231,562.

Erhardt, M. M., Oliveira, W. D. C., Fröder, H., Marques, P. H., Oliveira, M. B. P. P., & Richards, N. S. P. D. S. (2023). Lactic Bacteria in Artisanal Cheese: Characterization through Metagenomics. Fermentation, 9(1), 41.

Ferchichi, M., Hemme, D., Nardi, M., & Pamboukdjian, N. (1985). Production of methanethiol from methionine by *Brevibacterium linens* CNRZ 918. Microbiology, 131(4), 715-723.

Ferlay, J., Ervik, M., Lam, F., Colombet, M., Mery, L., Piñeros, M., et al. (2020). Global cancer observatory: Cancer Today, Lyon: International Agency for Research on Cancer; https://gco.iarc.fr/today. Access Date: 15.12.2021.

Fernández, M., Porcel, M., de la Torre, J., Molina-Henares, M. A., Daddaoua, A., Llamas, M. A., ... & Duque, E. (2015). Analysis of the pathogenic potential of nosocomial Pseudomonas putida strains. Frontiers in Microbiology, 6, 871.

Fox, P. F., Guinee, T. P., Cogan, T. M., & McSweeney, P. L. H. (2017). Microbiology of cheese ripening. In: Fundamentals of Cheese Science. Springer, Boston, MA, 333-390.

Gao, J., Azmi, A. S., Aboukameel, A., Kauffman, M., Shacham, S., Abou-Samra, A. B., & Mohammad, R. M. (2014). Nuclear retention of Fbw7 by specific inhibitors of nuclear export leads to Notch1 degradation in pancreatic cancer. Oncotarget, 5(11), 3444.

Gay, F., Aguera, K., Sénéchal, K., Tainturier, A., Berlier, W., Maucort-Boulch, D., ... & Bourgeaux, V. (2017). Methionine tumor starvation by erythrocyte-encapsulated methionine gamma-lyase activity controlled with per os vitamin B6. Cancer Medicine, 6(6), 1437-1452.

Gosalvitr, P., Cuellar-Franca, R., Smith, R., & Azapagic, A. (2019). Energy demand and carbon footprint of cheddar cheese with energy recovery from cheese whey. Energy Procedia, 161, 10-16.

Guillen, K. P., Kurkjian, C., & Harrison, R. G. (2014). Targeted enzyme prodrug therapy for metastatic prostate cancer–a comparative study of L-methioninase, purine nucleoside phosphorylase, and cytosine deaminase. Journal of Biomedical Science, 21(1), 1-8.

Guo, H. Y., Herrera, H., Groce, A., & Hoffman, R. M. (1993). Expression of the biochemical defect of methionine dependence in fresh patient tumors in primary histoculture. Cancer Research, 53(11), 2479-2483.

Han, Q., Tan, Y., & Hoffman, R. M. (2020). Oral dosing of recombinant methioninase is associated with a 70% drop in PSA in a patient with bone-metastatic prostate cancer and 50% reduction in circulating methionine in a high-stage ovarian cancer patient. Anticancer Research, 40(5), 2813-2819.

Han, L., Yuan, B., Shimada, R., Hayashi, H., Si, N., Zhao, H. Y., ... & Takagi, N. (2018). Cytocidal effects of arenobufagin and hellebrigenin, two active bufadienolide compounds, against human glioblastoma cell line U-87. International Journal of Oncology, 53(6), 2488-2502.

Hanif, F., Muzaffar, K., Perveen, K., Malhi, S. M., & Simjee, S. U. (2017). Glioblastoma multiforme: A review of its epidemiology and pathogenesis through clinical presentation and treatment. Asian Pacific Journal of Cancer Prevention, 18, 3–9.

Hassabo, A. A., Mousa, A. M., Abdel-Gawad, H., Selim, M. H., & Abdelhameed, R. M. (2019). Immobilization of l-methioninase on a zirconium-based metal–organic framework as an anticancer agent. Journal of Materials Chemistry B, 7(20), 3268-3278.

Higuchi, T., Han, Q., Miyake, K., Oshiro, H., Sugisawa, N., Tan, Y., ... & Hoffman, R. M. (2020). Combination of oral recombinant methioninase and decitabine arrests a chemotherapy-resistant undifferentiated soft-tissue sarcoma patient-derived orthotopic xenograft mouse model. Biochemical and Biophysical Research Communications, 523(1), 135-139.

Hoffman, R. M. (1984). Altered methionine metabolism, DNA methylation and oncogene expression in carcinogenesis: a review and synthesis. Biochimica et Biophysica Acta (BBA)-Reviews on Cancer, 738(1-2), 49-87.

Hoffman, R. M. (2015). Development of recombinant methioninase to target the general cancer-specific metabolic defect of methionine dependence: a 40-year odyssey. Expert Opinion on Biological Therapy, 15(1), 21-31.

Hoffman, R. M. (2017). The wayward methyl group and the cascade to cancer. Cell Cycle, 16(9), 825-829.

Hoffman, R. M. (Ed.). (2019). Methionine dependence of cancer and aging: methods and protocols. Humana Press.

Hoffman, R. M., Tan, Y., Li, S., Han, Q., Yagi, S., Takakura, T., ... & Kudou, D. (2019). Development of recombinant methioninase for cancer treatment. Methionine Dependence of Cancer and Aging: Methods and Protocols, 107-131.

Hori, H., Takabayashi, K., Orvis, L., Carson, D. A., & Nobori, T. (1996). Gene cloning and characterization of pseudomonas putida l-Methionine-α-deamino-γ-mercaptomethane-lyase. Cancer Research, 56(9), 2116-2122.

Hsu, J. F., Chu, S. M., Liao, C. C., Wang, C. J., Wang, Y. S., Lai, M. Y., Wang, H. C., Huang, H. R., & Tsai, M. H. (2021). Nanotechnology and nanocarrier-based drug delivery as the potential therapeutic strategy for glioblastoma multiforme: An update. Cancers, 13(2), 1–22.

Hu, J., & Cheung, N. K. V. (2009). Methionine depletion with recombinant methioninase: in vitro and in vivo efficacy against neuroblastoma and its synergism with chemotherapeutic drugs. International Journal of Cancer, 124(7), 1700-1706.

Jamerson, M. H., Johnson, M. D., & Dickson, R. B. (2004). Of mice and Myc: c-Myc and mammary tumorigenesis. Journal of Mammary Gland Biology and Neoplasia, 9, 27-37.

Kannaujia, P. K., Bhan, C., Asrey, R., & Prasad, H. (2015). Enzymes and its importance in food processing: A review. Journal of Progressive Agriculture, 6(1), 71-74.

Katsimpouras, C., & Stephanopoulos, G. (2021). Enzymes in biotechnology: Critical platform technologies for bioprocess development. Current Opinion in Biotechnology, 69, 91-102.

Kavya, D., & Nadumane, V. K. (2023a). Enhanced l-Methioninase production by Methylobacterium sp. JUBTK33 through RSM and its anticancer potential. Biocatalysis and Agricultural Biotechnology, 47, 102621.

Kavya, D., & Nadumane, V. K. (2023b). A combination of semi-purified L-methioninase with tamoxifen citrate to ameliorate breast cancer in athymic nude mice. Molecular Biology Reports, 50(3), 2925-2932.

Kawaguchi, K., Igarashi, K., Li, S., Han, Q., Tan, Y., Miyake, K., ... & Hoffman, R. M. (2018). Recombinant methioninase (rMETase) is an effective therapeutic for BRAF-V600E-negative as well as-positive melanoma in patient-derived orthotopic xenograft (PDOX) mouse models. Oncotarget, 9(1), 915.

Kawaguchi, K., Han, Q., Li, S., Tan, Y., Igarashi, K., Murakami, T., ... & Hoffman, R. M. (2019). Efficacy of recombinant methioninase (rMETase) on recalcitrant cancer patient-derived orthotopic xenograft (PDOX) mouse models: A review. Cells, 8(5), 410.

Kelleher, P., Murphy, J., Mahony, J., & van Sinderen, D. (2015). Next-generation sequencing as an approach to dairy starter selection. Dairy Science & Technology, 95, 545-568.

Kenyon, S. H., Waterfield, C. J., Timbrell, J. A., & Nicolaou, A. (2002). Methionine synthase activity and sulphur amino acid levels in the rat liver tumour cells HTC and Phi-1. Biochemical Pharmacology, 63(3), 381-391.

Khalaf, S. A., & El-Sayed, A. S. (2009). L-Methioninase production by filamentous fungi: I-screening and optimization under submerged conditions. Current Microbiology, 58, 219-226.

Khaw, A. K., Hande, M. P., Kalthur, G., & Hande, M. P. (2013). Curcumin inhibits telomerase and induces telomere shortening and apoptosis in brain tumour cells. Journal of Cellular Biochemistry, 114(6), 1257-1270.

Kitada, M., Ogura, Y., Monno, I., Xu, J., & Koya, D. (2021). Effect of methionine restriction on aging: its relationship to oxidative stress. Biomedicines, 9(2), 130.

Kokkinakis, D. M., Schold Jr, S. C., Hori, H., & Nobori, T. (1997). Effect of long-term depletion of plasma methionine on the growth and survival of human brain tumor xenografts in athymic mice. Nutrition and Cancer, 29(3), 195-204.

Kreis, W., & Hession, C. (1973). Biological effects of enzymatic deprivation of L-methionine in cell culture and an experimental tumor. Cancer Research, 33(8), 1866-1869.

Laakso, S., & Nurmikko, V. (1976). A spectrophotometric assay for demethiolating activity. Analytical Biochemistry, 72(1-2), 600-605.

Lenin, S., Ponthier, E., Scheer, K. G., Yeo, E. C., Tea, M. N., Ebert, L. M., ... & Gomez, G. A. (2021). A drug screening pipeline using 2D and 3D patient-derived in vitro models for pre-clinical analysis of therapy response in glioblastoma. International Journal of Molecular Sciences, 22(9), 4322.

Liu, S. Q., Yu, J. P., Yu, H. G., Lv, P., & Chen, H. L. (2006). Activation of Akt and ERK signalling pathways induced by etoposide confer chemoresistance in gastric cancer cells. Digestive and Liver Disease, 38(5), 310-318.

Lindsay, R. C., & Rippe, J. K. (1986). Enzymic generation of methanethiol to assist in the flavor development of Cheddar cheese and other foods. In: Biogenereration of Aromas (Croteau, R., Ed.), pp. 286–308 American Chemical Society, Washington, DC.

Lu, S., & Epner, D. E. (2000). Molecular mechanisms of cell cycle block by methionine restriction in human prostate cancer cells. Nutrition and Cancer, 38(1), 123-130.

Marshall, S.W. (2005). Prevalence and incidence. Encyclopedia of Social Medicine, 3, 141–147 .

Mobahat, M., Narendran, A., & Riabowol, K. (2014). Survivin as a preferential target for cancer therapy. International Journal of Molecular Sciences, 15(2), 2494-2516.

Machover, D., Rossi, L., Hamelin, J., Desterke, C., Goldschmidt, E., Chadefaux-Vekemans, B., ... & Saffroy, R. (2019). Effects in cancer cells of the recombinant l-methionine gamma-lyase from *Brevibacterium aurantiacum*. Encapsulation in human erythrocytes for sustained l-methionine elimination. Journal of Pharmacology and Experimental Therapeutics, 369(3), 489-502.

Majolo, F., Delwing, L. K. D. O. B., Marmitt, D. J., Bustamante-Filho, I. C., & Goettert, M. I. (2019). Medicinal plants and bioactive natural compounds for cancer treatment: Important advances for drug discovery. Phytochemistry Letters, 31, 196-207.

McEwan, M. V., Eccles, M. R., & Horsfield, J. A. (2012). Cohesin is required for activation of MYC by estradiol. PloS One, 7(11), e49160.

Mecham, J. O., Rowitch, D., Wallace, C. D., Stern, P. H., & Hoffman, R. M. (1983). The metabolic defect of methionine dependence occurs frequently in human tumor cell lines. Biochemical and Biophysical Research Communications, 117(2), 429-434.

Mohamed, A. H., Abou Zeid, A. A., El-Sayed, A. S., & Shawadfy, A. M. E. (2022). Short Review on Microbial L-methioninase and it’s Applications. Bulletin of Faculty of Science, Zagazig University, 2022(4), 107-133.

Mohamed, H. M., Barzideh, Z., Siddiqi, M., & LaPointe, G. (2023). Taxonomy, Sequence Variance and Functional Profiling of the Microbial Community of Long-Ripened Cheddar Cheese Using Shotgun Metagenomics. Microorganisms, 11(8), 2052.

Mohkam, M., Taleban, Y., Golkar, N., Berenjian, A., Dehshahri, A., Mobasher, M. A., & Ghasemi, Y. (2020). Isolation and identification of novel L-methioninase producing bacteria and optimization of its production by experimental design method. Biocatalysis and Agricultural Biotechnology, 26, 101566.

Montecucco, A., Zanetta, F., & Biamonti, G. (2015). Molecular mechanisms of etoposide. EXCLI journal, 14, 95.

Nelson, G., Platnick, N.I., 1981. Systematics and biogeography: cladistics and vicariance. Columbia University Press, New York, NY.

Ohgaki, H., & Kleihues, P. (2005). Epidemiology and etiology of gliomas. Acta Neuropathologica, 109(1), 93–108.

Ozdemir, M. D., & Gokturk, D. (2018). The effect of Rosmarinus officinalis and chemotherapeutic etoposide on glioblastoma (U87 MG) cell culture. Turkish Neurosurgery, 28, 853-857.

Ozdemir, M. D., & Gokturk, D. (2019). The concurrent effect of acyclovir and rosemary on glioblastoma cell culture. Cellular and Molecular Biology, 65(3), 66-71.

Overbeck, S. L. (2021). Comparison of microbial diversity of fifteen aged Cheddar cheeses from different regions using next generation sequencing (Doctoral dissertation, Utah State University).

Pakroo, S., Tarrah, A., Takur, R., Wu, M., Corich, V., & Giacomini, A. (2022). Limosilactobacillus fermentum ING8, a potential multifunctional non-starter strain with relevant technological properties and antimicrobial activity. Foods, 11(5), 703.

Palwai, N. R., Zang, X. P., Harrison, R. G., & Pento, J. T. (2007). Influence of L-methioninase targeted to the urokinase receptor on the proliferation and motility of lung and prostate cancer cells. Anticancer Research, 27(5A), 3435-3439.

Palwai, N. R., Zang, X. P., Harrison, R. G., Benbrook, D., & Pento, J. T. (2009). Selective growth inhibition of cancer cells by L-methioninase-containing fusion protein targeted to the urokinase receptor. Pharmacology, 84(5), 271-275.

Pancza, B., Szathmáry, M., Gyurján, I., Bánkuti, B., Tudós, Z., Szathmary, S., ... & Bánáti, F. (2021). A rapid and efficient DNA isolation method for qPCR-based detection of pathogenic and spoilage bacteria in milk. Food Control, 130, 108236.

Peron, K., Jones, T. N., Gauthier, S. A., Nguyen, T. N. T., Zang, X. P., Barriere, M., ... & Pento, J. T. (2003). Targeting of a novel fusion protein containing methioninase to the urokinase receptor to inhibit breast cancer cell migration and proliferation. Cancer Chemotherapy and Pharmacology, 52, 270-276.

Prakash, O. M., Kumar, A., & Kumar, P. (2013). Anticancer potential of plants and natural products. American Journal of Pharmacological Sciences, 1(6), 104-115.

Qiu, J., Shi, Z., & Jiang, J. (2017). Cyclooxygenase-2 in glioblastoma multiforme. Drug Discovery Today, 22(1), 148–156.

Rattray, F. P., & Fox, P. F. (1999). Aspects of enzymology and biochemical properties of *Brevibacterium linens* relevant to cheese ripening: a review. Journal of Dairy Science, 82(5), 891-909.

Rehman, N., Khan, S., Manzoor, S., Abubakar, M., Sami, R., Alharthy, S. A., ... & Shahid, R. (2022). Estrogen Induces c-myc Transcription by Binding to Upstream ERE Element in Promoter. Applied Sciences, 12(14), 6853.

Repetto, G., Del Peso, A., & Zurita, J. L. (2008). Neutral red uptake assay for the estimation of cell viability/cytotoxicity. Nature Protocols, 3(7), 1125-1131.

Roberts, M., Wijesundera, C., Bruinenberg, P. G., & Limsowtin, G. K. Y. (1995). Development of an aseptic cheese curd slurry system for cheese ripening studies1. Australian Journal of Dairy Technology, 50(2), 66.

Robinson, P. K. (2015). Enzymes: principles and biotechnological applications. Essays in Biochemistry, 59, 1.

Salim, N., Santhiagu, A., & Joji, K. (2019). Process modeling and optimization of high yielding L-methioninase from a newly isolated Trichoderma harzianum using response surface methodology and artificial neural network coupled genetic algorithm. Biocatalysis and Agricultural Biotechnology, 17, 299-308.

Salim, N., Santhiagu, A., & Joji, K. (2020). Purification, characterization and anticancer evaluation of l-methioninase from Trichoderma harzianum. 3 Biotech, 10(11), 501.

Salum, P., Erbay, Z., Kelebek, H., & Selli, S. (2017). Optimization of headspace solid-phase microextraction with different fibers for the analysis of volatile compounds of white-brined cheese by using response surface methodology. Food Analytical Methods, 10, 1956-1964.

Sanders, E. R. (2012). Aseptic laboratory techniques: plating methods. JoVE (Journal of Visualized Experiments), 63, e3064.

Selim, M. H., Karm Eldin, E. Z., Saad, M. M., Mostafa, E. S. E., Shetia, Y. H., & Anise, A. A. H. (2015a). Purification, characterization of L-methioninase from Candida tropicalis, and its application as an anticancer. Biotechnology Research International, 2015.

Selim, M. H., Elshikh, H. H., El-Hadedy, D. E., Saad, M. M., Eliwa, E., & Abdelraof, M. (2015b). L-Methioninase from some Streptomyces isolates I: Isolation, identification of best

producers and some properties of the crude enzyme produced. Journal of Genetic Engineering and Biotechnology, 13(2), 129-137.

Sevim, H., Parkinson, J. F., & McDonald, K. L. (2011). Etoposide-mediated glioblastoma cell death: dependent or independent on the expression of its target, topoisomerase II alpha?. Journal of Cancer Research and Clinical Oncology, 137, 1705-1712.

Shapiro, W. R., & Shapiro, J. R. (1998). Biology and treatment of malignant glioma. Oncology (Williston Park, NY), 12(2), 233-40.

Sharma, B., Devi, S., Kumar, R., & Kanwar, S. S. (2022). Screening, characterization and anti-cancer application of purified intracellular MGL. International Journal of Biological Macromolecules, 217, 96-110.

Sharpe, M. E., Law, B. A., Phillips, B. A., & Pitcher, D. G. (1977). Methanethiol production by coryneform bacteria: strains from dairy and human skin sources and *Brevibacterium linens*. Microbiology, 101(2), 345-349.

Sheng, L., Wan, B., Feng, P., Sun, J., Rigo, F., Bennett, C. F., ... & Hua, Y. (2018). Downregulation of Survivin contributes to cell-cycle arrest during postnatal cardiac development in a severe spinal muscular atrophy mouse model. Human Molecular Genetics, 27(3), 486-498.

Shin, S., Sung, B. J., Cho, Y. S., Kim, H. J., Ha, N. C., Hwang, J. I., ... & Oh, B. H. (2001). An anti-apoptotic protein human survivin is a direct inhibitor of caspase-3 and-7. Biochemistry, 40(4), 1117-1123.

Silantyev, Falzone, Libra, Gurina, Kardashova, Nikolouzakis, Nosyrev, Sutton, Panayioti, &Tsatsakis. (2019). Current and future trends on diagnosis and prognosis of glioblastoma: From Molecular biology to proteomics. Cells, 8(8), 863.

Soda, K. (2018). Polyamine metabolism and gene methylation in conjunction with one-carbon metabolism. International Journal of Molecular Sciences, 19(10), 3106.

Sontheimer, H. (2008). A role for glutamate in growth and invasion of primary brain tumors. Journal of Neurochemistry, 105(2), 287–295.

Stern, P. H., Wallace, C. D., & Hoffman, R. M. (1984). Altered methionine metabolism occurs in all members of a set of diverse human tumor cell lines. Journal of Cellular Physiology, 119(1), 29-34.

Suarez-Arnedo, A., Figueroa, F. T., Clavijo, C., Arbeláez, P., Cruz, J. C., & Muñoz-Camargo, C. (2020). An image J plugin for the high throughput image analysis of in vitro scratch wound healing assays. PloS One, 15(7), e0232565.

Suganya, K., Govindan, K., Prabha, P., & Murugan, M. (2017). An extensive review on L-methioninase and its potential applications. Biocatalysis and Agricultural Biotechnology, 12, 104-115.

Sunden, S. L., Renduchintala, M. S., Park, E. I., Miklasz, S. D., & Garrow, T. A. (1997). Betaine–homocysteine methyltransferase expression in porcine and human tissues and chromosomal localization of the human gene. Archives of Biochemistry and Biophysics, 345(1), 171-174.

Tan, Y., Xu, M., Guo, H., Sun, X., Kubota, T., & Hoffman, R. M. (1996). Anticancer efficacy of methioninase in vivo. Anticancer Research, 16(6C), 3931-3936.

Tanaka, H., Esaki, N., & Soda, K. (1977). Properties of L-methionine γ-lyase from Pseudomonas ovalis. Biochemistry, 16(1), 100-106.

Thomas, T., & Thomas, T. J. (2001). Polyamines in cell growth and cell death: molecular mechanisms and therapeutic applications. Cellular and Molecular Life Sciences CMLS, 58(2), 244-258.

Thompson, E. B. (1998). The many roles of c-Myc in apoptosis. Annual Review of Physiology, 60(1), 575-600.

Tokita, F., & Hosono, A. (1968). Production of volatile sulfur compounds by *Brevibacterium linens*. Japanese Journal of Zootechnical Science, 39, 127-132.

Tong, X., Yang, P., Wang, K., Liu, Y., Liu, X., Shan, X., ... & Wang, J. (2019). Survivin is a prognostic indicator in glioblastoma and may be a target of microRNA-218. Oncology Letters, 18(1), 359-367.

Ulagesan, S., & Kim, H. J. (2018). Antibacterial and antifungal activities of proteins extracted from seven different snails. Applied Sciences, 8(8), 1362.

Van Rite, B. D., Lazrak, Y. A., Pagnon, M. L., Palwai, N. R., Neves, L. F., McFetridge, P. S., & Harrison, R. G. (2011). Enzyme prodrug therapy designed to target L-methioninase to the tumor vasculature. Cancer Letters, 301(2), 177-184.

Van Rite, B. D., Krais, J. J., Cherry, M., Sikavitsas, V. I., Kurkjian, C., & Harrison, R. G. (2013). Antitumor activity of an enzyme prodrug therapy targeted to the breast tumor vasculature. Cancer Investigation, 31(8), 505-510.

Wang, J., Yang, Z. J., Wang, Y. D., Cao, Y. P., Wang, B., & Liu, Y. (2021). The key aroma compounds and sensory characteristics of commercial Cheddar cheeses. Journal of Dairy Science, 104(7), 7555-7571.

Weimer, B., Dias, B., Ummadi, M., Broadbent, J., Brennand, C., Jaegi, J., ... & Sisson, D. V. (1997). Influence of NaCl and pH on intracellular enzymes that influence Cheddar cheese ripening. Le Lait, 77(3), 383-398.

Xu, J., Chen, Y., & Olopade, O. I. (2010). MYC and breast cancer. Genes & Cancer, 1(6), 629-640.

Yeo, E. C. F., Brown, M. P., Gargett, T., & Ebert, L. M. (2021). The role of cytokines and chemokines in shaping the immune microenvironment of glioblastoma: Implications for immunotherapy. Cells, 10(3), 1–25.

Yoshioka, T., Wada, T., Uchida, N., Maki, H., Yoshida, H., Ide, N., ... & Sugita, K. (1998). Anticancer efficacy in vivo and in vitro, synergy with 5-fluorouracil, and safety of recombinant methioninase. Cancer Research, 58(12), 2583-2587.

Zhang, Y., Qi, Y., Lo, E. C., McGrath, C., Mei, M. L., & Dai, R. (2021). Using next-generation sequencing to detect oral microbiome change following periodontal interventions: A systematic review. Oral Diseases, 27(5), 1073-1089.

Zingg, J. M., & Jones, P. A. (1997). Genetic and epigenetic aspects of DNA methylation on genome expression, evolution, mutation and carcinogenesis. Carcinogenesis, 18(5), 869-882.